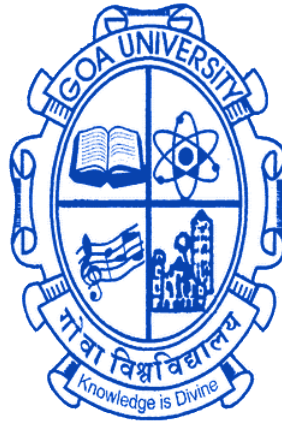


**UNDERSTANDING THE MORPHOLOGICAL BEHAVIOUR AND EVOLUTION  
OF DEEP SEA CHANNEL SYSTEMS VIS-À-VIS FLUVIAL SYSTEMS**



**THESIS SUBMITTED TO  
GOA UNIVERSITY**

**FOR THE AWARD OF THE DEGREE  
DOCTOR OF PHILOSOPHY  
IN  
EARTH SCIENCE**

*by*  
**R. PRERNA**

**Under the Guidance of**

**Dr. Mahender Kotha**  
School of Earth, Ocean and Atmospheric  
Sciences, Goa University, Goa

**Dr. Dhananjai K Pandey**  
National Centre for Polar and Ocean  
Research, Ministry of Earth Sciences, Goa

**SCHOOL OF EARTH, OCEAN AND ATMOSPHERIC SCIENCES  
GOA UNIVERSITY**

**MAY, 2020**

## CERTIFICATE

This is to certify that the thesis entitled “Understanding the morphological behaviour and evolution of deep sea channel systems vis-à-vis fluvial systems” submitted to Goa University, by Ms R. Prerna for the award of the degree of Doctor of Philosophy in Earth Science is a record of original and independent work carried out by her during the period of February 2015 – May 2020 under my supervision and the same has not been previously submitted for the award of any diploma, degree, associateship or fellowship or any other similar title.

Goa University

May, 2020

**Dr Mahender Kotha (Supervisor)**

School of Earth, Ocean and Atmospheric Sciences,

Goa University, Taleigao Plateau, Goa – 403206

**Dr Dhananjai K Pandey (Co-Supervisor)**

National Centre for Polar and Ocean Research,

Ministry of Earth Sciences,

Headland Sada, Vasco-da-Gama, Goa – 403804

## DECLARATION

I hereby declare that the matter embodied in this thesis entitled “Understanding the morphological behaviour and evolution of deep sea channel systems vis-à-vis fluvial systems” submitted to Goa University, for the award of the degree of Doctor of Philosophy in Earth Sciences is a record of original and independent work carried out by me during the period of February 2015 – May 2020 under the supervision of Dr Mahender Kotha, School of Earth, Ocean and Atmospheric Sciences, Goa University and Dr Dhananjai K Pandey, National Centre for Polar and Ocean Research (NCPOR), Ministry of Earth Sciences, India and that it has not been previously formed the basis for award of any diploma, degree, associateship or fellowship or any other similar title.

Goa University

May, 2020

**R. Prerna**

## ACKNOWLEDGEMENT

*The inception of this research began with a deep sea cruise in the Arabian Sea, back in 2013. Our objective was to ensonify a block in the Laxmi Basin region as part of a site survey for an IODP sediment core drilling expedition. Little did I realize then, that the opportunity to participate in the site survey would open avenues leading to my doctoral research. I shall be ever grateful to Dr Dhananjai K Pandey, who envisaged the scientific value to explore deeper into the subject and motivated me to prepare a research proposal. His perennial support and encouragement was a true inspiration that has finally led to the culmination of my doctoral research. My team members onboard ORV Sagar Kanya – Dr Ravi Mishra, Mr Ajeet Kumar, Mr Kishor Gaonkar and Mr Prathap Akkapolu, and the entire crew of SK 306 are thanked for their cooperation. I also gratefully acknowledge Mr Sarath Chandran and his team from Norinco Pvt. Ltd. who were exceptionally cooperative in helping me understand the fundamentals of bathymetric data acquisition and the nitty-gritty of surveying—right from planning to execution.*

*Dr Mahender Kotha has been supportive towards my research proposal from day one. His keen insight into the geomorphology of fluvial and submarine features and overall subject expertise was helpful in executing my research. As an established mentor, his guidance throughout my research tenure is deeply appreciated and gratefully acknowledged.*

*Dr Ramprasad T, VC nominee, has been a constant source of encouragement. Through his keen outlook and eye for detail, he provided valuable feedback at every stage of my research which was always welcome. I express my earnest thankfulness for his active involvement and support.*

*I extend my sincere gratitude to Director, National Centre for Polar and Ocean Research (NCPOR), Ministry of Earth Sciences, Goa for his kind support. Scientists from the EEZ Division, NCPOR are also sincerely thanked for processing and facilitating part bathymetric data utilised in this research.*

*Dr Peter Clift and Dr Tim Henstock are thanked for their gracious support to include bathymetric data collected by them onboard RV Pelagia in this study. Dr SW Cooley for sharing valuable information through his portal on GIS for geomorphology; and the web GIS community is graciously thanked for providing tools/information for betterment of this research.*

*My fellow colleagues at NCPOR, Goa – Dr Nisha Nair, Mr N Lachit Singh, Mr S Khogenkumar Singh, Dr Sanjay Singh Negi and Mr Bala Laxman Mhagdut are sincerely thanked for their valuable suggestions and support. I would also like to thank Mrs Sangita Tilve, other staff members and Mr Purushottam Verlekar from the School of Earth, Ocean and Atmospheric Sciences at Goa University for their kind support and assistance.*

*I extend paramount gratitude to my parents, Lt Col K Ramesh and Mrs Veena Ramesh, and my elder sister Ms Archana Ramesh for imbibing perseverance in me to accomplish what I began. Their love, support, patience and most importantly, their confidence in my goals has inspired me all the way along for which I shall be ever grateful.*

*I thank God Almighty for giving me the courage and strength to fulfil this endeavour.*

**R Prerna**

## CONTENTS

<b>Certificate</b> .....	<b>i</b>
<b>Declaration</b> .....	<b>ii</b>
<b>Acknowledgement</b> .....	<b>iii</b>
<b>Contents</b> .....	<b>v</b>
<b>List of figures</b> .....	<b>viii</b>
<b>List of tables</b> .....	<b>xiii</b>
<b>Thesis Structure</b> .....	<b>xiv</b>
<b>Glossary</b> .....	<b>xv</b>
<b>Chapter 1: Introduction</b> .....	<b>1-24</b>
1.1. Preface .....	<b>1</b>
1.2. Submarine fan systems: an overview .....	<b>4</b>
1.2.1. Scientific significance .....	<b>4</b>
1.2.2. Controlling factors .....	<b>9</b>
1.2.3. Submarine-fluvial analogy .....	<b>11</b>
1.3. Rationale .....	<b>13</b>
1.3.1. What are the similarities? .....	<b>14</b>
1.3.2. What are the dissimilarities? .....	<b>16</b>
1.4. Research objectives .....	<b>21</b>
<b>Chapter 2: Physiographic and geological setting</b> .....	<b>25-34</b>
2.1. The fluvial Indus Basin .....	<b>26</b>
2.1.1. Indus River .....	<b>28</b>
2.1.2. Indus Delta .....	<b>29</b>
2.2. The submarine Indus Fan .....	<b>30</b>
2.2.1. Indus Canyon .....	<b>32</b>
2.2.2. Indus Fan channel levee complex .....	<b>33</b>

<b>Chapter 3: Data and Methods</b>	<b>35-58</b>
3.1. Datasets .....	36
3.2. DEM data (for fluvial analysis) .....	39
3.2.1. Stream network and basin delineation .....	40
3.2.1.1 Step 1: Creation of depressionless DEM .....	40
3.2.1.2 Step 2: Flow direction .....	41
3.2.1.3 Step 3: Flow accumulation .....	42
3.2.1.4 Step 4: Filtration of flow accumulation .....	43
3.2.1.5 Step 5: Stream ordering .....	44
3.2.1.6 Step 6: Basin delineation .....	45
3.2.2. Geomorphometric parameter estimation of the Indus River .....	48
3.2.2.1 Longitudinal profile .....	48
3.2.2.2 Channel width profile .....	50
3.2.2.3 Sinuosity profile .....	52
3.2.2.4 Planform .....	52
3.2.2.5 Slope profile .....	53
3.2.3. Elevation-relief analysis of the Indus Basin .....	53
3.2.4. Geomorphometric account of the Indus system .....	54
3.3. MBES data (for submarine analysis) .....	55
<b>Chapter 4: Data analysis and interpretation</b>	<b>59-109</b>
4.1. Indus River and its basin .....	60
4.1.1. Stream network identification .....	60
4.1.2. Longitudinal profiling and channel width analysis .....	62
4.1.3. Sinuosity analysis and planform classification .....	68
4.1.4. Slope analysis .....	75
4.1.5. Elevation-relief analysis .....	79
4.1.6. Demarcation of Upper, Middle, Lower Indus Basin .....	82
4.1.7. Gist of fluvial analysis .....	89
4.2. Indus Fan and its channel levee complex .....	90

4.2.1.	Upper Indus Fan .....	91
4.2.2.	Middle Indus Fan .....	94
4.2.3.	Lower Indus Fan .....	99
4.2.4.	Gist of submarine analysis .....	100
4.3.	Comparison of fluvial rivers vis-à-vis submarine channel levee complexes ....	101
4.3.1.	Upper Indus Basin vs. Upper Indus Fan .....	101
4.3.2.	Middle Indus Basin vs. Middle Indus Fan .....	105
4.3.3.	Lower Indus Basin vs. Lower Indus Fan .....	108
<b>Chapter 5: Discussion and conclusion</b>		<b>110-130</b>
5.1.	Holistic observations .....	111
5.2.	Causative factors .....	119
5.3.	Conclusion .....	124
5.4	Scope for further research .....	128
5.5	Epilogue .....	129
<b>References</b> .....		<b>131-148</b>
<b>Publications and participations</b> .....		<b>149</b>
<b>Annexures</b> .....		<b>150-151</b>

## LIST OF FIGURES

<b>Fig 1.1</b>	Graphical representation of a typical fluvial and submarine system with associated features depicting direct and indirect association of the canyon head with the fluvial system with sea level change. (Figure from Prerna and Kotha, 2020) .....	3
<b>Fig 1.2</b>	World distribution of major submarine fan systems like Bengal, Indus, Amazon, Mississippi, Zaire, Niger, Baranof present on both active and passive continental margins.....	7
<b>Fig 1.3</b>	Planform of (A) submarine channel from the Indus Canyon and (B) subaerial fluvial Indus River showing remarkable physical similarities. [Data source: (A) Clift and Henstock, 2015; (B) ESRI™ World Imagery (WGS84)] .....	12
<b>Fig 2.1</b>	Physiographic/tectonic map of the Indus Basin modified from Yin (2006), Afzal et al. (2009), Chen and Khan (2010), Asim et al. (2014), Mukherjee (2015) and Prerna et al. (2018). Major faults like the Karakoram, Chaman; positive relief features like the Kohat and Potwar Plateaus having direct implications on the Indus River’s morphology are indicated, yellow stars denote the river’s source and mouth .....	27
<b>Fig 2.2</b>	Physiographic map of the Indus Fan and surrounding regions. Middle and Lower Indus Fan boundaries (as -3400 and -3900 m contours) adopted from Kolla and Coumes (1987). A close-up of Indus Canyon as a major bathymetric incision on the western continental margin of India is provided as inset a (Clift and Henstock, 2015). Yellow star denotes Indus River’s mouth 40 km away from the Indus Canyon head. RS: Raman Seamount, WG: Wadia Guyot .....	31
<b>Fig 3.1</b>	Physiographic map of study area. Indus Fan boundaries are adopted from Kolla and Coumes (1987) and Indus Basin boundaries from Prerna et al. (2018). Blocks F1 (CartoDEM), F2 (SRTM), S1 (Clift and Henstock, 2015), S2 (NCPOR, n.d.), S3 (Mishra et al., 2015), R1 (Kenyon et al., 1987); R2 (Kodagali and Jauhari, 1999), R3 (Bourget et al., 2013) represent the extent of data blocks. (Figure from Prerna and Kotha, 2020) .....	38
<b>Fig 3.2</b>	Schematic workflow for stream network extraction from DEM. (Figure from Prerna and Kotha, 2020) .....	40
<b>Fig 3.3</b>	Difference in cross-sections of (A) original DEM and (B) filled DEM .....	41
<b>Fig 3.4</b>	Illustration showing how flow direction is estimated (Source: ESRI™) .....	42
<b>Fig 3.5</b>	Illustration showing how flow accumulation is estimated (Source: ESRI™) ....	43
<b>Fig 3.6</b>	Stream order as per (A) Strahler (1952) and (B) Shreve (1966) .....	44

<b>Fig 3.7</b>	Process of basin delineation showing (A) a part of DEM from the study area showing streams and estimated ridge lines and (B) ridge lines and stream flow direction used to delineate basin boundaries .....	<b>45</b>
<b>Fig 3.8</b>	(A) Location of 77 CartoDEM and 01 SRTM data tile with grid code used in the study; [(B)-(F) process of stream and basin identification of one tile (i44g) shown as sample] (B) Depressionless DEM (C) Flow direction raster; (D) Flow accumulation raster; (E) Stream order; (F) Basin delineation .....	<b>46</b>
<b>Fig 3.9</b>	Model for stream and basin delineation built using ArcMap® Model Builder ...	<b>47</b>
<b>Fig 3.10</b>	(A) 4 sample profiles – P1, P2, P3, P4 along channel course shown in planform; (B) Cross-sections of P1, P2, P3, P4 with respective thalweg points; (C) Illustrative longitudinal profile generated from elevation of thalweg points. (Figure from Prerna et al., 2018) .....	<b>49</b>
<b>Fig 3.11</b>	Channel width estimation using <i>DrawPerpendicularSeg</i> tool. (A) channel with axis; (B) regular interval points generated on either bank of the channel; (C) perpendicular lines generated from points representing channel width .....	<b>51</b>
<b>Fig 3.12</b>	Flowchart of methodology followed to construct morphometry of the Indus system .....	<b>55</b>
<b>Fig 3.13</b>	Geomorphometric parameter estimation for a part of Middle Indus Fan channels using MBES data. 1: Construction of longitudinal profile by plotting thalweg points at 10 km interval; 2: construction of channel width profile using straight line transects at 100 m interval; 3: calculation of SI using sinuous distance (A) fixed at 10 km divided by straight line distance (B); and 4: calculation of slope (percentage rise) for every reach of 10 km. (Figure from Prerna and Kotha, 2020)	<b>57</b>
<b>Fig 3.14</b>	Summarized methodology for morphometric comparison of fluvial and submarine channel behaviour on a one-to-one basis—i.e. basin vs fan. Blue and yellow boxes represent fluvial and submarine process/method respectively.....	<b>58</b>
<b>Fig 4.1</b>	Mosaicked grid from 78 tiles of DEM data superimposed with the extracted Indus drainage network. Bold blue line represents the Indus River, lighter blue lines represent tributaries, and yellow stars denote the river’s source and mouth. (Figure from Prerna et al., 2018) .....	<b>61</b>
<b>Fig 4.2</b>	Longitudinal profile of the Indus River with channel width denoted at every 100 m. Channel width is represented as distance from channel axis to either bank, for e.g., if the width at a given point is 500 m, the graph would show 250 m on either side from 0 (primary ordinate). Different colour bands indicate the extent of each planform type (I to VIII) across the course of the river, discussed in Section 4.1.3 (Fig 4.6). Confluence points of Indus with its tributaries and major dams/barrages along its course are also marked. (Figure from Prerna et al., 2018)	<b>63</b>

<b>Fig 4.3</b>	Tectonic map of the Indus Basin with major thrust zones/faults marked; modified from Yin (2006), Afzal et al. (2009), Chen and Khan (2010), Asim et al. (2014), Mukherjee (2015) and Prerna et al. (2018). 15 major tributaries of the Indus River are plotted .....	<b>64</b>
<b>Fig 4.4</b>	Plot of sinuosity values measured for every 10 km reach superimposed on the longitudinal profile of the Indus. SI ranges from 1.007 to 3.221. Demarcation of Upper, Middle, Lower Indus Basin shown here is discussed in Section 4.1.6. (Figure from Prerna et al., 2018).....	<b>70</b>
<b>Fig 4.5</b>	(A) Anastomosis of Gar Zangbo in the Tibetan plateau – channel splits from singular to multiple to single again due to drop in valley gradient causing loss of energy; (B) Sênggê Zangbo undergoes anastomosis – channel avulsion may have caused abandonment of one channel, broad channel belt indicates paleo-course; (C) Braided channel belt with multiple streams divided by depositional features; (D) Braided channel with exposed floodplains/sand bars etc. caused by lateral aggradation of the Indus River (Source: Google Earth™). (Figure from Prerna et al., 2018).....	<b>71</b>
<b>Fig 4.6</b>	Planform types identified along the course of the Indus River with their characteristics (refer Fig 4.2 for location) (Figure from Prerna et al., 2018) .....	<b>73</b>
<b>Fig 4.7</b>	Correlation and linear regression plot showing very low positive correlation between sinuosity and slope in the Indus River system. (Figure from Prerna et al., 2018) .....	<b>76</b>
<b>Fig 4.8</b>	Plot of percentage rise measured for every 10 km reach superimposed on the longitudinal profile of Indus River. Slope (percentage rise) varies from – 0.09 to 1.42%. (Figure from Prerna et al., 2018) .....	<b>78</b>
<b>Fig 4.9</b>	(A) Hypsometric curve for the Indus Basin. Normalized area (primary abscissa) is plotted against normalized elevation (primary ordinate) and the secondary axes show percentage areas within each elevation slab (of 100 m interval); (B) shapes of hypsometric curves belonging to youthful stage, mature stage and monadnock Stage with HI of 79.5%, 43% and 17.6% respectively (Strahler, 1952). (Figure from Prerna et al., 2018) .....	<b>81</b>
<b>Fig 4.10</b>	Hypsometric curve for the Indus Basin with corresponding percentage areas. (Figure from Prerna et al., 2018) .....	<b>82</b>
<b>Fig 4.11</b>	(A) Satellite imagery of 1984, Guddu Barrage in Pakistan shows the then active channel with ox-bow formation developing towards the lower reach; (B) Satellite imagery of 2017 shows severe lateral migration of active channel, disappearance of ox-bow and remarkable change of channel belt planform. (Source: Google Earth™)[Completed in 1962, the influence of the barrage on the river course is phenomenal but due to data limits, images are restricted to 1984] (Figure from Prerna et al., 2018) .....	<b>84</b>

<b>Fig 4.12</b>	(A) Satellite imagery of 2001, Indus River after Tarbela Dam - shows a highly braided reach of the river with well-developed depositional features; (B) Satellite imagery of 2017 - shows visible difference in channel width (marked in boxes) at several locations within and beyond the channel belt, caused either by climatic or anthropogenic influences. (Source: Google Earth™). (Figure from Prerna et al., 2018) .....	<b>85</b>
<b>Fig 4.13</b>	(A) Satellite imagery of 2010, near Manchhar Lake, Pakistan - shows a highly sinuous channel of Indus; (B) Satellite imagery of 2017 - shows one fully and two nearly developed ox-bows on either side of the active channel which has undergone major lateral migration. (Source: Google Earth™). (Figure from Prerna et al., 2018) .....	<b>86</b>
<b>Fig 4.14</b>	Indus Basin divided into Upper, Middle and Lower Basin; locations of major dams/barrages are marked along the river. (Figure from Prerna et al., 2018) .....	<b>88</b>
<b>Fig 4.15</b>	(A) 3D surface map of the Indus Canyon (Block S1, refer Fig 2 for location). Vertical exaggeration (VE) is 12x. (B) 2D surface map of the Indus Canyon showing location of cross-sections P1 to P9. Note transition from side wall slumping to flat terraces and near-vertical boundaries along the channel thalweg. (C) Enlarged representation of box drawn on P6 showing how channel width is estimated. [CT: channel thalweg; CW: channel width; ML: meander loop; NVB: near-vertical boundary]. (Figure from Prerna and Kotha, 2020).....	<b>92</b>
<b>Fig 4.16</b>	(A) 3D surface map of channel levee complex in the Upper Indus Fan (Block S2, refer Fig 2 for location). Vertical exaggeration (VE) is 12x. (B) 2D surface map of channel levee complex in the Upper Indus Fan showing location of cross-sections P1 to P5. Note transition in levee height down-fan along the channel thalweg. (C) Enlarged representation of box drawn on P2 showing how channel width is estimated. [CT: channel thalweg; CW: channel width; BL: Bounding levees; ML: meander loop]. (Figure from Prerna and Kotha, 2020) .....	<b>93</b>
<b>Fig 4.17</b>	(A) 3D surface map of channel levee complex in the Middle Indus Fan (Block S3, refer Fig 2 for location) showing three channels numbered 1 to 3. Vertical exaggeration (VE) is 12x. Channel 3 does not show surface impressions in the middle segment denoted by white dashed line. (B) 2D surface map of channel levee complex in the Middle Indus Fan showing location of cross-sections P1 to P7. Note distinction between incisional channel 1 without bounding levees and aggradational channels 2 and 3 with bounding levees. The positive relief feature is the Laxmi Ridge. [CT: channel thalweg; CW: channel width; BL: Bounding levees; ML: meander loop] (Figure from Prerna and Kotha, 2020) .....	<b>96</b>
<b>Fig 4.18</b>	Channel network in the Indus Fan with canyon complexes 1-3 (youngest to oldest, modified from McHargue and Webb, 1986; Amir et al., 1996). Blue lines represent channels identified from study Blocks [S1, S2, S3] and reference Blocks [R1, R2, R3] modified from Kenyon et al. (1995), Kodagali and Jauhari (1999) and Bourget et al. (2013) respectively. Fan boundaries are modified from	

	Kolla and Coumes (1987), black dashed lines indicate probable channel network and orange circle represents the location of Site U1456 in Laxmi Basin. (Figure from Prerna and Kotha, 2020).....	97
<b>Fig 4.19</b>	Geomorphometric comparison of Upper Indus Basin [UIB] and Upper Indus Fan [UIF]. (A) Longitudinal profile of UIB; (A1) Channel-width profile of UIB; (A2) Sinuosity profile of UIB; (A3) Slope gradient (in percentage rise) of UIB; (B) Longitudinal profile of UIF;(B1) Channel-width profile of UIF, data extent marked on B; (B2) Sinuosity profile of UIF; (B3) Slope gradient represented (in percentage rise) of UIF. Dotted lines represent data gap .....	102
<b>Fig 4.20</b>	Representative channel cross-section from (A) Upper Indus Basin; (B) Upper Indus Fan (canyon); and (C) Upper Indus Fan (channel levee). [CT: Channel thalweg; Z: Depth] .....	104
<b>Fig 4.21</b>	Geomorphometric comparison of Middle Indus Basin [MIB] and Middle Indus Fan [MIF] (A) Longitudinal profile of MIB; (A1) Channel-width profile of MIB; (A2) Sinuosity profile of MIB; (A3) Slope gradient (in percentage rise) of MIB; (B) Longitudinal profile of MIF; (B1) Channel-width profile of MIF, data extent marked on B; (B2) Sinuosity profile of MIF; (B3) Slope gradient (in percentage rise) of MIF. Dotted lines represent data gap. All profiles superimposed on longitudinal profile A and B .....	107
<b>Fig 4.22</b>	Representative planforms from Upper, Middle, Lower Indus Basin and Upper, Middle, Lower Indus Fan. [Data source: (A-C) ESRI™ World Imagery (WGS84); (D) Clift and Henstock, (2015); (E) NCPOR (n.d.); (F) Ward (2007)]	109
<b>Fig 5.1</b>	Combined longitudinal profile with Upper, Middle, Lower boundaries of the fluvial Indus Basin and the submarine Indus Fan. Dominant planform type, channel width, sinuosity and channel gradient through each zone of the Indus Basin and Indus Fan denote the transformation of a land-to-deep sea system (Figure from Prerna and Kotha, 2020).....	116
<b>Fig 5.2</b>	Dominant planforms and representative cross-section from the Indus River (A1 to A6) and the Indus Fan channels (B1 to B6). Blue polygons on every cross-section denote channel width. [Data source: Indus Basin (Block F1); Upper Indus Canyon (Block S1); Upper Indus Fan (Block S2); Middle Indus Fan (Block S3); Lower Indus Fan (Ward, 2007)] (Figure from Prerna and Kotha, 2020).....	117
<b>Fig 5.3</b>	Schematic comparison of a typical (A) multi-point source system and (B) single-point source system .....	120

## LIST OF TABLES

<b>Table 1.1</b>	Summarized similarities/dissimilarities between fluvial and submarine systems .....	<b>20</b>
<b>Table 3.1</b>	Datasets used for morphometric analysis (Source – Prerna and Kotha, 2020) .....	<b>37</b>
<b>Table 4.1</b>	Interpretations of HI/E values (Source – Prerna et al., 2018) .....	<b>79</b>
<b>Table 4.2</b>	Stages of development within the Indus Basin based on Hypsometric Curve (Source – Prerna et al., 2018) .....	<b>81</b>
<b>Table 5.1</b>	Summarized observations on comparison of fluvial and submarine channels (Source – Prerna and Kotha, 2020) .....	<b>118</b>

## THESIS STRUCTURE

### **Chapter 1: Introduction**

Chapter includes the basic tenets of the research, beginning with a preface to fluvial rivers and submarine channels—their formation and processes, followed by a detailed background of the fluvial-submarine morphometry debate. With the scientific rationale, aims and objectives are discussed, followed by a brief description of the methodology and results.

### **Chapter 2: Physiographic and geological setting**

A description of significant physiographic features and geotectonic units that influence the fluvial basin, submarine fan and associated features is detailed in this chapter.

### **Chapter 3: Data and Methods**

A thorough description of the techniques adopted in the study is detailed in the third chapter of the thesis, presented in two parts owing to the two different data types used.

### **Chapter 4: Data analysis and interpretation**

This chapter is divided sequentially to unfold the basic objectives given in Chapter 1 with each sub head giving a description of a component of the study. All components are first explained and then amalgamated to load the interpretation and results. Discussion of every geomorphometric parameter entails further to facilitate a one-to-one comparison between fluvial rivers and submarine channels.

### **Chapter 5: Discussion and conclusion**

Summarized observations from the research indicating nonconformity between the morphometric patterns observed in fluvial and submarine channel systems forms the final chapter of the thesis. A section discussing the causative factors to help explain the variance is also provided before the concluding remarks.

## GLOSSARY

<b>Term</b>	<b>Definition</b>
Channel levee complex	: A collection of smaller order channel levee systems, fed by a common source e.g. a submarine canyon (Deptuck et al., 2003).
Channel levee system	: A single channel belt with associated levees (Deptuck et al., 2003).
Channel width	: Calculated as a straight line distance from channel axis to either bank.
Digital Elevation Model (DEM)	: A gridded digital representation of terrain, with each pixel value corresponding to a height above a datum (Hawker, et al., 2018).
Elevation-relief ratio (E)	: An indicator of the proportion of remnant rock in a given basin. Calculated as mean elevation minus minimum relief divided by relief (Pike and Wilson, 1971).
Fluvial system	: Pertaining to a river and its basin, their processes and resulting features.
Geomorphometry	: A science of quantitative topographic analysis with focus on the extraction of land-surface parameters from elevation data (Pike, 1995).
Levees	: Fine-grained sedimentary deposits formed on the channel flanks as a result of overspill.
Longitudinal profile	: A graphical representation of change in gradient with increasing length.
Multibeam Echosounder (MBES)	: A type of sonar (sound navigation ranging) used to map the seabed.

<b>Term</b>	<b>Definition</b>
Morphometry	: A quantitative measure of size and shape, often used to evaluate the form of any geographical feature.
Multi-point source system	: A cumulative system where tributaries contribute towards a higher order stream/river.
Planform	: An aerial/plane view of a feature's form.
Sinuosity	: A measure of deviation of a channel from its central path along its course (Prerna et al., 2018).
Single-point source system	: A distributary system with one, and only one, source of flow.
Sinuosity index (SI)	: A ratio of the curvilinear distance (channel length) to the shortest-path distance (valley length) (Brice, 1974).
Submarine canyon	: An incision on the shelf formed as a result of sediment scouring by turbidity currents, directly or indirectly linked to a terrigenous sediment source e.g. a river.
Submarine fan	: An accumulation of sediment deposited by the action of turbidity currents, funnelled by canyons at the land-sea termini (Menard, 1955).
Submarine system	: Pertaining to submarine channels and its fan, their processes and resulting features.
Turbidity currents or sediment-gravity flows	: Sediment laden currents flowing under the influence of gravity creating turbidite deposits on the seafloor.
Thalweg	: The locus of lowest bed elevation or maximum flow depth within a watercourse (Dey, 2014).

**CHAPTER 1**  
**INTRODUCTION**

# CHAPTER 1

## INTRODUCTION

### 1.1. Preface

Rivers are formed when headwaters flowing downstream gradually gain momentum and converge under the influence of gravity. These headwaters that mostly generate from melt water or springs/lakes enhance their erosive capability while gaining stream velocity. The process results in the genesis of an expansive stream network with one major channel called as river, and other lesser order streams as tributaries. Rivers function as conduits that carry sediments eroded from interior landmasses and transport them downstream until the river mouth. The entire region drained by a river and its tributaries towards an outlet is termed as a river basin.

When the sediment-saturated rivers drain into the sea, turbidity currents or sediment-gravity flows are often initiated. Turbidity currents are sediment laden currents flowing under the influence of gravity creating turbidite deposits on the seafloor. If the right conditions prevail, these currents, usually denser than the ambient flow, could incise the seafloor, and deposit coarser sediments at the bottom while forming fine-grained sediment deposits called levees on the channel flanks. As a product of coeval erosion and deposition on the seafloor, an accumulation with incised channels is created, widely referred to as a channel levee complex. Based on collective research on various channel-fan systems, Deptuck et al. (2003) simplify the definition of a channel levee complex as a series of stacked channel levee systems fed by the same canyon.

The land-sea terminus, therefore, can be recognized as a juncture where a fluvial river may transform into a submarine channel levee complex(s) and continue to develop on the abyssal plains of the ocean floor up till the point where sediment flux is present and

erosion/deposition is active. The entire accumulation of sedimentary deposition thus created is termed as a submarine fan. Menard (1955) in one of the earliest accounts on modern submarine fans, defined a submarine fan as an accumulation of sediment deposited by the action of turbidity currents, funnelled by canyons at the land-sea termini. Theorised to be conical, modern fans vary from elongate, lobate to trapezoidal and other complex shapes (Shanmugam and Muiola, 1988). These fans can be considered as the submarine analogy of river basins that we see on land. Both terms define the encompassment of drainage by fluvial rivers and channels, in the subaerial and submarine environment.

Factors like sedimentary composition, shelf/slope morphology, tectonic effects and more importantly, eustatic changes are major controls behind submarine channel complex formation (Stow et al., 1985). In the Indus system, specifically, the direct association of sediment supply to canyon head is known to have been largely controlled by eustatic changes (Kolla and Coumes, 1987; Shanmugam and Muiola, 1988; Prins et al., 2000, Clift et al., 2014). Fig 1.1 is a simplified schematic representation of the fluvial river basin and the submarine fan system, also depicting direct and indirect association of the canyon head with the fluvial system during low and high sea-stands, respectively.

It would not be inaccurate to say that submarine fans and channel levee complexes are products of terrestrial drainage. Due to the inherent nature of fluids to erode, deposit and transport, fluvial and submarine systems are often considered to be alike. Much as the rivers on land, submarine channels on seafloor could also be erosive, with the ability to create depositional features and be conduits for sediment transport. Simply put, deep sea channels are the spatial extensions of subaerial rivers; and submarine fans are detrital accumulations of terrigenous sediment brought down by rivers of fluvial drainage basins.

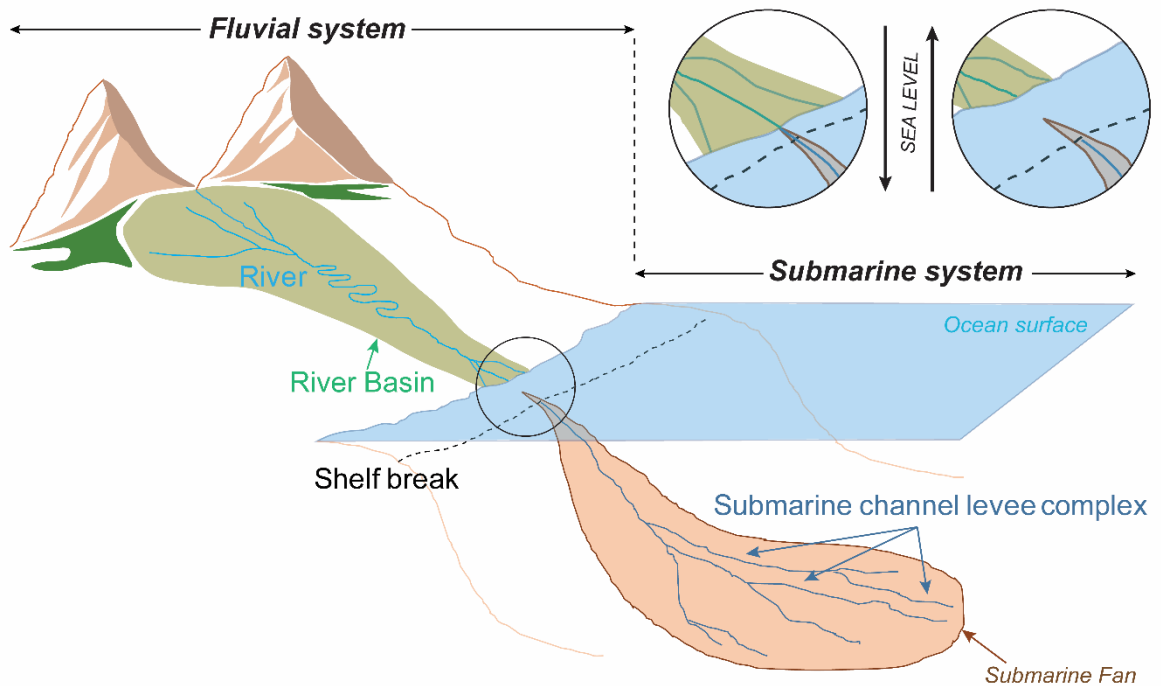


*Fig 1.1: Graphical representation drawn to show a typical fluvial and submarine system with associated features depicting direct and indirect association of the canyon head with the fluvial system with sea level change. (Figure from Prerna and Kotha, 2020)*

This study aims to assess the variations in the two systems by examining the morphometry of the fluvial rivers on land and the submarine channels on the seafloor. Morphometry—a quantitative measure of size and shape, is often used to evaluate the form of any geographical feature and geomorphometry is the science of quantitative topographic analysis with focus on the extraction of land-surface parameters from elevation data (Pike, 1995). Its application covers a range of disciplines like earth sciences, environmental engineering, oceanography etc. that aim to capture land-surface parameters like slope, aspect, curvature, stream power and many other morphometric variables from topographic data (Florinsky, 2017). For effective comparison of these features and their morphometric trends, data has been taken from a single river system i.e. the Indus Basin and the Indus Fan. The following sections introduce the submarine systems and their scientific impact—elucidating the need to monitor these marvellous systems by means of morphometric estimation.

## **1.2. Submarine fan systems: an overview**

Submarine canyons and their associated channel levee complexes have fascinated researchers ever since they were first identified. Identification of submarine canyons and the subsequent channel systems through echo-sounding as well as manual surveys began as early as the 1900s (Spencer, 1903; Hull, 1912; Shepard, 1934; Veatch and Smith, 1939). Later works by Shepard et al. (1969), Nomark (1970), Mutti and Ricci Lucchi (1978) and others on submarine canyons and channel systems are also noteworthy, efficiently summarized as historical accounts of submarine fan systems by Mulder (2011) and Shanmugam (2016). But more recently, since the 1980s, major discoveries of hydrocarbons from turbidite systems along with the invention of sophisticated geophysical tools like side-scan sonars, swath bathymetry mapping systems, multi-channel seismic profiling and 3D seismics have escalated the studies on submarine channel levee complexes (Amir et al., 1996, Kolla et al., 2001). Over the last few decades, submarine systems have been studied from different angles. Extensive literature is available on their morphology—shape/size/volume; geology—provenance/stratigraphy; sediment transport—kinematics of sediment flows/velocities; evolution—upper to lower fan/ancient to modern fans, formation—tectonics/eustatic effects/discharge rates; along with physical observations—geochemistry/geophysical data acquisition etc., covering various aspects of the canyon-channel complexes.

### *1.2.1. Scientific significance*

Understanding the submarine fan systems plays a manifold role in expanding our knowledge of the marine environs. The close association of the fluvial-submarine transformation and their intrinsic components are crucial in understanding the system holistically. Nature of the sediments, episodic/catastrophic flow, eustatic effects, shelf-slope topography and many other factors interplay towards the formation of submarine fans. Even within the submarine system,

the characteristics of canyons, channel levee systems, gullies, lobes etc. must be understood to closely ascertain the processes involved in their development.

Presence of proximal canyons are known to influence deltaic development, for instance, in the Indus system, the incised Indus Canyon presumably hindered the formation of the deltaic front as the sediments got funnelled offshore (Giosan et al., 2006 and references therein). The distributary network of the channel levee complex must be known in order to effectively predict flow paths of sediments during instances of accelerated flux. Slope failures, landslides, mass deposits and gullying are increasingly gaining the attention of researchers due to their role in hazard studies (Mountjoy and Micallef, 2018; Deptuck and Sylvester, 2018). Recent scientific drilling in the offshore Indus fan (Pandey et al., 2016) identified one of the most extensive mass-transport deposits on Earth's passive margins (Dailey et al., 2019). Named as the Nataraja Slide (Calvès et al., 2015), it is a giant region extending from Gujarat-Saurashtra margin offshore western India till the Laxmi Ridge in Eastern Arabian Sea. Evidence of tsunamis—triggered by earthquakes caused by massive submarine landslides have been reported from several parts of the globe. The potential of these catastrophic events to cause havoc on offshore facilities is steadily being realised. Williams (2016) reported numerous incidents from Alaska, Venezuela and the Mississippi Delta, highlighting the need to understand and model these events. The Tohoku Tsunami in 2011 was also partly attributed to a submarine landslide (Tappin et al., 2014). Submarine pipelines and communication cables bypassing seafloors and offshore platforms are often disrupted by transient turbidity flows/submarine landslides (Bea et al., 1983; Piper et al., 1988; Hsu et al., 2008). In order to assess the susceptibility against disturbances and mitigate any damage caused by sediment flows, knowledge of channel systems and their pathways, and the architecture, structure and evolution of submarine canyon-channel complexes is vital.

Submarine fans are also excellent preservers of sedimentary archives—crucial for high-resolution paleo-climate reconstruction studies, making them valuable indicators of past environmental conditions. Covault (2011) stated that the turbidite deposits collected in submarine fans contain valuable information for assessing past climatic signals by way of onshore weathering, erosional and depositional processes. The offshore depositional history is also an important indicator of global/regional/local eustatic changes and tectonic activity (Bastia and Radhakrishna, 2012). Speaking of the study area of this research, the Indus system is the product of Himalayan orogeny (Molnar and Tapponnier, 1977; Amir et al., 1996) and is, therefore, a natural laboratory for decoding the chronology of events shaping the Himalayas. The Indus Fan records the erosion patterns of the western Himalayas and Karakoram since India began to collide with Asia during the Eocene at ~50 Ma (Clift et al., 2002). Weathering and erosional record of the Himalayan orogeny and its long term links with the regional climate are relatively well preserved in the Indus Fan sediments (Clift et al., 2001). This is attributable to the sedimentary drainage brought down by channel systems, providing long-term reliable paleoclimate proxies for reconstruction models. International Ocean Discovery Program (IODP) and its predecessor – Deep Sea Drilling Project (DSDP) have orchestrated several drilling operations across the globe including the Indus Fan since 1970s. Over the last decade, a growing understanding of the tectonic-climatic linkage has come into shape by dating sediment cores derived from the Indus Fan. More recently in 2015, IODP Expedition 355 retrieved deep-sea cores from the Laxmi Basin, Arabian Sea to document the coevolution of mountain building, weathering, erosion, and climate over a range of timescales with basement rock samples to unravel the tectonic setting of the western continental margin of India (Pandey et al., 2016). Intensification of the Indian summer monsoon, episodic exhumation of the Himalayas and its tectonic uplift, plus the overall impact on the sediment flux of the Indus has been studied time and again to better constrain the tectonic-climate linkages (Tada et al., 2016;

Clift, 2017, Kumar et al., 2019). Fig 1.2 gives the distribution of the major submarine fan systems of the world.

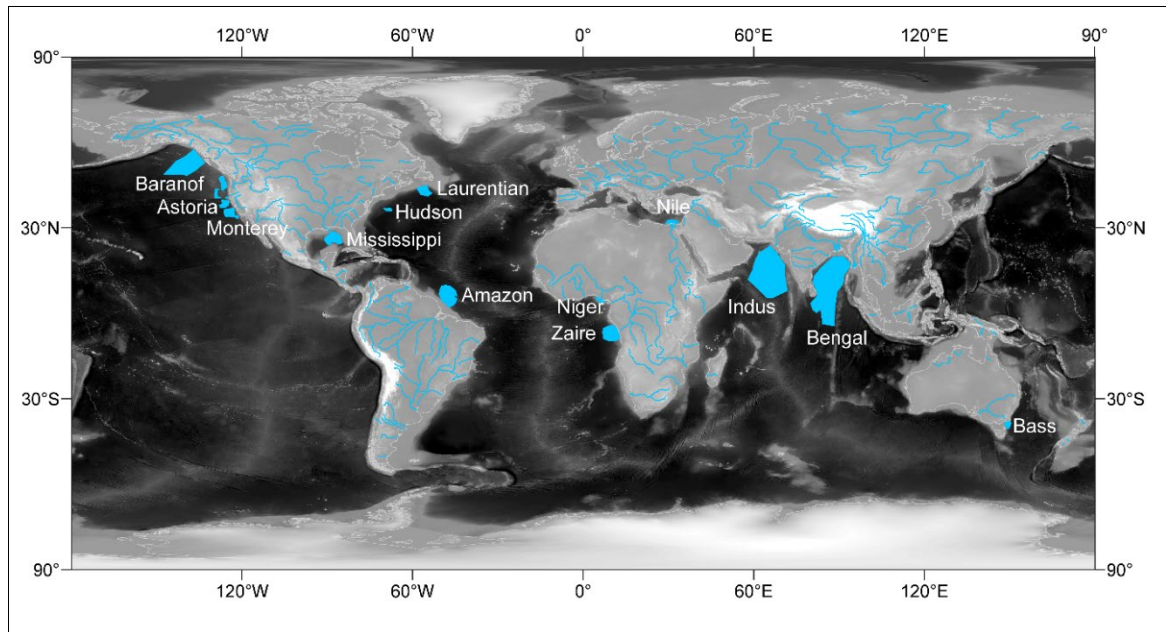


Fig 1.2: World distribution of major submarine fan systems like Bengal, Indus, Amazon, Mississippi, Zaire, Niger, Baranof present on both active and passive continental margins.

Coming to their economic value, the submarine fan systems with their associated turbidite channel conduit networks are increasingly gaining popularity as potential hydrocarbon reservoirs (Bouma et al., 1985a; Shanmugam and Moiola, 1988; Amir et al., 1996; Kolla et al., 2001; Pettingill and Weimer, 2002; Lomas and Joseph, 2004; Babonneau et al., 2010; Covault, 2011; Covault et al., 2012). Hydrocarbon potential of reservoirs like the Monterey Fan, Los Angeles Basin off California in the Pacific Ocean, Cellino Formation in Central Italy, Balder Fan in North Sea (Shanmugam and Moiola, 1988), offshore West Nile Delta (Cross et al., 2009) and many more are being extensively studied for accurate prediction of their occurrence. Other major concentration zones exist in the Gulf of Mexico, Brazil and West Africa (Pettingill and Weimer, 2002). Vittori et al. (2000) while studying the Quaternary

Congo deep sea fan identified that the main reservoirs are the sandy turbidite and related mass-flow deposits located in ancient meandering channel complexes. Sand-rich characteristic formation (as seen mostly in active margin settings) are found to have great potential, however, fans developed on passive margins such as the Indus also have increasing potential down fan as their composition transforms from mud-rich to sand-rich sediments (Shanmugam and Moiola, 1988). McHargue and Webb (1986) while zoning the Indus Canyon suggested that the cessation of high-amplitude discontinuous facies at the proximal mouth was indicative of reservoir quality sandstone. Preliminary studies based on geophysical and well data had confirmed reservoir potential in the offshore extent (Quadri and Shuaib, 1986; Shah, 1997). Research continues to determine the reservoir potential of the Indus Fan sediments and assess the challenges for commercial discovery (Carmichael et al., 2009). Pettingill and Weimer (2002) opined that at present, given the economic limitations of resource exploration from submarine fans/turbidite systems, their potential is not fully developed but could turn into a major focus in the future. This emphasises the fact that hydrocarbon exploration of the turbidite systems requires a thorough knowledge about the channel systems, their genesis, extent, architecture and sediment transport. Sand-rich systems may act as reservoirs but are highly risky to drill as compared to fine and porous sediments. For proper risk assessment and to counteract the limitations faced today, in-depth studies about every aspect of these vital sedimentary systems is essential.

Turbidites deposited as levees are also important components of the fan system. Bastia and Radhakrishna (2012) reported a summary of three-decade long extensive research of turbidite systems of some of the largest fans in the world, highlighting the significance of studying their architectural, transportational and depositional behaviour for evaluating hydrocarbon development potential.

Projects have also been pursued to understand the sedimentary structure and transportation processes of submarine channel systems in order to formulate precise models for reservoir identification (Babonneau et al., 2002). Miall (2002) while recording the architecture of the fluvial systems of the Malay Basin observed wide variations in channel styles with the uniform fluvial styles and warned against making simplistic assumptions during architectural/reservoir modelling and paleo-hydraulic reconstruction. Crude analogies could pose severe ramifications on modelling outputs, and therefore, accurate parameters of channel style and morphology become a precondition for any reservoir modelling. To do that effectively, a thorough understanding of the different processes involved and resulting features must first be undertaken. Kolla et al. (2012) considered comparative studies between fluvial and submarine deep-water sinuous channel systems as one of the key approaches to understand the distribution, architecture and potential of submarine reservoirs.

Conclusively, submarine fans and their associated features have a lot to offer in terms of understanding the seafloor morphology, sediment transport, mass balance, records for paleo-tectono-climatic studies, eustatic fluctuations, or hydrocarbon potential. With growing realisation of their significance, more and more work can be expected from every submarine fan system in the coming years, and studies such as this are effective contributors.

### *1.2.2. Controlling factors*

Other than the sedimentary flux coming from onshore fluvial rivers, factors like sedimentary composition (sand-rich/mud-rich), tectonic effects (passive/active margin), morphology (width, gradient of shelf/slope) and eustatic changes also control the formation of submarine channel systems (Stow et al., 1985). Fluvial systems that culminate into sediment saturated flows at the land-sea terminus usually extend to form submarine channel levee complexes if the aforementioned factors interplay favourably. Sedimentary transport flows initiate from the

shelfal regions and further to submarine fans when sediment accommodation is breached at the shelf. The concept of accommodation (Jervey, 1988) refers to the cumulative space created for the accumulating sediments, either by tectonic or eustatic movements. The direct association of fluvial sediments and canyon heads get disrupted during highstands as deposition shifts landward, while during lowstands, there is emergence of direct association (Shanmugam and Muiola, 1988) leading to accommodation towards the deep sea fans. Based on sediment core analysis from the Upper and Middle Indus Fan, Prins et al. (2000) established that increased sediment supply during low sea-levels were attributed to accentuated erosion of the Indus Canyon and/or direct drainage of Indus River into the Canyon, followed by a major reduction in sediment supply and starvation of the fan during high sea-levels. Hence the interaction of sediment supply and accommodation is a key governing factor behind the formation and development of submarine fan and channel levee systems.

It must also be noted that not all submarine complexes are dependent on fluvial systems for sediment flux. Mass slumping, landslides on steep shelves, heavy storm surges etc. could also be triggering factors for sediment-gravity flows, (Shanmugam and Muiola, 1988) however, they are not as significant as channelized turbidity currents carrying terrigenous sediment supply. Acoustic characterization of sediment layers in the Indus Fan also revealed evidences of slumping along the Indian margin (Naini and Kolla, 1982).

In the present study, focus is on turbidite flows generated by a single-point source such as a canyon-fed system, seen in submarine fans like Bengal Fan, Indus Fan, Amazon Fan, Zaire Fan (former Congo), Niger Fan, Mississippi Fan etc. These are the most common instances for submarine channel levee complex formation. Mostly all large canyons are seen as incisions, and further as shelf valleys on continental shelves, maintaining a direct link with fluvial drainage systems (Harris, 2012). Such canyon-fed systems function on a distributary flow pattern where the turbidity influx is spread across the fan through multiple conduits or channels

of the fan system. Fluvial rivers, on the other hand, operate in a multi-point source system, where tributaries connect to the main stream, supplement the overall flow velocity of the river and increase its erosive capability as it progresses downstream.

### *1.2.3. Submarine-fluvial analogy*

Given the hugely disparate conditions of subaerial and submarine environs, it seems almost natural that the functioning of their system and the morphology of their features would also differ. But on the contrary, ever since submarine channels were identified, the visual similarities in sinuosity, architecture, planform etc. have encouraged researchers to consider them analogous. Especially, when it comes to morphology, fluvial rivers and submarine channels may appear quite similar. At first glance, given the sinuous planform, presence of ox-bows or scroll bars, formations of levees etc., fluvial rivers and submarine channels look almost like. Their stark resemblance has lent credence to the long-standing analogy between fluvial and submarine systems. Some of the most frequently discussed points of commonality are— channel evolution and morphology; planform; internal geometry; architectural elements; sinuosity; depositional features; drainage pattern etc. Fig 1.3 shows visual similarity between a segment of Indus Fan's submarine channel and the subaerial Indus River. The close resemblance of sinuous planform and presence of ox-bows in both environments make them apparently similar.

Conversely, there is an equally potent view that considers them as non-analogous or different. Variations in the very same parameters of sinuosity, planform etc. and their trends in formation have been found to differ significantly between fluvial and submarine river/channel systems. Density contrasts among ambient flows; hydrodynamic characteristics; different role of lateral and vertical component of aggradation; migration; rate of meander/levee development; effect of centrifugal/coriolis forces; relation between slope gradient and

sinuosity; base level controls; stratigraphic records etc. broadly indicate a contrast in fluvial and submarine channels.

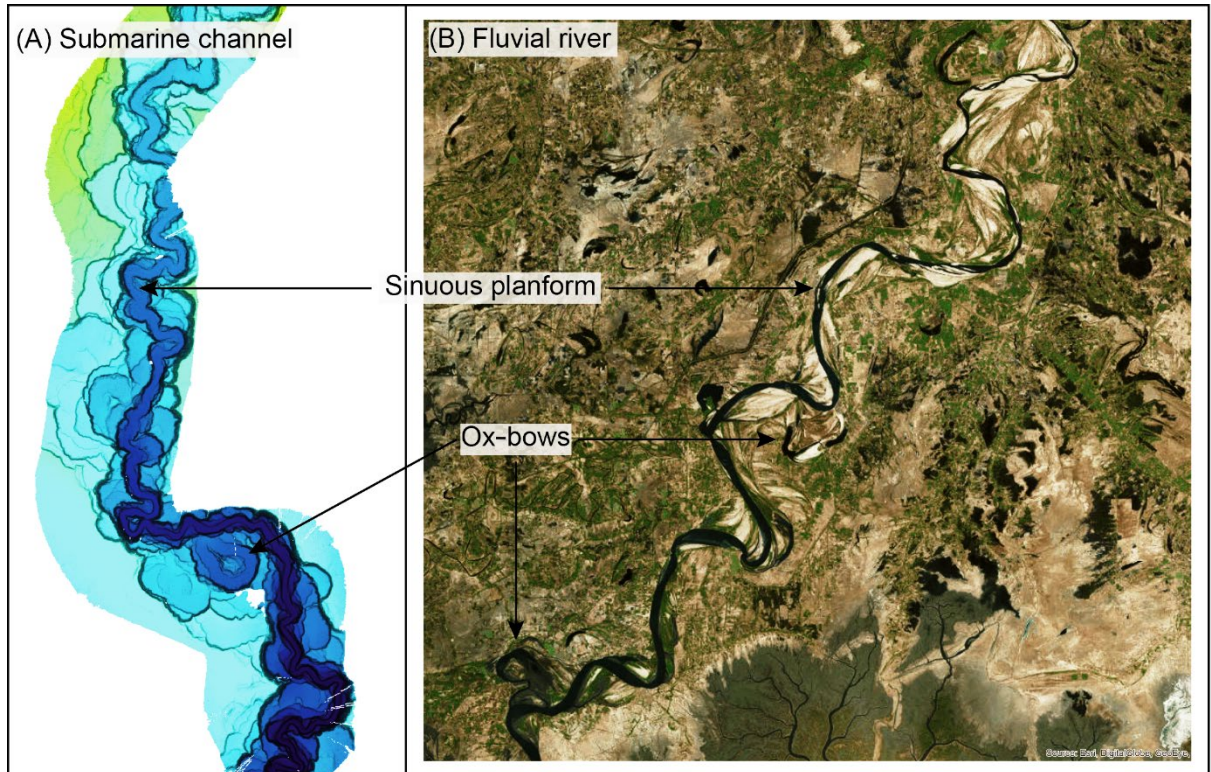


*Fig 1.3: Planform of (A) submarine channel from the Indus Canyon and (B) subaerial fluvial Indus River showing remarkable planform similarities. [Data source: (A) Clift and Henstock, 2015; (B) ESRI<sup>TM</sup> World Imagery (WGS84)].*

What concerns the present study is specific to the morphology of submarine channel complexes and their long standing analogy with land based fluvial systems, because in spite of the extant literature discussing their comparison, a concrete and substantive conclusion based on empirical analysis is absent.

### 1.3. Rationale

The fluvial-submarine comparison is not a new concept in geomorphic research. Data from offshore submarine fans has been compared with fluvial systems on land, both on a global and regional extent. Some of the most noteworthy studies and their outcomes are discussed briefly here. Clark et al. (1992) summarized data from 16 submarine fan channels and compared them with fluvial/flume data (Leopold and Wolman, 1960; Schumm and Khan, 1972) to conclude that the geometries of sinuous submarine channels are comparable to fluvial channels as a consequence of analogous physical processes functioning in both systems. Kolla et al. (2001) very efficiently summarized similarities and differences observed in fluvial and submarine systems with respect to channel morphology, evolution and processes using 3D seismic data from the submarine Congo Fan, however, evidences from fluvial systems were taken from other studies (Flood and Damuth, 1987; Clark et al., 1992, Imran et al., 1999; Peakall et al., 2000 etc.). Later, Kolla et al. (2007) presented a comparative paper stressing on the dissimilarities, this time supported with 3D seismic fluvial channel data from *offshore* Indonesia, with submarine channel data from different fans of the world. In another interesting comparative study, Konsoer et al. (2013) presented a comparative inventory of 177 submarine channel cross-sections and 216 river cross-sections to substantiate observed differences in channel geometry, evolution and discharge. Jobe et al. (2016) compared 297 submarine and fluvial channel belts from numerous systems across the globe to conclude that channel trajectory is the primary control on stratigraphic architecture and that apparently similar channel forms can create clearly different stratigraphy. Numerous flume-based/laboratory experiments and numerical simulations have also aimed at comparing fluvial and submarine channel behaviour (Imran et al., 1999; Corney et al., 2006; Keevil et al., 2006, 2007; Kane et al. 2008, Lajeunesse et al., 2010; Darby and Peakall, 2012; Foreman et al., 2015).

These studies form a few examples of comparative accounts between fluvial and submarine channel structures, albeit, only a few are substantiated with ground-truth data from actual submarine fans and river basins. Others are based on theoretical or laboratory-experiments that replicate submarine processes in an attempt to correlate with fluvial systems. A thorough morphometric study offering a one-to-one comparison of fluvial river and channel morphology *within the same system*, with exhaustive data from onshore as well as offshore basins is by far rare.

The lacuna to be filled through this study is to confirm the variance between fluvial rivers and submarine channels. As observed from in-situ data observations, their likeness has stirred researchers to think that they must also function in a manner similar to subaerial rivers creating similar forms as seen on land, but there are also those who recorded disparity. To better explain the current status of similarities and dissimilarities from extant literature is discussed below:

#### *1.3.1. What are the similarities?*

- (i) Sinuous/meandering flow pattern observable in fluvial and submarine systems is the most commonly discussed similarity. Brice (1974), McGregor et al. (1982), Pickering et al. (1986), Flood and Damuth (1987) found the two systems similar in terms of sinuosity, meandering flow and also noticed common morphological features. Kolla et al. (2007) described sinuosity as a common process occurring in both systems wherein the alluvial plains/seafloor interact with the sediments and gradually attain equilibrium.
- (ii) The mechanism and evolution of channel form is also found to be identical as per some studies. Stelting et al. (1985) opined that similar sediment transport mechanisms active in both systems result in similar channel geometries. Detailed characterization of channel morphology and migration geometry by Babonneau et al. (2010) showed that

the evolution of the submarine channel path is very similar to fluvial meandering systems considering lateral meander growth; downward thalweg translation; and meander cutoffs.

- (iii) Presence of similar looking depositional features like point-bars, scroll-bars, channel levees and flood bank deposits etc., produce matching planform characteristics and similarities in erosional/depositional behaviour (McHargue, 1991; Clark et al., 1992; Amir et al., 1996; Kolla et al., 2001; Abreu, 2003; Posamentier, 2003). Babonneau et al., (2010) believed that the similar looking fluvial and sigmoidal shaped turbidite point-bars were indicative of similarity between the basal part of the turbidity currents within the channel and the fluvial river flow.
- (iv) Dimension of fluvial rivers and submarine channels are often considered approximate and therefore imply analogy. Damuth and Flood (1985) looked into meander wavelength, amplitude, frequency, channel and levee dimensions of the Middle Amazon Fan channels and found them to be equal to larger than the lower Mississippi River on land.
- (v) Dendritic pattern of channel flow that is typical of fluvial systems has been observed in submarine morphologies too (Kenyon et al., 1978; McGregor et al., 1982; Taylor and Smoot, 1984; Foreman et al., 2006; Antobreh and Krastel, 2006; Metz et al., 2009).
- (vi) Avulsion—a relatively sudden displacement or switching of the channel from one part of the valley to another by development of new course, forcing the river's stability to cross its threshold (Jones and Schumm, 1999) occur in both fluvial and submarine systems. Also, the concept of achieving base level equilibrium exists in both (Pirmez and Flood, 1995, Kolla et al., 2001).

### 1.3.2. *What are the dissimilarities?*

- (i) Running water is responsible for shaping the morphology of fluvial river systems, while in the submarine extent, density flows are the erosive agents (McGregor et al., 1982). Also, the density of turbidity/sediment-gravity flows and river flows are phenomenally disparate. Turbidity currents are sediment suspension driven in a subaqueous environment, whereas fluvial currents are fluid driven in a subaerial environment (Middleton, 1993). They are the principal causative factor behind major differences in the internal architecture and modes of evolution of fluvial and submarine environments (Kolla et al., 2007). Also, density contrasts between these flows and ambient fluids is a key differentiator. In sediment-gravity currents, flow occurs due to the relatively small difference in unit weight between the gravity fluid and the ambient fluid. The flow of rivers, on the other hand, are seldom considered as gravity currents due to the large difference in unit weight of water and that of air (Middleton, 1993). The compositional difference of the two agents greatly influences the erosive or depositional capacities of rivers/channels. Much greater superelevation of channel flow around bends in submarine systems than in fluvial rivers is also found to be attributable to flow density contrasts (Imran et al., 1999).
- (ii) The velocity profile of turbidity currents has implications on sinuosity in submarine channels (Deptuck and Sylvester, 2018) and are found to be far more complex than rivers (Peakall and Sumner, 2015) thereby, resulting in differential patterns of sinuosity and aggradation. Konsoer et al. (2013) suggested that the added friction between turbidity and ambient flows cause steeper channel gradients in submarine systems.
- (iii) Sinuosity is observed in both systems but the precise mode of sinuosity evolution may differ; in submarine systems high sinuosities generally develop through repeated channel aggradation and subsequent lateral migration and not by lateral migration alone

as observed in fluvial channels (Kolla et al., 2001). Also, in submarine systems, sinuosity usually reduces down fan due to reduced flow velocity but on land, it is normally the opposite.

- (iv) Channel width and depth progressively reduce downstream in submarine systems suggesting that the total volume or channelized turbidity current flow also decreases down fan. This is in contrast to subaerial rivers where tributaries converge with the main river adding more water and increasing the sediment discharge downstream (Flood and Damuth, 1987). After comparing hundreds of submarine channel and fluvial river cross-sections, Konsoer et al. (2013) concluded that submarine channels' cross-sectional dimensions often surpass the dimensions of the largest rivers on land by an order of magnitude; and that the slope of submarine channels can be up to two orders of magnitude greater than the slope of rivers even when the channel dimensions are similar.
- (v) The relationship between channel gradient and sinuosity may not be as simple in submarine systems as in fluvial and remains complex in turbidite environments (Babonneau et al., 2010). This is because in submarine systems, apart from the gradient and sinuosity, valley entrenchment also acts as a factor. Deeply incised or entrenched channel valleys, mostly in the canyon or upper fan region, hinder meander formation as compared to distal areas where valley slope is reduced and channel migration can occur freely (Babonneau et al., 2010).
- (vi) Formation of meanders and frequency of bend cut-offs also differ. Peakall et al. (2000) believed that the very small number of identifiable bend cut-offs in submarine channels as compared to fluvial channels with frequencies one to two orders of magnitude higher, to be a prominent dissimilarity.

- (vii) Rarity of braiding in submarine systems is a well discussed aspect in the fluvial-submarine debate. Wynn et al. (2007) attributed this to the lack of favourable conditions required for braiding and the shortage of well constrained data from truly sinuous channel systems. Experimental studies performed by Foreman et al. (2015) and Lai et al. (2017) demonstrate the inception of braiding in laboratory-based submarine conditions. However, despite the close resemblance created experimentally, they also believe that the thicker density flows with accentuated channel relief and high levee deposition rates observed in submarine systems inhibit the creation of wide and shallow channel formation which is essential for braiding. Also, gradient of submarine channels is by and large found to be far more than those of large meandering fluvial rivers (Flood and Damuth, 1987), which again obstructs braiding to occur.
- (viii) Dimension of levees seen on land and on the ocean floor differ greatly. Amir et al. (1996) pointed that the marine channel levees are typically greater in thickness than in fluvial rivers. As per Peakall et al. (2000), continuous overbank spilling in submarine channels causes large levees to be formed throughout as opposed to piecemeal levee build-up in fluvial rivers. Wynn et al. (2007) considered these hundred meters plus high aggradational levees as the most spectacular distinction in submarine and fluvial systems.
- (ix) Base level for a fluvial river is sea-level, but for submarine channels, it is ultimately the deepest point of the basin (Kolla, 2007). Base level in submarine systems are controlled by flow parameters, sediment grain size and the changing seafloor gradient making it a dynamic variable, which does not limit vertical aggradation as much as it does in fluvial systems (Kolla et al., 2007). This makes the submarine channels more unstable than fluvial rivers, and prone to avulsion as they seek shorter courses to their base level.

- (x) In submarine channel complexes, lateral migration and vertical aggradation could occur in a variety of forms i.e. either continuous, or discrete or in combinations, thereby resulting in different channel architectures (Kolla et al., 2007). Jobe et al. (2016) compared stratigraphy of fluvial and submarine channel and concluded that vertical aggradation is stronger in submarine systems with lateral accretion being more dominant in fluvial systems, and Kolla et al. (2001) stated that vertical channel aggradation is always combined with lateral migration in deep-water systems. Hence the functioning of erosive/depositional elements of channel morphology is not alike in the two systems.
- (xi) Other factors like effects of Coriolis and centrifugal forces, steady flows and catastrophic flows, vertical and horizontal density gradients are believed to have a diametric influence on shaping the geometry of fluvial and submarine channels (Imran et al., 1999; Kolla et al., 2001, 2007; Peakall and Sumner, 2015). Variation in helical flow behaviour, which profoundly impact the sediment transport processes, is also found to be reversed in submarine and fluvial channel flows (Corney et al., 2006; Keevil et al., 2006, 2007).

Table 1.1 summarizes the key points of similarities and dissimilarities. It is quite evident that the differences outplay the similarities observed between fluvial and submarine systems. However, in order to truly ascertain the extent of variance, the behaviour of river and channel morphology must be investigated. And to do that more effectively, the marine and fluvial response of a single system is examined—the Indus.

Table 1.1: Summarized similarities/dissimilarities between fluvial and submarine systems

Aspect	Similarities	Dissimilarities
Sinuosity	Gradient dependent and gradual sinuosity development in both systems	Channel sinuosity decreases downfan; High valley entrenchment in submarine systems hinders meandering
Channel development	Sediment transport mechanism is identical;  Lateral migration, thalweg deepening, meander cut-off observed in both systems	Density contrasts between fluvial running water and submarine turbidity currents, and with ambient medium result in variable channel development;  Result in different erosional/depositional behaviour
Depositional features	Point-bars/scroll bars, levees/flood plains etc. are present in both river basins and submarine fans	Much larger/thicker submarine levees are attributable to density contrasts;  Mostly continuous overbank spilling in submarine channels result in large levees as opposed to piecemeal built-up in fluvial rivers during flooding
Channel dimension	Meander wavelength, amplitude, levee size etc. found to be similar	Channel width, depth, sinuosity invariably increases in fluvial rivers and decreases in submarine channels
Planform	Similar planform with sinuous, braided or dendritic patterns observed	Planform transforms from simple (straight) to complex (sinuous/braided) in fluvial, and complex to simple in submarine
Avulsion	Observed in both systems	More active in submarine

The Indus Fan and its associated channel levee systems is one of the most complex and expansive submarine fan systems of the world, and with the presence of another proximal ancient canyon complex having its own recorded history of channel levee development, it gets

all the more intriguing. On land as well, the Indus River and its basin drain through a massive territory of the Indian subcontinent, creating unique morphometric forms as it flows through several tectonic units. A thorough analysis of this system could entail a wider picture of the entire source-to-sink system, which as described by Nyberg et al. (2018) is a system that includes surrounding catchments, alluvial and coastal plains, the continental shelf, slope the submarine fan.

Therefore, in this study, a morphometry-based comparison of the fluvial Indus River and its submarine counterpart—the Indus Fan channel system is presented using information from satellite-based elevation models and bathymetric data. This research work is a first-ever morphometric comparison with exhaustive data from onshore as well as offshore basins within the same system. But before attempting a systematic comparison, exhaustive data on the morphology of submarine channel levee systems and fluvial rivers is gathered and analysed.

#### **1.4. Research objectives**

Looking at the wide range of scientific opinions pertaining to the analogy discussed above, the outstanding question remains: are the fluvial rivers and submarine channels actually similar in function and form? Function here refers to the processes (erosional, depositional and evolutionary) and form refers to the morphometry (internal architecture, channel width, depth, cross-section dimension, planform, sinuosity etc.). The only triggering thought behind the study was that if function varies, form must also vary. It is important to state that the study began on a neutral note, unbiased between similarity or dissimilarity, but over the course of research the indices used to assess morphometry were found to be skewed toward dissimilarity. Hence, the aim transformed to highlight their dissimilarity backed with supporting evidences from morphometric indices using Digital Elevation Models (DEMs) and Multi-beam Echosounder (MBES) data. This study also attempts to explain causative factors behind the

variation and persuade the dilution of the analogy between fluvial rivers and submarine channels.

In order to achieve the aforementioned scientific aim, two research objectives are formulated:

1. To understand the architecture and evolution of the submarine Indus Fan and its associated channel system. This includes (a) mapping the existent channel structure using available data; (b) studying the variation of channel morphology from shelf to abyssal plains; (c) examining variations in the channel form through the various stages and processes of development.
2. To compare the morphology of Indus Fan and its submarine channels vis-à-vis Indus Basin and its river. This involves (a) identification of river flow pattern in the fluvial Indus Basin; (b) morphometric measurements across various stages of river development; (c) stage-wise comparison of submarine and fluvial channel behaviour with respect to each geomorphometric parameter.

As a complimentary objective of this research, a detailed morphometric account of the Indus River is obtained for the first time, from the source to mouth. The entire river and basin have been mapped along with its longitudinal and hypsometric profile, and parameters like channel width, sinuosity and slope gradient at regular intervals are estimated using DEMs. These data were a prerequisite for comparison with the Indus Fan submarine channel behaviour. Previous research on submarine channel behaviour in the Arabian Sea (Mishra et al., 2015, 2016; Prerna et al., 2015) provided an impetus to undertake this study. Literature review of past studies from the Indus as well as other fan systems built the grounds to detect the inherent variations between river/channel behaviour.

To accomplish the aforementioned objectives, two data types are employed in this research—DEM data for fluvial analysis and MBES data for submarine analysis. Hydrology

modelling tools using the Spatial Analyst and 3D Analyst Toolboxes of the ArcMap® software and its model builder are effectively utilised for extracting stream flow and basin boundaries from DEM data. For MBES data, manual digitization of channel width is adopted to ensure precision in calculation. Building profiles of channel width, sinuosity, slope gradient and cross-sections are performed using other various semi-automated tools of the ArcMap® software. Profiles of all geomorphometric parameters are built after exporting data points into MS Excel. 2D/3D plotting of the Indus Fan channel systems is done using Surfer® software.

Comparison of the fluvial and submarine system follows a two-way approach: (a) parametric and (b) stage-wise. Parametric refers to the comparison of the fluvial river with submarine channels based on the longitudinal profile, channel width, sinuosity, slope and planform. By stage-wise comparison, the variance in the stage of development between fluvial rivers and submarine channels has been assessed. The idea is to emphasize on the different processes that operate in each stage of river/channel development and shape the morphometry of these features, and also to quantify the dissimilarity in function and form through the different stages of development. Hence, every geomorphometric parameter calculated for the Indus River is compared with the same parameter for the Indus Fan channel levee complex, part by part i.e. upper basin with upper fan, middle basin with middle fan and lower basin with lower fan. Detailed description of data and methods is provided in Chapter 3.

It is envisaged that the methodology employed will be effective to ascertain the inherent diametric variations prevalent in the fluvial and submarine channel systems. From the discussion of similarities and dissimilarities presented earlier, it is well established that the fluvial and submarine environments and processes controlling them are disparate, and as a result, their morphometric imprints ought to vary as well. So far, the range of this difference has not been estimated from onshore and offshore data of a single river's basin/fan system, hence, a key deliverable from this study is the quantification of observed differences is.

Chapter 4 elucidates the results obtained from the morphometric comparison. Principal causative factors that could have led to the contrasting channel behaviour are also discussed in Chapter 5. The outcomes of this study could provide means to a greater end by including complex aspects of fluvial and submarine channel morphometry. A section on further scope states the need for including more research to understand complexities of channel planforms and evolution to augment the findings of this research and a build a more robust model for estimating channel behaviour of various submarine fans worldwide.

**CHAPTER 2**

**PHYSIOGRAPHIC AND GEOLOGICAL**

**SETTING**

## CHAPTER 2

### PHYSIOGRAPHIC AND GEOLOGIC SETTING

Two major river systems—the Ganges and the Indus came into existence on either sides of the Indian plate as a consequence of Indian-Eurasian Plate collision and the resulting tectonic upliftment-erosional cycle through the Himalayan and Tibetan orogenic belt (Molnar and Tapponnier, 1975). These major river systems perennially carried Himalayan detritus and created the Bengal and Indus Fans on the east and west respectively (Amir et al., 1996, Bastia and Radhakrishna, 2002). The Indus Fan is known to have been receiving orogenic detritus since the start of India-Eurasia collision around Middle Eocene, ~45 Ma (Clift et al., 2001), as has the Bengal Fan in the east (Emmel and Curray, 1985). Much of the sediment flux transported through the Indus into the Arabian Sea is attributed to the erosional load from the western Himalayas (Clift et al., 2001; 2002). The Indus River progresses through several major geological/tectonic units from its source to mouth—creating remarkable morphological signatures along its course.

The Indus Fan is relatively less studied than many of the major fan systems of the world, primarily due to paucity of high quality offshore data. Elementary geophysical surveys in the Indus Fan mostly spanned between 1970's to 1990's (Naini and Kolla, 1982; McHargue and Webb, 1986; Kenyon et al., 1987; Kolla and Coumes, 1987; von Rad and Tahir, 1997; Kodagali and Jauhari, 1999), with some additional surveys conducted more recently (Bourget et al., 2013; Clift and Henstock, 2015, Mishra et al., 2015). This study integrates all prevailing datasets to characterize channel behaviour from shelfal margins to the deeper Lower Indus Fan, with a parallel analysis of fluvial river attributes from the Indus Basin. The following sections detail the physiographic-geological setting of the fluvial and submarine components of the Indus system.

## **2.1. The fluvial Indus Basin**

The transboundary Indus Basin, spreading across Afghanistan, China, India and Pakistan, with an area of 1.16 million km<sup>2</sup> (Winston et al., 2013) forms the twelfth largest drainage basin in the world (Wohl, 2008). Together with major tributaries like the Satluj, Beas, Jhelum, Chenab, Ravi, Gilgit, Kabul, Kurram and others, the significance of this river and its basin, especially in the Asian subcontinent is paramount. With the addition of the paleo-Saraswati River draining subparallel to the Indus River, the entire drainage purportedly supported the Indus Valley (Harappan) civilization before 10 ka (Clift et al., 2012; Khonde et al., 2017). In present day, the Indus Basin is one of the most densely populated regions of the world, with its inhabitants directly or indirectly dependent on it. With annual available water resources estimated at 286.93 billion m<sup>3</sup>, and a population of 215.8 million dependant on it, the annual per capita water availability is 1329 m<sup>3</sup> (Babel and Wahid, 2008). The significance of international water sharing treaties, like the Indus Water Treaty (1960) is of profound importance in such geopolitical settings. India and Pakistan signed this treaty to facilitate a peaceful platform for optimum yet equitable usage of the river's waters for economic development etc. (FAO, 2011).

The river begins its journey in the Trans-Himalayan Tibetan region, cutting across the high relief Himalayan zone, into the Punjab plains and through the semi-arid/arid Lower Indus Basin. Along the Neotethyan Indus Suture Zone, it flows around the Nanga-Parbat syntaxis, through the tectonic blocks of the Karakoram and the Himalayan Arc, to the plains of Punjab before draining into the Arabian Sea (Garzanti et al., 2005; Inam et al., 2008; Clift, 2017). The Indus Basin, which spreads across multiple geotectonic units, is also bound by the Chaman Fault and the Karakoram Fault from the W-SW and N-NE respectively. Fig 2.1 is a physiographic/tectonic map of the Indus Basin and surrounding regions.

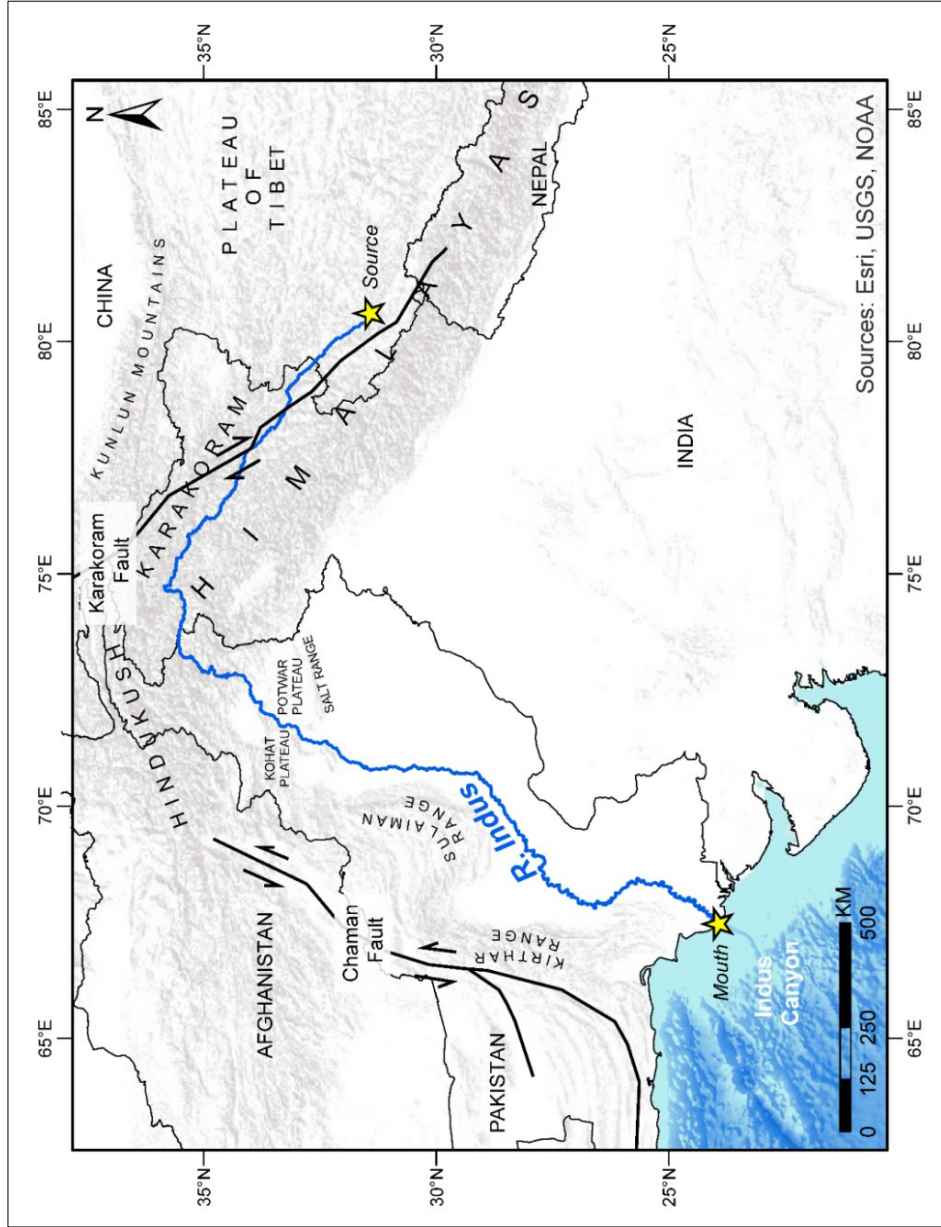


Fig 2.1: Physiographic/tectonic map of the Indus Basin modified from Yin (2006), Afzal et al. (2009), Chen and Khan (2010), Asim et al. (2014), Mukherjee (2015) and Prerna et al. (2018). Major faults like the Karakoram, Chaman; positive relief features like the Kohat and Potwar Plateaus having direct implications on the Indus River's geomorphometry are indicated, yellow stars denote the river's source and mouth.

Prerna et al. (2018) explain the demarcation of the Indus Basin based on the physiographic features and morphometric channel behaviour. The Upper Indus Basin, covering the high-relief section, extends from the source till the Tarbela Dam shortly after which it exits the Himalayan Arc. In the Middle Indus Basin, the Kohat Potwar fold belt and the Salt Range are the most significant geotectonic zones which significantly alter the planform of the Indus River (Kazmi and Jan, 1997). After the confluence of the river with its left bank tributaries, the Lower Indus Basin starts—traversed by several basement highs and thrust belts of Kirthar and Sulaiman Ranges (Clift, 2017).

### *2.1.1. Indus River*

The Indus River flows for a total length of 3329 km sourcing from the Gangdise Shan Range on the Tibetan Plateau till its delta (Prerna et al., 2018). The annual estimated water discharge of the Indus River is 240 billion m<sup>3</sup> with 50 million tonnes of average annual suspended sediment discharge (Gupta, 2004); peaked discharge occurring during summer months as a coupled result of glacier melting and summer monsoon (Clift et al., 2001).

Evidences of river course modification along the Indus, caused by tectonic influences, are plentiful. Deformations are well recorded in the Himalayan zone as well as beyond—in the north western Himalayan forelands of Pakistan. The development of the Salt ranges coupled with the Potwar Plateau led to a southward shift in the drainage of the river during Pliocene at ~5 Ma (Burbank and Beck, 1991; Gupta, 2004). Najman et al. (2003) also discuss the paleo-Indus route in the Potwar Plateau region using provenance indicators. Even further south, probable effects of the growth of Sulaiman Range are seen to have caused a course alteration up to 200-300 km (Clift, 2002). A proposed event of major river capturing by the Indus of its present-day tributaries (the Punjab rivers—Satluj, Ravi, Jhelum and Chenab) after ~5 Ma are also attributed to tectonic effects active in the region supplemented with a stronger monsoon

(Clift and Blusztajn, 2005). These findings clearly indicate very strong tectonic implications on the drainage and course development of the Indus and perhaps on its tributaries as well.

The resourcefulness of the Indus River has been optimized with a high number of functional dams/barrages/reservoirs etc. that provide hydropower, irrigation support, flood control, ease of navigation etc. But as a consequence, after the 1950s, a major reduction in water and sediment discharge has been noted (Giosan et al., 2006) which unequivocally dampens the sustenance of the delta.

### *2.1.2. Indus Delta*

The Indus River created a lobate shaped delta covering most of the Lower Indus Basin in the Sindh province of Pakistan during Holocene (Giosan et al., 2006; Inam et al., 2008). The vast paleo delta was a typical fluvial landform with the mighty river bifurcating into smaller streams distributing the overall flow velocity. However, as a consequence of variable discharge, monsoonal and tidal effects, the delta has undergone severe modifications (Inam et al., 2008). The river does not have much of a depositional delta left in its current form—owing to damming and other human interventions over the past few decades, reducing the delta to a marshy and saline water logged expanse (Milliman and Meade, 1983; Haq et al., 1997; Giosan et al., 2006; Coleman et al., 2008, Ziring and Burki, 2019) estimated to stand at a reduced area of 260 km<sup>2</sup> from 2600 km<sup>2</sup> (Kazmi and Jan, 1997). It extends in the east merging into the vast mudflat region of the Great Rann of Kutch. At the delta front, the river and its basin approach their terminal on land but the extensive erosive flux of the fluvial system is transported through the Indus Canyon into the Arabian Sea—creating the world's second largest detrital accumulation i.e. the Indus Fan (Clift et al., 2014).

## **2.2. The submarine Indus Fan**

Deposited on the passive western continental margin of the Indian subcontinent, the Indus Fan sediments mainly comprise of material eroded from the western Himalaya, Karakoram, and Hindukush (Clift et al., 2002), with an estimated volume of 5 million km<sup>3</sup> (Johnson, 1994) covering an area of ~1.1-1.25 million sq. km (McHargue and Webb, 1986). It is noteworthy that the Indus Fan approximates the Indus Basin in terms of area, but to quantify the contrasting morphometric form of the fluvial rivers and submarine channels is the key research question here.

The Indus Fan extends ~1800 km latitudinally from the Indus Canyon to the Carlsberg Ridge, bound by the Chagos Laccadive Ridge on the east, Owen Fracture Zone to the west and Murray ridge to the north-west (Fig 2.2), thereby restricting the fan's lateral growth (McHargue and Webb, 1986). Division of the fan into Upper, Middle and Lower Indus Fan given by Kolla and Coumes (1987) is based on echo character from high frequency sub-bottom reflectors, low frequency seismic profiles and sediment characteristics. Similar approach was followed for the Amazon and Magdalena Fan boundaries (Damuth and Kumar, 1975; Kolla and Buffler, 1985). The Upper Indus Fan extends from the foot of the continental slope to the 3400 m contour; the Middle Indus Fan extends till the 3800-4000 m and; the Lower Indus Fan extends till the Carlsberg Ridge with depths exceeding 4600 m (Kolla and Coumes, 1987). The study area hence runs from the source of the river at 4682 m above sea-level to ~4500 m below sea-level in the deep Indus Fan, creating an overall relief of 9.1 km.

Evidences of the paleo-Indus Fan in the Katawaz Basin of Pakistan and off the Makran margin have been recorded previously (Shuaib, 1982; Kolla and Coumes, 1987, Qayyum et al., 1996). Analysis of seismic reflection and well data from the Upper Indus Fan indicate that sediments predate the uplift of the Murray Ridge during Early Miocene at ~22 Ma, further implying that the Arabian Sea received sediments since the Paleogene (Clift et al., 2001).

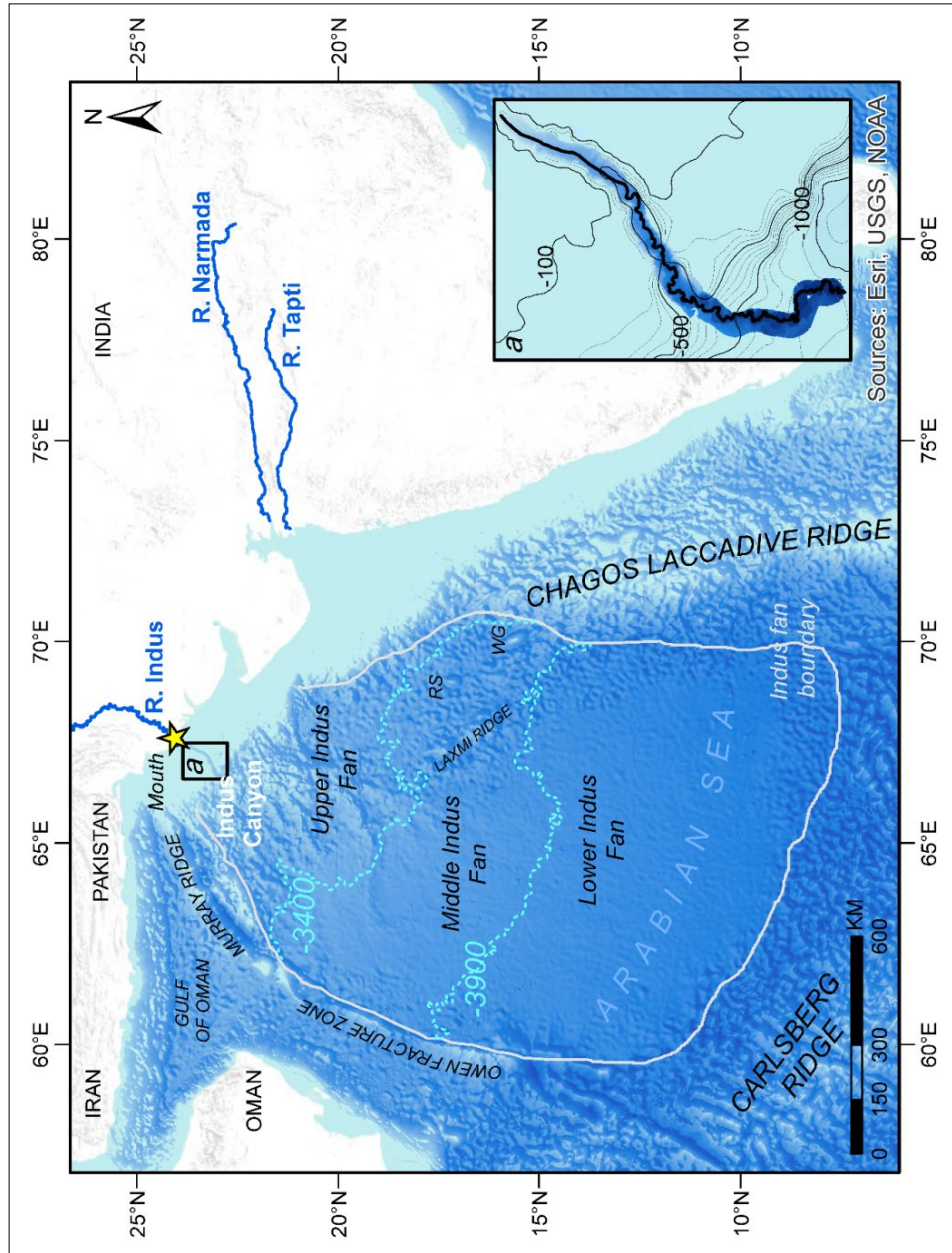


Fig 2.2: Physiographic map of the Indus Fan and surrounding regions. Middle and Lower Indus Fan boundaries (as -3400 and -3900 m contours) adopted from Kolla and Coumes (1987). A close-up of Indus Canyon as a major bathymetric incision on the western continental margin of India is provided as inset a (Clift and Henstock, 2015). Yellow star denotes Indus River's mouth 40 km away from the Indus Canyon head. RS: Raman Seamount, WG: Wadia Guyot.

Present-day fan sediments are up to 9 km thick off the deltaic front marking the thickest section of the fan (Clift et al., 2001; Gaedicke et al., 2002). Other than turbidity currents, pelagic sedimentation and mass-wasting aeolian deposition are significant contributors to the fan growth (Inam and Tahir, 2004, Prins et al., 2000). Principal contribution of illite, the most dominant mineral in the Indus Fan comes from the illite-rich clay minerals carried by the Indus River (Ramaswamy et al., 1991). Secondary contributors like Narmada and Tapi Rivers draining the Deccan Traps of western and southern India carry smectite-rich sediments (Kolla, 1976). A lesser magnitude canyon named Saraswati, off Western India was suggested as a sediment funnel during pre-Holocene whence the paleo-Saraswati River flourished (Kolla and Coumes, 1987). However, with new evidence presented here, *prima facie* connection between the Middle Indus Fan channels and the Saraswati Canyon seems dubious (discussed later in Section 4.2.2).

### *2.2.1. Indus Canyon*

The Indus Canyon is a pre-Holocene relict feature, known to have formed during the low sea-levels of the Quaternary when the Indus River extended over the exposed continental shelf coeval with the turbidity currents scouring the shelf (Inam et al., 2008). Also known as the Swatch, the canyon is a deeply entrenched feature on the western continental shelf of the Indian plate and the principal point source feeder of the Indus Fan channel levee complex. Less than 40 km SSE from the delta, the canyon is evident as a bathymetric incision (Fig 2.2, inset *a*). Three canyon complexes, forming an extensive erosional zone called the Indus Trough, were mapped near the mouth of the Indus River by Kolla and Coumes (1987). The youngest of the canyon complexes, which is the present-day Indus Canyon, lying east of the other two paleo canyons was later identified as the main feeder of the channel levee complexes of the Upper and Middle Indus Fan by Kenyon et al. (1995), while the older two canyons were considered

as the initial sediment conduits before turbidite processes developed during Oligocene-Miocene (Naini and Kolla, 1982). It is an established fact that there has been gradual/periodic shifting of the canyon eastward due to various reasons, leading to a consequential attempt by the channels to occupy the adjacent topographically low-lying areas (Kolla and Coumes, 1987). Also on land, evidence of deltaic deposits similar to present-day Indus delta sediments occurring further eastward, is credible to suggest a westward shift of the delta (Kazmi and Jan, 1997). Nevertheless, bathymetric data used in this study confirm that there is a slight west-east offset between the mainstream Indus River from its delta to the canyon head.

Dimensions of the active Indus Canyon are mapped from high-resolution swath bathymetry data (Clift and Henstock, 2015) detailed in Chapter 4. The Canyon is 180-190 km in length, averaging 8 km in width, sloping from 20 to 1715 m below sea-level at ~1:100 gradients. Seismic reflection data analysed by Kolla and Coumes (1987) revealed fine-grained sediments of moderate amplitudes in the canyon. Slumping and terraces (with sub-vertical, sharp boundaries) are common features of the canyon morphology (Kolla and Coumes, 1987; Clift et al., 2014; Hansen et al., 2017; von Rad and Tahir, 1997). Recent sediment cores retrieved from within the Indus Canyon helped to estimate a high recent sedimentation rate of 10 cm per year in the canyon head (Clift et al., 2014).

### *2.2.2. Indus Fan channel levee complex*

Beginning in the Oligocene-Early Miocene, sedimentation via channelized turbidity currents dominated the upper fan that dissipated sediments till the lower fan through both channelized and unchannelized sediment flows (Kolla and Coumes, 1987). Overspill of thick turbidites from channels resulted in the build-up of exhaustive levees and probable lobes (in the Lower Indus Fan) (Inam and Tahir, 2004). Clift et al. (2001) suggested that the first major channel levee complex construction began in Middle Miocene at a time when sedimentation rates were

accentuated. Therefore, the development of the channels/levee systems predate the Indus Canyon, thereby implying that fluvial drainage was directly linked to the fan with active turbidity currents feeding the erosive-depositional system of the channel levee complexes. With the high stands of Holocene causing a remarkable drop in the supply of terrigenous sediments, the functioning of this system dispelled and the fan faced sediment starvation; a dominance of pelagic/hemi-pelagic sediments prevailed with frequently avulsing channels creating new channel levee systems (Inam and Tahir, 2008). Avulsion in the Upper-Middle Indus Fan, which is also a region of gradient lowering, is particularly pronounced creating complex depositional patterns (Amir et al., 1996, Bastia and Radhakrishna, 2002).

Seismic reflection data analysis from the Upper and Middle Indus Fan revealed that channel fills contain coarse-grained sediments fining upward indicated by high-amplitude, random reflections underlying weak to moderate amplitude reflections; bordered by wedge-shaped, concave-upward transparent reflection packages denoting levee structures (Naini and Kolla, 1982; Kolla and Coumes, 1987). Lower fan deposits that are acoustically transparent, present in the form of isolated sediment pockets denote pelagic sedimentation (Naini and Kolla, 1982).

**CHAPTER 3**  
**DATA AND METHODS**

## **CHAPTER 3**

### **DATA AND METHODS**

Several methods and techniques are adopted in this work for effective data analyses. Models and methods vary depending on the type of data employed. For instance, stream identification using DEM data has been performed directly using GIS based modelling but the same could not be applied for bathymetric data where manual digitization worked more precisely. Similarly, automated stream network results derived from DEM data could be verified for errors with open source high-resolution satellite data but for channel identification, multi-beam bathymetric data was the only available source. Considering that a unified protocol was not viable for processing subaerial and submarine data, moderately variant approaches were designed for optimizing results. These variations and their implications are discussed further in this chapter. Barring those, the overall methodology for data generation and morphometric parameter estimation from both DEM and MBES data, is similar.

For the ease of understanding, this chapter is divided in two parts based on data type—DEM data (for fluvial analysis) and MBES data (for submarine analysis). The geomorphometric parameters estimated for both fluvial and submarine systems are longitudinal profile and cross-sections, channel width, sinuosity, planform and slope. After the calculation of all parameters, the morphometric behaviour is compared one-to-one, following a two-way approach, based on (a) individual parameters, as well as (b) stages of development wherein, the upper basin is compared with the upper fan, the middle basin with middle fan and the lower basin with lower fan. Such stage-wise comparisons help in:

- identifying the variation in the processes operating in fluvial and submarine environments;
- assessing the variance in the respective stages of development; and
- controlling the extent of comparison.

### **3.1. Datasets**

Two types of data are employed in this study — (1) Digital Elevation Models (DEM) data for fluvial analysis and (2) Multi-beam Echosounder (MBES) data for submarine analysis. [MBES and bathymetric data are used interchangeably hereinafter].

DEM data comprises of 77 tiles of CartoDEM data (CartoDEM v-3 R1 2015) and 01 tile of SRTM data (Jarvis et al. 2008) marked as Block F1, F2 (Fig 3.1). A wide range of DEM data sources (e.g. interferometric/radargrammetric or stereoscopic) are available today. Choice of a particular DEM may vary based on the objective, topography, resolution etc. Selecting a particular data source for the Indus Basin, considering its widely ranging topography was therefore, tricky. However, after considering the high efficiency in drainage network extraction using CartoDEM compared with other data sources like SRTM and ASTER (NRSC, 2011), 30 m CartoDEM [derived from Cartosat-1, PAN (2.5 m)] was chosen for this study. Due to unavailability of CartoDEM data in Block F2 region, 01 tile of SRTM data was used instead.

MBES data from the Indus Fan is relatively sparse as compared to the seamless DEM data for the fluvial Indus Basin. Due to this, continuous analysis for the Indus Fan could not be performed. Nonetheless, high-resolution data available for smaller blocks, spread across different parts of the Indus Fan were utilised to enable a one-to-one comparison of channel morphometry.

The channel behaviour in the Upper and Middle Indus Fan has been analysed using data from three sources marked as Block S1, S2 and S3. Block S1 was acquired in 2008-2009

onboard RV *Pelagia* and processed subsequently (Clift and Henstock, 2015). Block S2 forms part of Exclusive Economic Zone surveys carried out by the National Centre for Polar and Ocean Research (NCPOR). Lastly, Block S3 was also acquired by NCPOR in 2013 as part of site survey for IODP Expedition 355. Channels identified in this block from the Middle Indus Fan have also been extensively discussed in Mishra et al. (2015, 2016) and Prerna et al. (2015).

To further constraint the findings, inferences from previous works in the Indus Fan by Kenyon et al. (1987) [Block R1]; Kodagali and Jauhari (1999) [Block R2] and Bourget et al. (2013) [Block R3] are also added. Table 2.1 tabulates the datasets utilised in the study and Fig 3.1 shows the extent of data blocks.

Table 3.1: Datasets used for morphometric analysis (Source – Prerna and Kotha, 2020)

<b>Block</b>	<b>DEM data (for fluvial analysis)</b>	<b>Region</b>
F1	CartoDEM (CartoDEM v-3 R1, 2015), 30m ground resolution, 1° x 1° tile	Indus Basin
F2	Shuttle Radar Topography Mission (SRTM) (Jarvis et al., 2008), 90m ground resolution, 5° x 5° tile	
<b>Block</b>	<b>MBES data (for submarine analysis)</b>	<b>Region</b>
S1	Kongsberg EM302 processed bathymetry data, 3.5 kHz frequency, Indus Canyon and shelf, <i>RV Pelagia</i> , Cruise PE300 (Clift and Henstock, 2015)	Indus Fan
S2	Processed bathymetry data (NCPOR, n.d.)	
S3	SeaBeam 3012 processed bathymetry data, 12 kHz frequency, Laxmi Basin, <i>ORV Sagar Kanya</i> , Cruise SK 306 (Mishra et al., 2015)	
<b>Block</b>	<b>Reference data from previous work</b>	<b>Region</b>
R1	GLORIA long-range side-scan sonar, 3.5 kHz high-resolution profiler and precision echo sounder, GLORIA study of the Indus Fan, <i>RRS Charles Darwin</i> , Cruise 20 (Kenyon et al., 1987)	Indus Fan
R2	Hydrosweep processed bathymetry data, 15.5 kHz, Lower Indus Fan, <i>ORV Sagar Kanya</i> , Cruise SK 074 (Kodagali and Jauhari, 1999)	
R3	Kongsberg-SIMRAD EM120, 12 kHz, Fanindien 2009 and Owen surveys, <i>R/V Beautemps-Beaupré</i> (Bourget et al., 2013)	

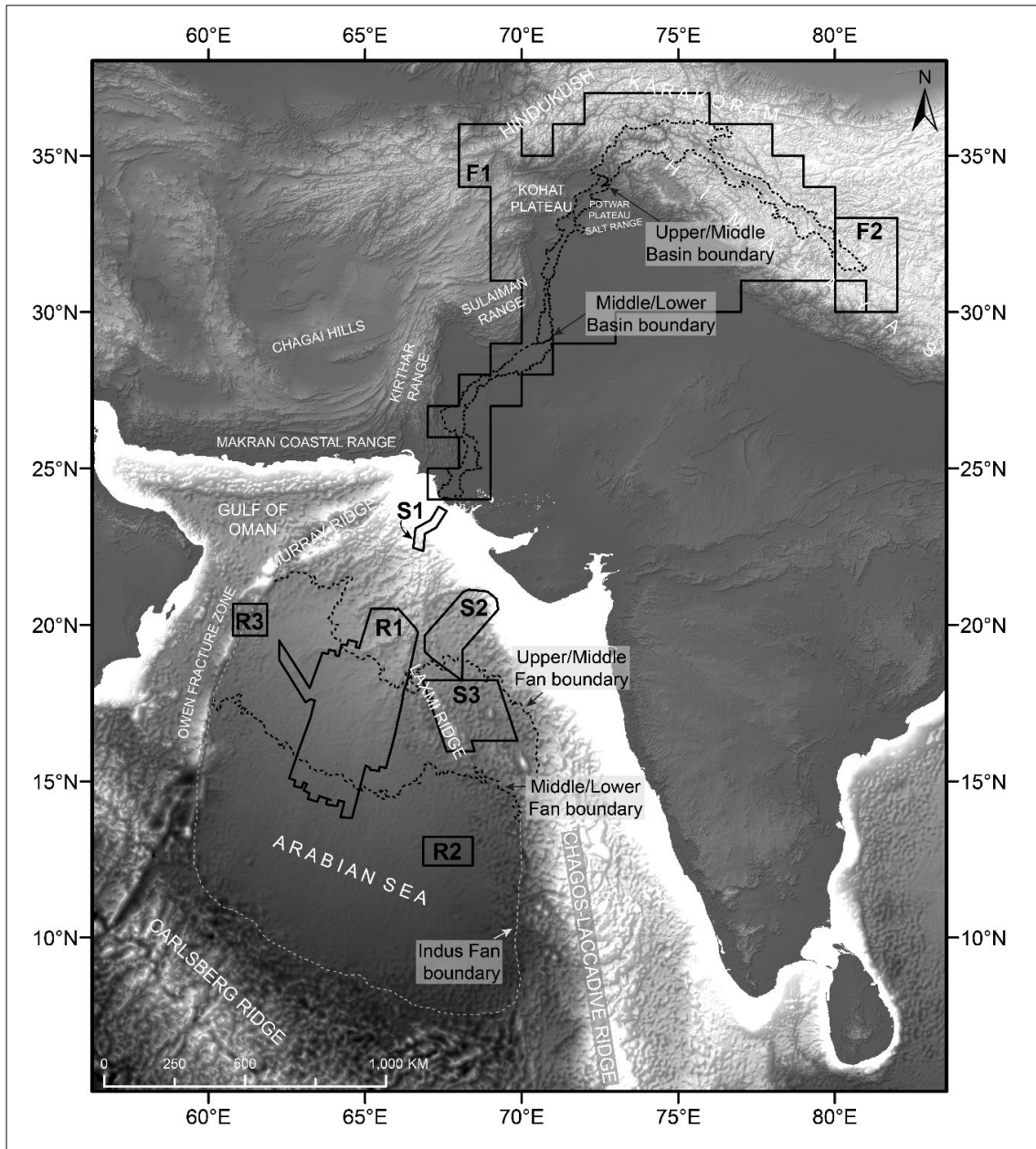


*Fig 3.1: Physiographic map of study area. Indus Fan boundaries are adopted from Kolla and Coumes (1987) and Indus Basin boundaries from Prerna et al. (2018). Blocks F1 (CartoDEM), F2 (SRTM), S1 (Clift and Henstock, 2015), S2 (NCPOR, n.d.), S3 (Mishra et al., 2015), R1 (Kenyon et al., 1987); R2 (Kodagali and Jauhari, 1999), R3 (Bourget et al., 2013) represent the extent of data blocks. (Figure from Prerna and Kotha, 2020)*

### **3.2. DEM data (for fluvial analysis)**

Several processes, both surficial and sub-surficial are role players in sculpting the morphology of landmasses—like fluvial, aeolian, karstic or glacial. Out of these, fluvial processes are considered to be the most active agent dominating the continental landmass. Other processes are mainly active in limited regions of the continents (Strahler and Strahler, 1996; Babar, 2005).

Morphometry based analyses of river basins using geospatial techniques have been in practise, mainly to quantify the drainage-network relationships between streams and their catchment, as well as to assess the interrelationship between hydrology, geology and geomorphology. Effective implementation of GIS based hydrological modelling on specific watersheds of the Indus Basin to address soil conservation, disaster control, sustainable water management and for climate change projection are evident in the works of Awasthi et al. (2002), Singh and Sarangi (2008), Singh (2009), Khan et al. (2014), Khan et al. (2017) and others. Significant research in the stream network extraction and basin categorization has been performed, however, most study areas are restricted to smaller catchments/watersheds.

As mentioned earlier, in the present study, DEM data has been rigorously used to extract values of five geomorphometric parameters: (a) Longitudinal profile; (b) channel width; (c) sinuosity; (d) planform; and (e) slope for the complete length of Indus River. The existing inter-relation between elevation/relief, gradient, planform pattern and stream behaviour can be effectively understood using these select parameters. Elevation-relief analysis of the Indus Basin is also performed to further corroborate explanation. It is an important indicator of the development stages of the fluvial Indus River and also aids in the demarcation of the Indus basin into Upper, Middle and Lower basins. The methodology for fluvial analysis is unfolded in four sections: (a) Stream network and basin delineation; (b) geomorphometric parameter estimation; (c) elevation-relief analysis; and (d) morphometric account of the Indus system.

### 3.2.1. Stream network and basin delineation

Analysis begins with the extraction of stream network from the DEMs, one of the most widely used applications of remotely sensed data. The drainage network attained using the Spatial and 3D Analyst toolboxes of ArcGIS® software was further used as input for identifying the geomorphometric parameters subsequently. The 6-step workflow is explained below (Fig 3.2).

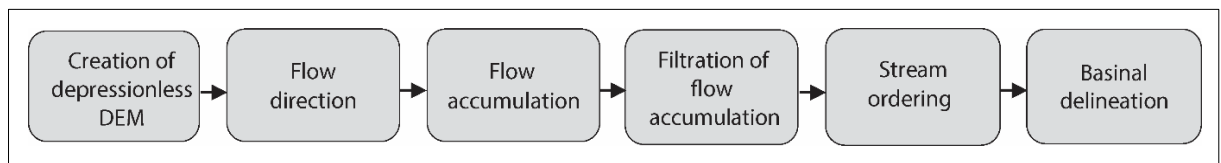


*Fig 3.2: Schematic workflow for stream network extraction from DEM. (Figure from Prerna and Kotha, 2020)*

#### 3.2.1.1 Step 1: Creation of depressionless DEM

Most data representing the elevation or bathymetry of a region may sometimes have erroneous sinks or depressions. Jenson and Domingue (1988) stated DEMs often contain depressions that hinder flow routing. Omission of such depressions has a positive influence on enhancing the quality of elevation models (Lin et al., 2008). For this, several techniques have been developed which eliminate these undesired sinks—discussed by Jenson and Domingue (1988), Fairfield and Leymarie (1991) and Garbrecht and Martz (1997). The sinks may occur as a singular pixel or a group of pixels with relatively lesser values than their surroundings pixels. Depending on the number of pixel or pixels, the process to fill up the sinks may be direct or iterative. A z-limit value to define the maximum depth of a sink to be filled can be given optionally. Cross-sections from original and filled DEM is shown below for comparison (Fig 3.3).

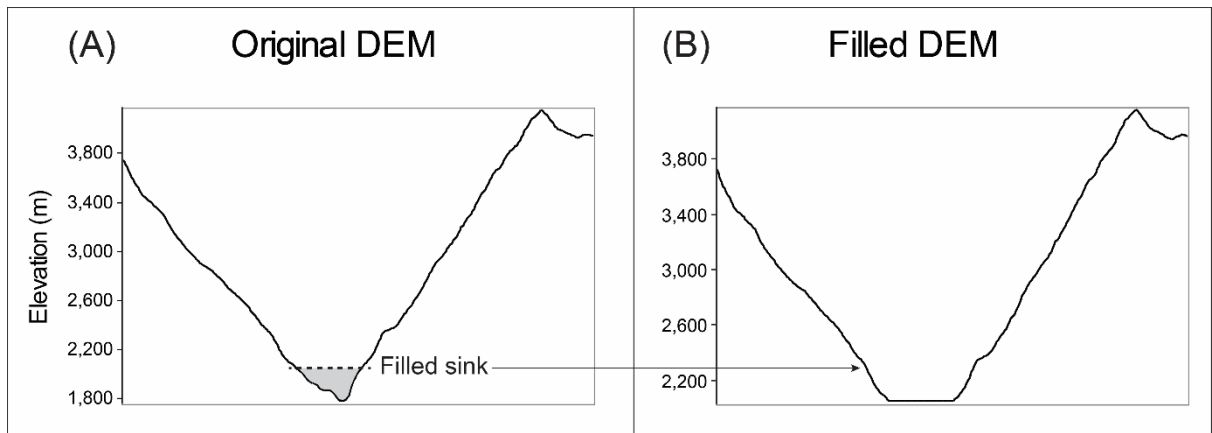


Fig 3.3: Difference in cross-sections of (A) original DEM and (B) filled DEM.

### 3.2.1.2 Step 2: Flow direction

The second step is to compute a flow direction raster using the D8 algorithm given by O'Callaghan and Mark (1984). This raster helps in understanding the direction of the steepest flow of water from each cell to its adjoining cells. Starting from the east incrementing in the clockwise direction, the values depicting flow direction range from 1 to 128, coded as powers of 2 from 0 to 7, i.e.  $2^0 = 1$ ;  $2^1 = 2$ ; .....  $2^7 = 128$ , in a way that the surrounding conditions correspond to unique values when the powers of two are summed for any unique set of neighbours (Jenson and Domingue, 1988). Fig 3.4 is an illustration showing elevation surface and its flow direction values calculated based on the D8 algorithm in the ArcMap® environment.

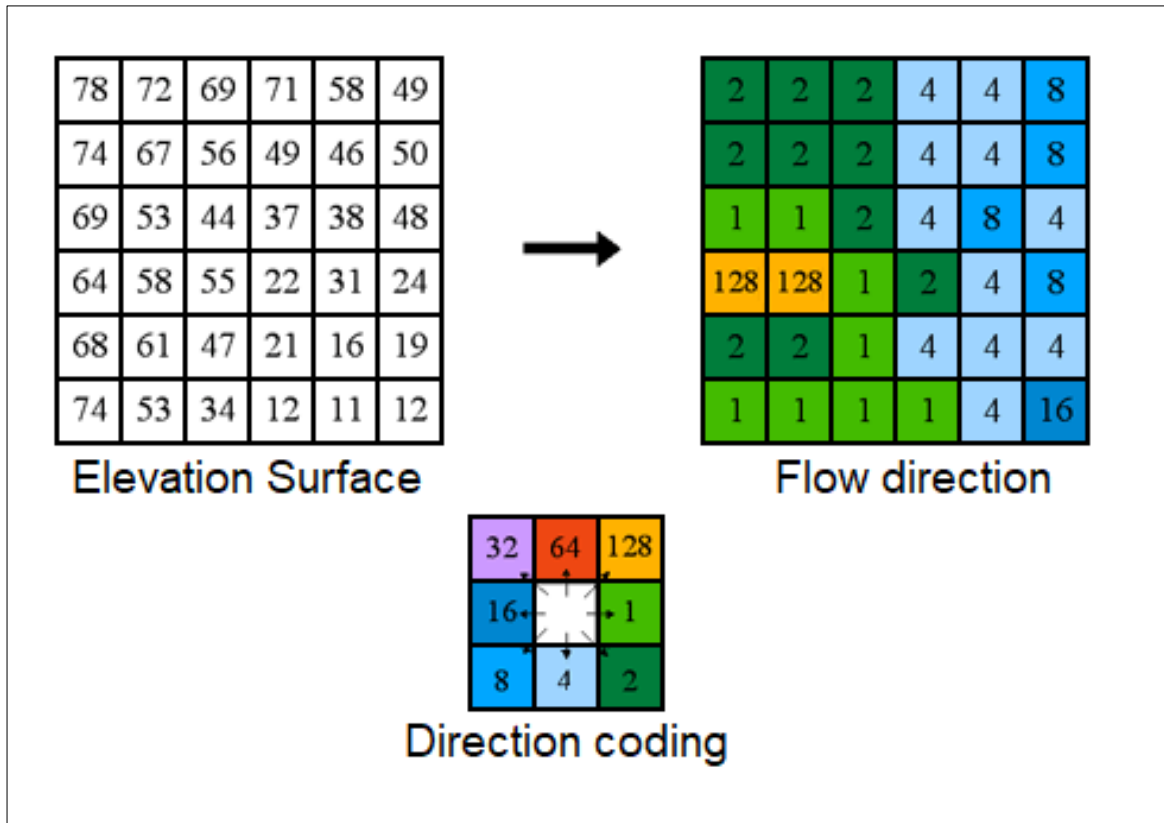


Fig 3.4: Illustration showing how flow direction is estimated (Source: ESRI™).

### 3.2.1.3 Step 3: Flow accumulation

The flow direction raster is used as the input for calculating flow accumulation. Here each cell is assigned a value equal to the number of cells that flow to it (O'Callaghan and Mark, 1984). Along any given channel, the value of accumulated flow generally increases downstream. Flow accumulation is crucial for identifying streams because higher accumulation values imply greater flow from surrounding cells. The values continue to increment downslope with the length of the stream channel, hence there is no upper range, but 0 valued pixels indicating no inbound flow are possible. These cells are normally observed to be the local topographic highs. Fig 3.5 is an illustration showing the estimation of flow accumulation based on flow direction in the ArcMap® environment.

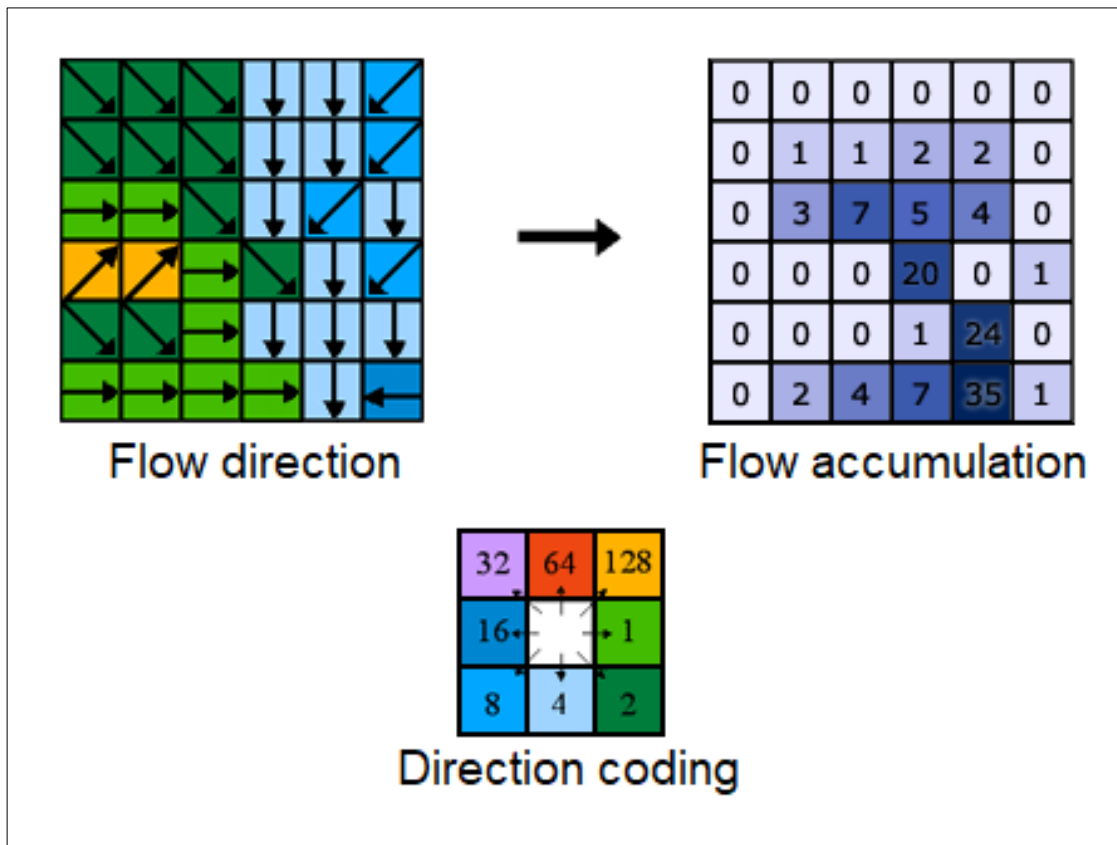


Fig 3.5: Illustration showing how flow accumulation is estimated (Source: ESRI™).

#### 3.2.1.4 Step 4: Filtration of flow accumulation

The flow accumulation raster calculates values for all pixels receiving flow from surrounding areas but it needs filtration because not all pixels are part of the drainage network. A locally applicable threshold can be defined to filter the flow accumulation raster resulting into a binary inferred stream raster, where 0 denotes “no flow” and 1 denotes “stream flow”. Standard conditional tools like CON or SETNULL can be used. After the major streams are classified, other ephemeral streams/tributaries can be included progressively by lowering the threshold.

### 3.2.1.5 Step 5: Stream ordering

Every stream needs identification as a value that represents its order in the stream network. Only when the order is known, the higher order streams can be identified as the major river and lower order streams as tributaries or ephemeral streams. There are two methods for stream ordering given by Strahler (1952) and Shreve (1966) based on order and magnitude respectively. Shreve's method considers every stream additively, thus calculating the magnitude downstream but in Strahler's method, stream order increases only when two lower order streams converge. Given the very high number of streams in the study area, Strahler's method is considered suitable as it avoids exorbitant stream ordering. Fig 3.6 represents the stream order difference in the two methods.

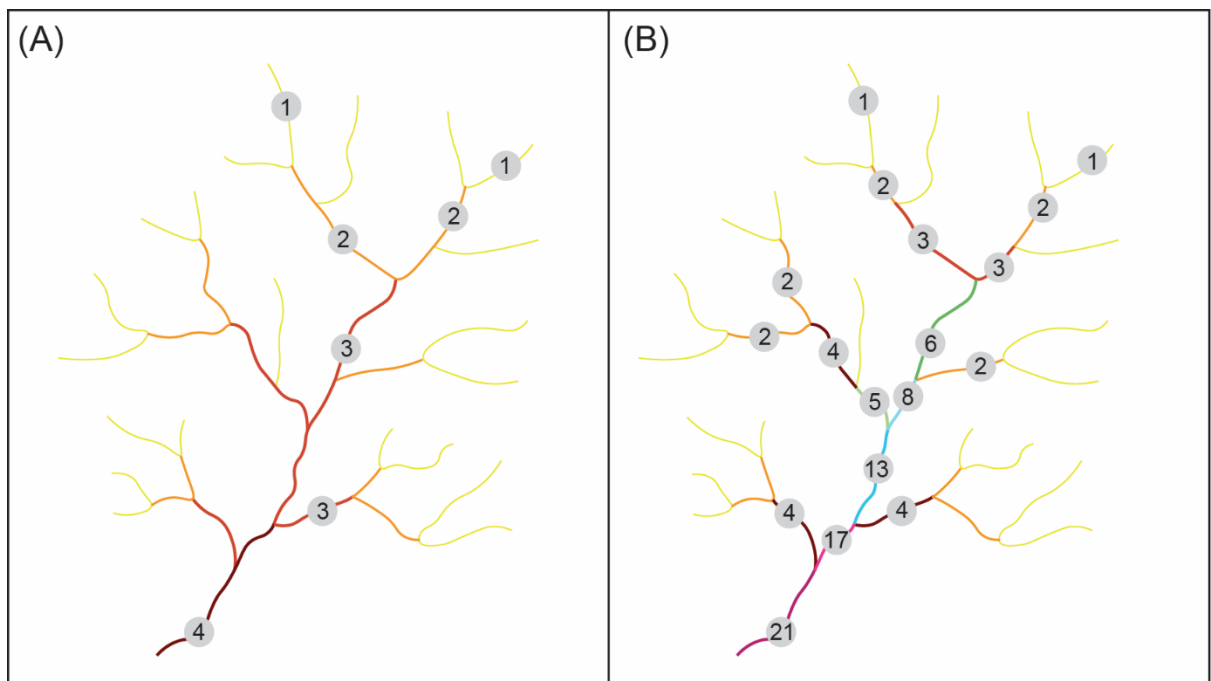
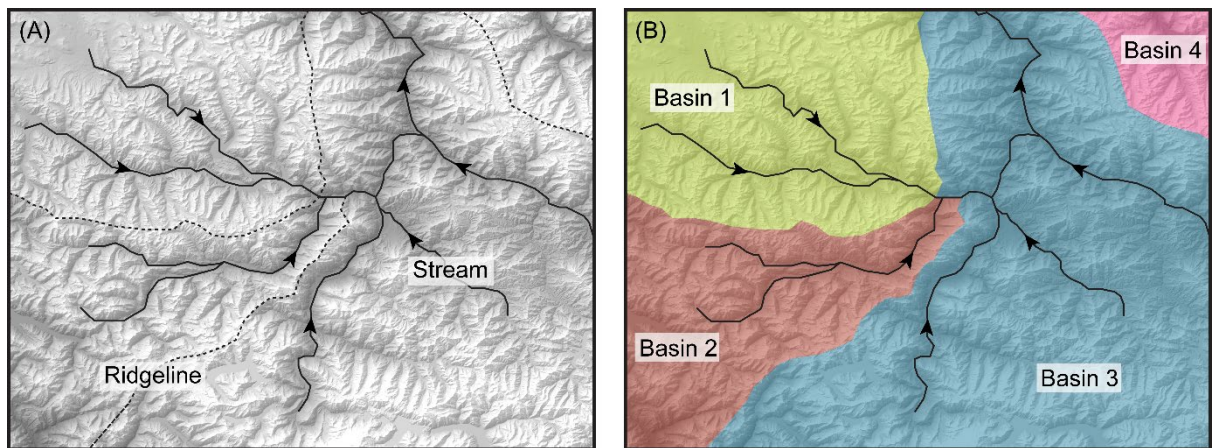


Fig 3.6: Stream order as per (A) Strahler (1952) and (B) Shreve (1966).

### 3.2.1.6 Step 6: Basin delineation

Lastly, the flow direction raster is used to identify ridge lines (a line joining the highest points of a ridge) which in turn is used to delineate basins for every data tile. All streams that flow into a common pour-point are circumvented and included into a singular drainage basin (Fig 3.7). If a large number of basin margins are created, they can be merged subsequently.



*Fig 3.7: Process of basin delineation showing (A) a part of DEM from the study area showing streams and estimated ridge lines and (B) ridge lines and stream flow direction used to delineate basin boundaries.*

Functional depiction of Steps 1 to 6 of stream network and basin delineation on one tile from the full dataset is presented in Fig 3.8 and the execution model built using ArcMap® Model Builder is given in Fig 3.9. This model was run iteratively for every data tile used for analysis. Once stream network and basin delineation is completed for all data tiles, geomorphometric parameter estimation follows.

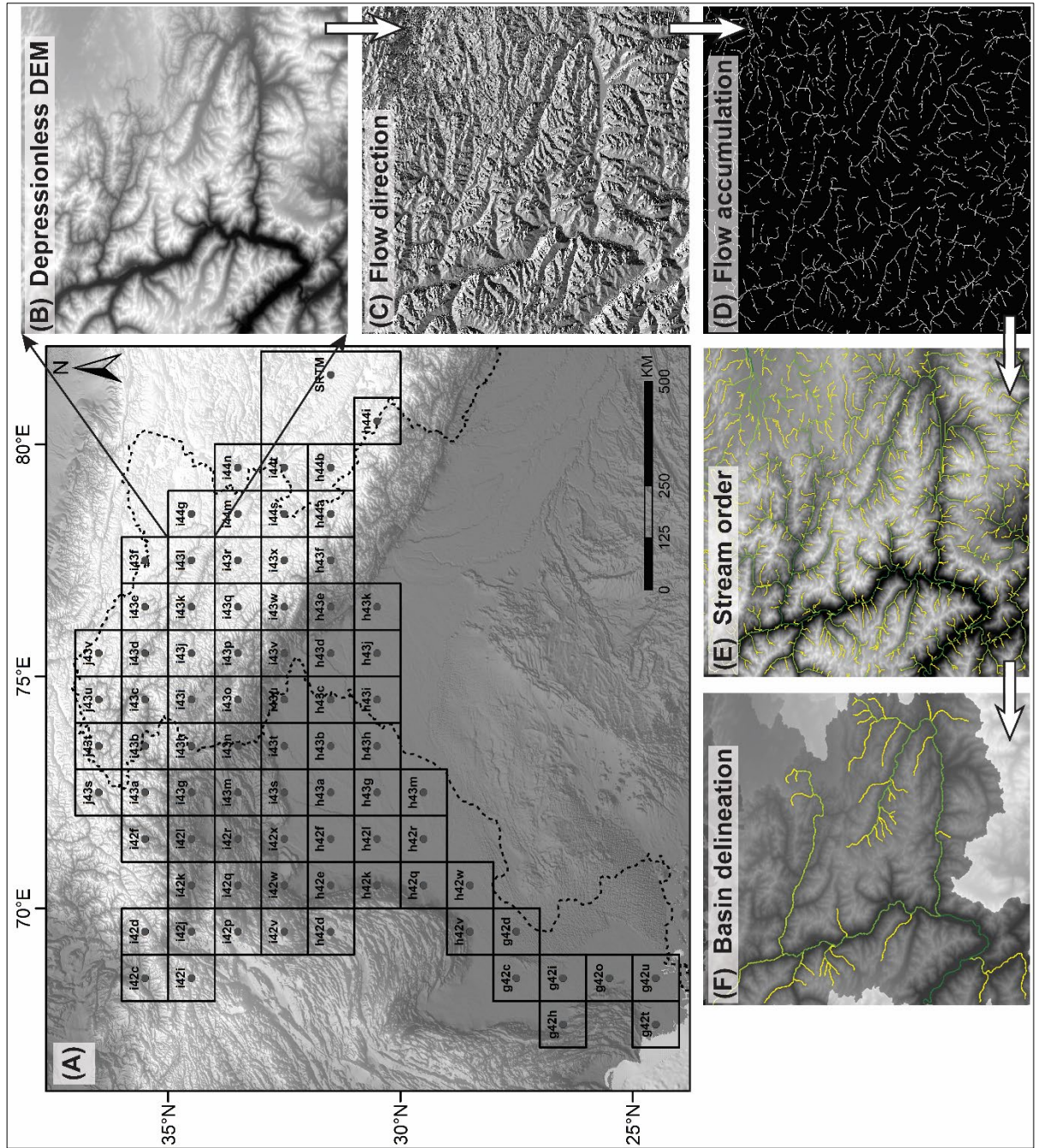


Fig 3.8:

(A) Location of 77 CartoDEM and 01 SRTM data tile with grid code used in the study; [(B)-(F) process of stream and basin identification of one tile (i44g) shown as sample] (B) Depressionless DEM (C) Flow direction raster; (D) Flow accumulation raster; (E) Stream order; (F) Basin delineation.

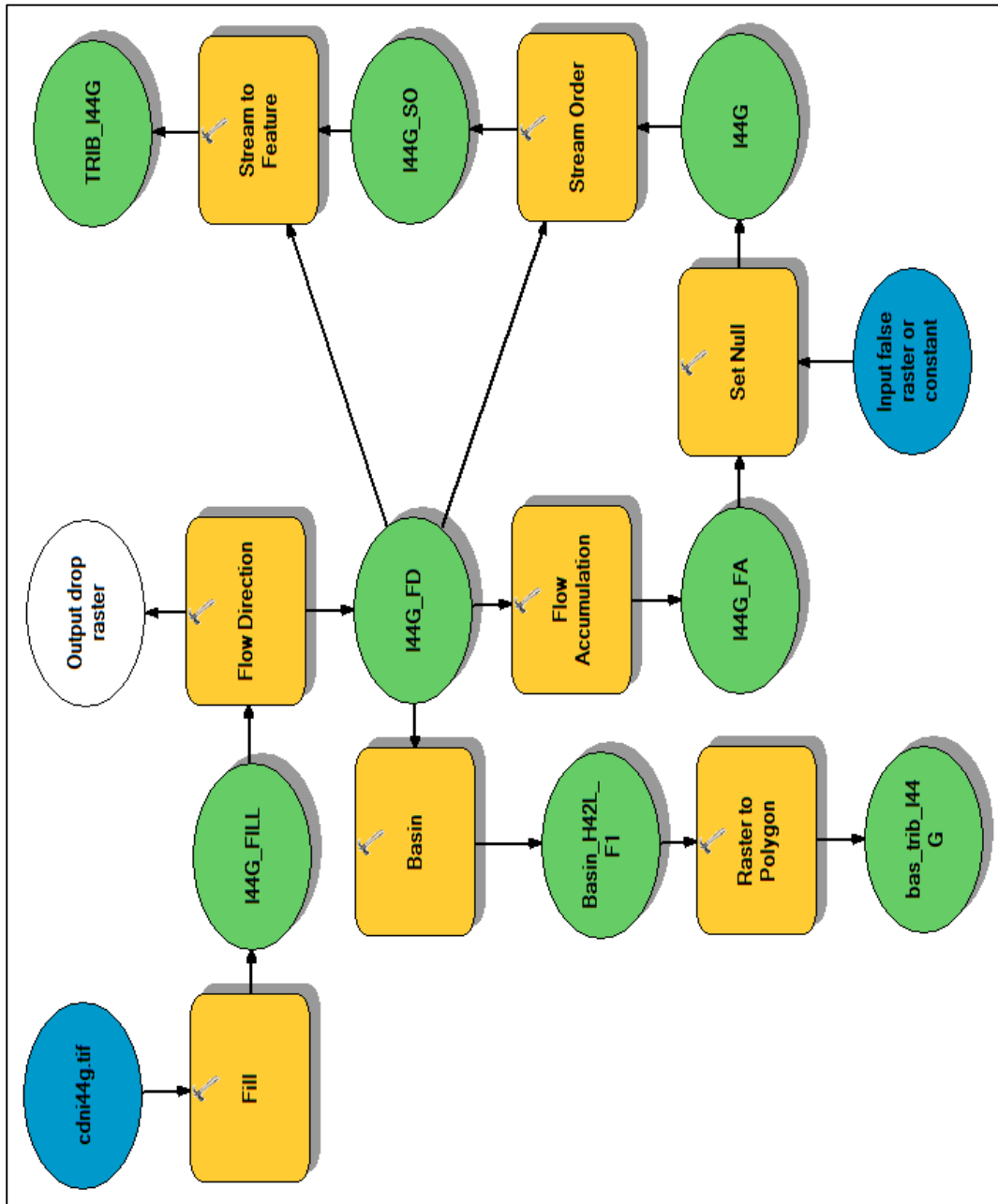


Fig 3.9: Model for stream and basin delineation built using ArcMap® Model Builder.

### 3.2.2. *Geomorphometric parameter estimation of the Indus River*

There are several geomorphometric parameters used by analysts to describe the morphology of a river, for e.g. radius of curvature, stream-length index, valley width-to-height ratio etc. In this study, the longitudinal profile is studied in conjunction with channel width, sinuosity and slope along with basin divisions of the Indus Basin to provide a holistic morphometric description. With more data in the future, additional parameters can be included to further strengthen the analysis performed here. The five parameters estimated are discussed below:

#### 3.2.2.1 Longitudinal profile

A longitudinal profile is a graphical representation of change in gradient with increasing length. It helps analyse geological and geomorphic interactions operating on a particular feature at different time scales (Sonam and Jain, 2018). Sudden or steep changes in lateral gradient are clearly identifiable on such profiles, from which inferences can be drawn about a river's course into different stages of development (Prerna et al., 2018). As a precursor though, cross-sectional profiling is useful for identifying channel thalweg—the locus of lowest bed elevation or maximum flow depth within a watercourse (Dey, 2014). Therefore, the longitudinal profile of the Indus was constructed for its complete length, from source to mouth, using cross-sections constructed at every 10 km. This approach was preferred over creating a 3D profile along the course of the river directly, because it is only from cross-sections that the thalweg values can be accurately extracted, which in effect makes the longitudinal profile more efficient—representing only the deepest points at regular intervals downstream. The 10 km interval effectively captured all major topographic undulations along the course of the river. An illustration to explain the working process behind building a longitudinal profile is given in Fig 3.10.

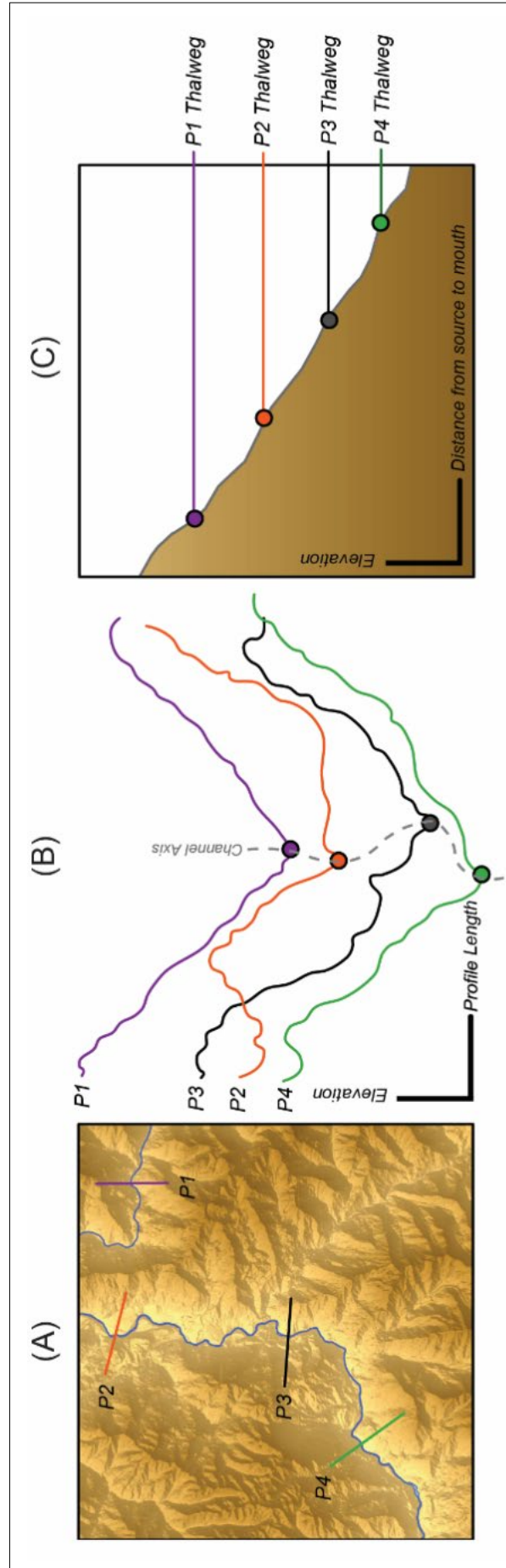
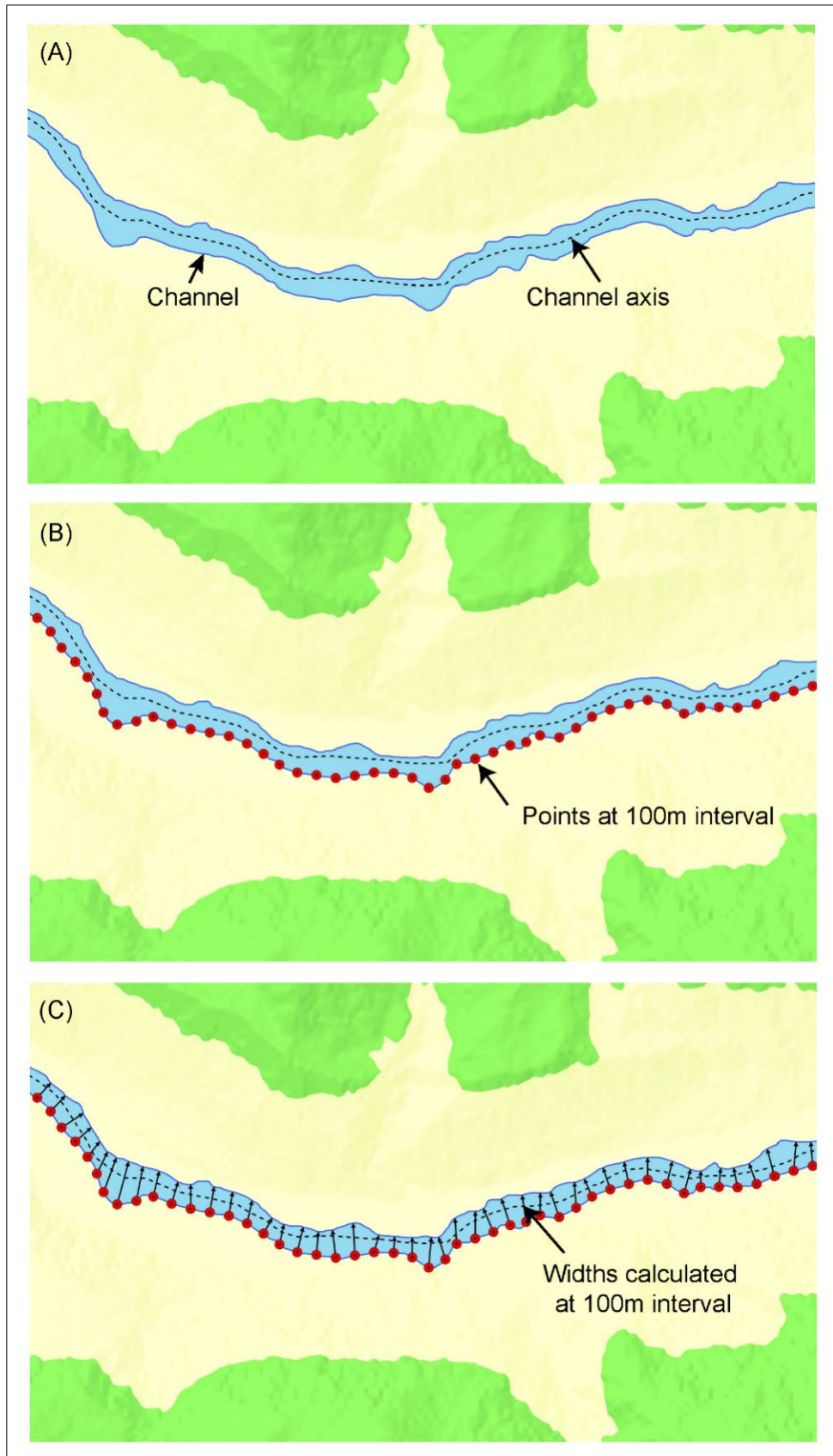


Fig 3.10: (A) 4 sample profiles – P1, P2, P3, P4 along channel course shown in planform; (B) Cross-sections of P1, P2, P3, P4 with respective thalweg points; (C) Illustrative longitudinal profile generated from elevation of thalweg points. (Figure from Prerna et al., 2018)

### 3.2.2.2 Channel width profile

Channel width is calculated as a straight line distance from channel axis to either bank (Prerna et al., 2018). Combining this profile with other parameters like the longitudinal profile or sinuosity profile helps in identifying regions with large channel width which could represent potential of high deposition or lesser channel width indicating increased channel incision. Sharp changes in channel width are often indicative of certain endogenic/exogenic effects thereby helps in focusing on the areas of distress. Physiographic modifications in river planform caused by anthropogenic effects are clearly identifiable using channel width plots. A river often starts to deposit sediments in the form of temporary islands/sand bars amidst its channel belts when the sediment load exceeds the river's carrying capacity. This behaviour is identified as braiding. Increased braiding, especially in the Lower Basin, could be attributable to the construction of several barrages and dams. Hence in this study, the channel width includes these depositional features such that segments of the river which are highly braided can be immediately identified.

Since there is no method of accurately deriving channel width from DEM data, the main river has to be digitized, in this case from base maps available on ArcGIS® Online. A wide variety of high-resolution satellite images are utilised along with Google Earth™ for mapping the outer banks of the Indus River. Thereafter channel width estimation is done by constructing straight line transects from either bank of the main channel at every 100 m (performed using *DrawPerpendicularSeg tool – AddIn* tool available on ArcGIS® Online). After close consideration, an interval of 100 m was found to capture the channel width variation precisely. Fig 3.11 depicts the process flow of channel width estimation for a segment of the Indus River.



*Fig 3.11: Channel width estimation using DrawPerpendicularSeg tool. (A) channel with axis; (B) regular interval points generated on either bank of the channel; and (C) perpendicular lines generated from points representing channel width.*

### 3.2.2.3 Sinuosity profile

Sinuosity of a river is a measure of deviation of a channel from its central path along its course (Prerna et al., 2018). All flowing channels, whether fluvial, submarine or extra-terrestrial, exhibit a degree of deviation in their flow from their straight-line downslope path. It is the basic nature of liquids to flow over a surface by maintaining equilibrium between its erosive power and the resistivity of the surface. Sinuosity index (SI) is a ratio of the curvilinear distance (channel length) to the shortest-path distance (valley length) (Brice, 1974). Sinuosity is an essential indicator to identify the different planforms exhibited by the river along its course.

To compute the SI for the Indus River, the ratio of sinuous distance fixed at a 10-km interval i.e. (A) and the shortest-path distance between the start and end of every reach i.e. (B) was tabulated.  $SI = (A) / (B)$ . An interval higher or lesser than 10 km resulted in subdued variations or extremely jagged sinuosity. Hence, a standard interval applicable to all systems for undertaking any morphometric analysis cannot be determined. Based on the scale of detail required to understand a particular phenomenon, measurements may permute (Prerna et al., 2018).

### 3.2.2.4 Planform

Planform is an aerial/plane view of a feature's form (Prerna et al., 2018). Along any river's course, a variety of planform types can be identified. This parameter is more of a qualitative than quantitative descriptor of a river/channel's behaviour. Considering the channel width and sinuosity of the Indus, as many as eight different planform types are identified. Each type denotes the effect of operating factors active through its course, and therefore, the extent is also important. A description of planform types and their extent along the longitudinal profile is provided in Chapter 4 (Sections 4.1.2. and 4.1.3.).

### 3.2.2.5 Slope profile

Slope or gradient along a river's course is directly indicative of its erosional behaviour (Prerna et al., 2018). As a river progresses through various stages of development, slope makes a key morphometric player for estimating the erosive power of the channel/river. Slope is measured as ratio of elevation difference between Point A (upslope) to Point B (downslope) to the distance along the flow pathway i.e.  $\Delta y/\Delta x$ . It can be represented as a ratio; percentage rise or in degrees. In the current analysis of the Indus River, percentage rise with respect to the downslope course has been plotted. For the purpose of calculating  $\Delta y$  for every 10 km reach ( $\Delta x$ ), thalweg points of the river extracted for constructing the longitudinal profile are employed. [Percentage slope rise =  $(\Delta y/\Delta x) * 100$ ].

Followed by geomorphometric estimation of the river is the elevation-relief analysis of the basin—an important indicator of the basin's development with respect to the fluvial processes acting upon it.

### 3.2.3. *Elevation-relief analysis of the Indus Basin*

Elevation-relief ratio and hypsometry are considered close estimates to study the effects of denudation and tectonic uplift—key players of landform development (Prerna et al., 2018). As per Strahler (1952), the form of hypsometric curve and the value of the hypsometric integral are important elements in understanding topographic form and geologic structure.

Wood and Snell (1960) developed a more direct and equally competent measure—the Elevation-Relief ratio (E) due to the complexity of measuring the Hypsometric Integral (HI). The equivalent E method has been empirically tested and mathematically proven to be at par with the HI (Strahler, 1952) by Pike and Wilson (1971) establishing that  $E \approx HI$ .

$$E \approx HI = \frac{\text{Mean elevation} - \text{Min elevation}}{\text{Max elevation} - \text{Min elevation}}$$

For calculating E, it is essential that the drainage basin be accurately derived from an elevation model, in this case, the mosaicked DEM of the Indus Basin (Prerna et al., 2018). The elevation range, from the summit top to the basin mouth is calculated and divided into sub-ranges. Surface area of tributary basins like those of Satluj, Ravi, Beas, Gilgit, Kabul, Kurram, etc. have not been included in the basin of Indus. Hence, only the watersheds contributing directly to the Indus River have been extracted to model its immediate basin which is 127,453 km<sup>2</sup>.

#### *3.2.4. Geomorphometric account of the Indus system*

The morphometric account of the Indus system is an amalgamation of the morphometric data extracted from the river and its basin using DEM data and ancillary satellite images. As described in Section 3.2.2 and 3.2.3, the river and the basin is first studied separately and then put together to divide the basin into Upper, Middle and Lower Indus Basin. Despite immense research on this drainage basin, there seems to be a lack of scientific reasoning in the identification of Indus Basin margins. It is crucial to perform this exercise because the river and basin inter-relationship can be better understood with respect to the stage of development. In a system as enormous as the Indus, basin categorisation is fundamental in understanding the intricacies of hydro-geological phenomenon operational in a system. Fig 3.12 summarizes the methodology adopted.

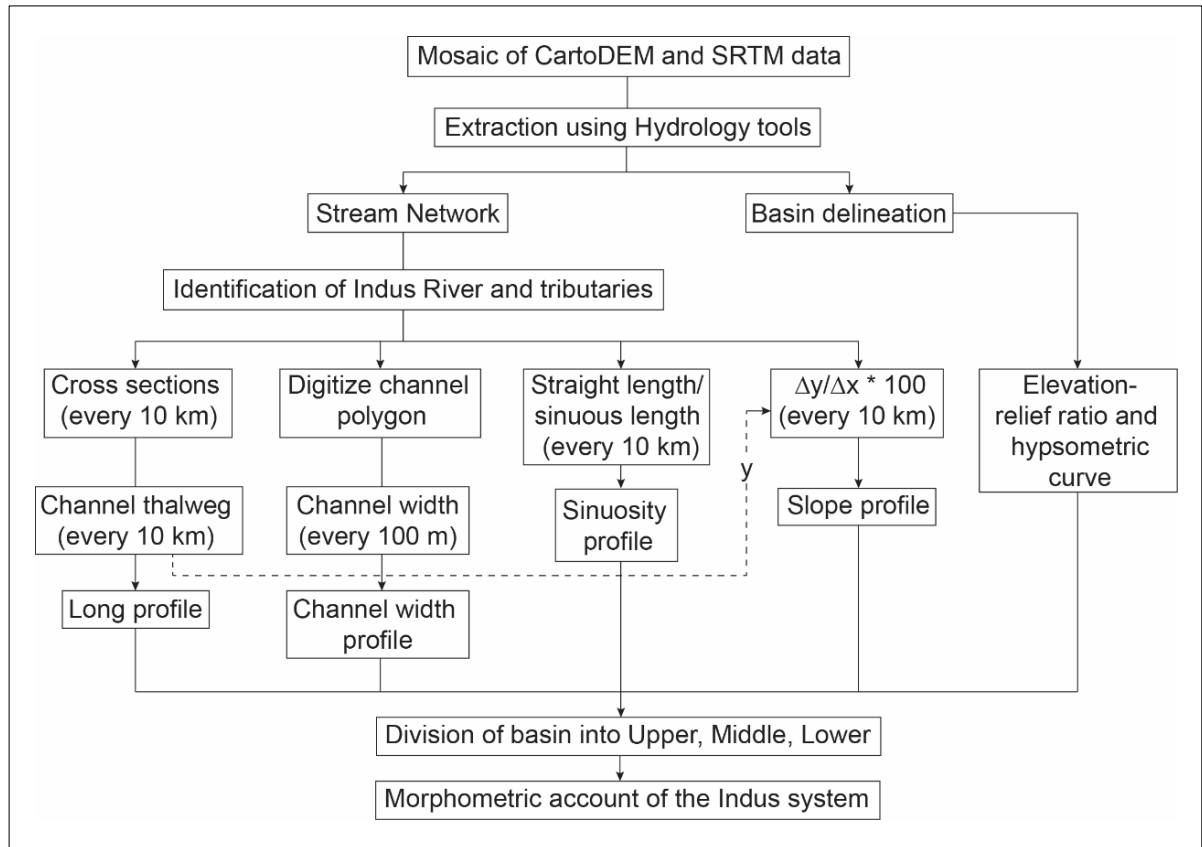


Fig 3.12: Flowchart of methodology followed to construct morphometry of the Indus system.

### 3.3. MBES data (for submarine analysis)

Parametric estimation for submarine analysis is similar to fluvial analysis, difference being that, automated extraction of stream network using Hydrology modelling tools of the Spatial Analyst/3D Analyst Toolboxes could not be applied on bathymetric data. Instead, manual digitization of the channels is done. Running direct tools on bathymetric data for stream identification can be done to derive probable pathways based on sink points. This technique is quite efficient for estimating the possibility of channels in areas where high-resolution bathymetric data is not available. Prerna et al. (2015) demonstrate this technique for generating a *projected channel system* in the Arabian Sea. However, for minute observations such as in this study, direct digitization of channels is found to be more accurate. Once the channels are mapped, building cross-sections for thalweg identification and longitudinal profiling;

calculation of channel width; estimation of sinuosity and slope gradient for the Indus Fan channels is performed just as for the Indus River.

Channel thalweg is extracted for every 10 km for constructing the longitudinal profile. In areas where high-resolution MBES data was unavailable, seafloor depth from TOPEX mission data (Smith and Sandwell, 1997) are utilised to construct a continuous longitudinal profile of the Indus Fan and channel pathway estimates were adopted from Prerna et al. (2015). For the channel width profile, straight line transects were drawn perpendicular to the channel axis using *DrawPerpendicularSeg tool – AddIn* at 100 m interval for effectively capturing variations in width. Using the cross-sectional area (CSA) approach presented by Qin et al. (2016), channel width is estimated with the lower channel bank as the starting limit, where channel banks occur at different depths. Sinuosity and slope gradient (percentage rise) are estimated at 10 km interval. Other than the longitudinal profile, the remaining parameters are estimated only where MBES data is available.

For representation, the methods for calculating these parameters for a single channel in the Middle Indus Fan are shown in Fig 3.13 (from Prerna and Kotha, 2020). [1, 2, 3, 4 represent four different approaches for extracting each parameter, respectively].

After compiling morphometric data for—the Indus Basin and river, and for the Indus Fan and its channel levee system, comparison based on (a) parameter and (b) stage of development is performed. Fig 3.14 summarizes the entire methodology adopted in this study.

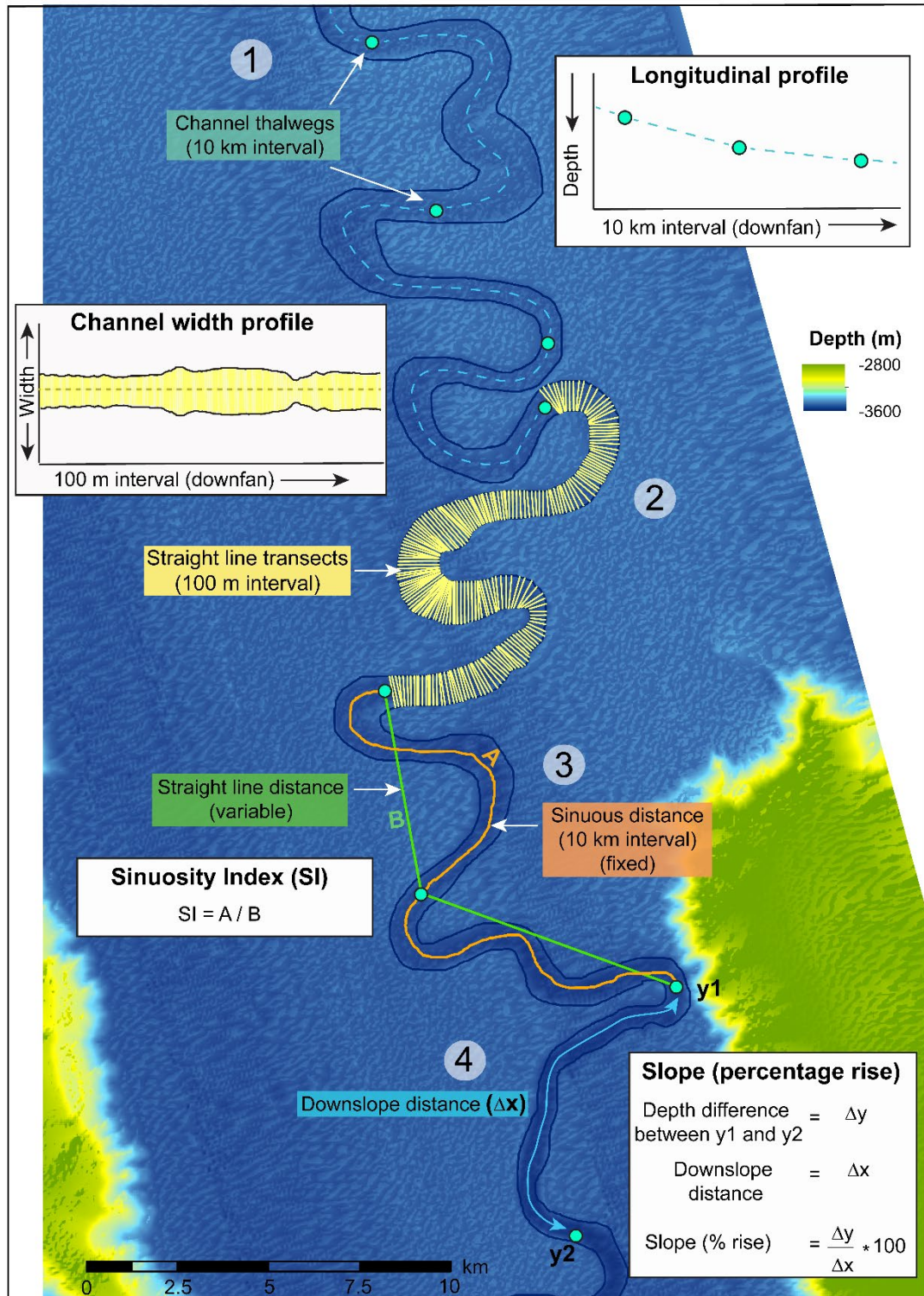


Fig 3.13: Geomorphometric parameter estimation for a part of Middle Indus Fan channels using MBES data. 1: Construction of longitudinal profile by plotting thalweg points at 10 km interval; 2: construction of channel width profile using straight line transects at 100 m interval; 3: calculation of SI using sinuous distance (A) fixed at 10 km divided by straight line distance (B); and 4: calculation of slope (percentage rise) for every reach of 10 km. (Figure from Prerna and Kotha, 2020)

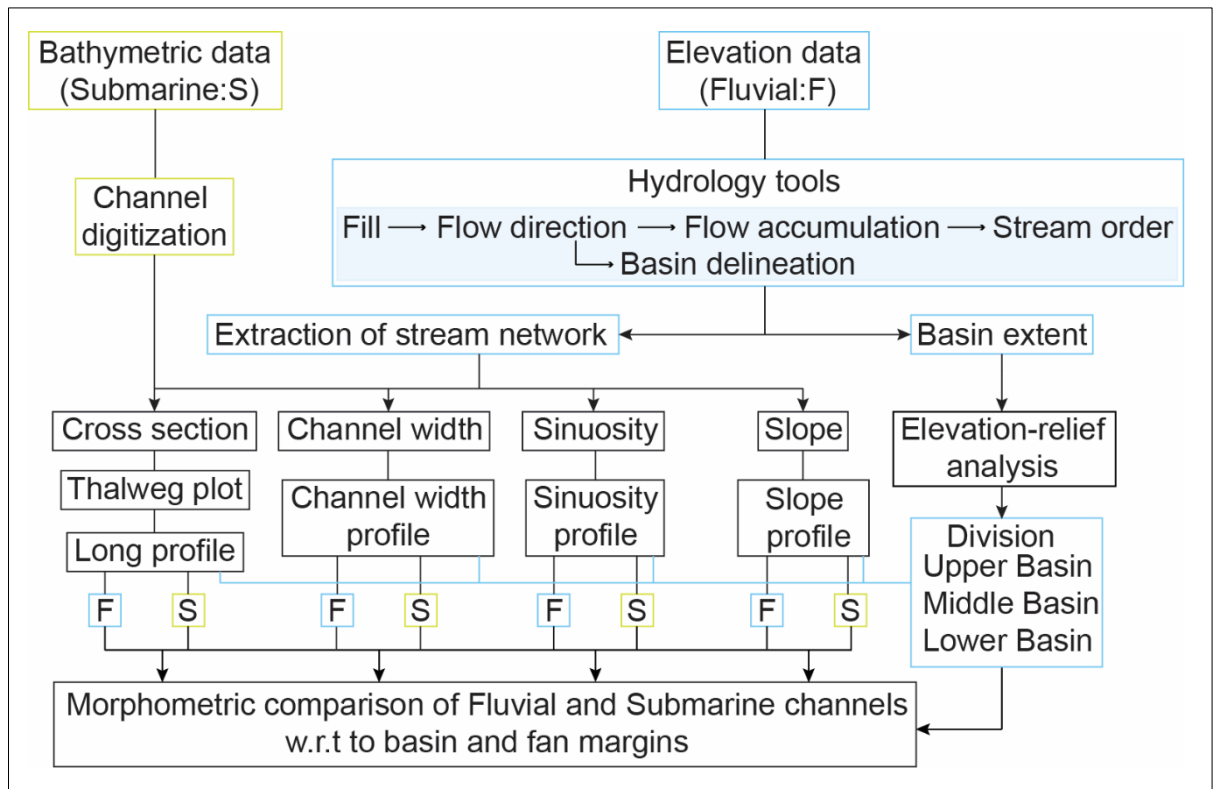


Fig 3.14: Summarized methodology for morphometric comparison of fluvial and submarine channel behaviour on a one-to-one basis—i.e. basin vs fan. Blue and yellow boxes represent fluvial and submarine process/method respectively.

Here, it is also important to discern the implications of utilising variable datasets and consequentially, different methods, for data generation. As stated above, for the bathymetric analysis, manual digitization was more befitting as opposed to automated extraction, primarily because—(a) data from Blocks S1, S2 and S3 were of variable spatial resolution, and (b) data was fragmented; with voids in certain pockets. On the other hand, manual digitization for the entire grid of DEM tiles seemed fairly inept, and therefore, an appropriate GIS model was implemented. Furthermore, the spatial resolution of DEM data was consistent. With these being the only notable differences, it would be fair to say that the methodologies are designed to smoothen out the variations inherent in the data and bring forth comparable data products.

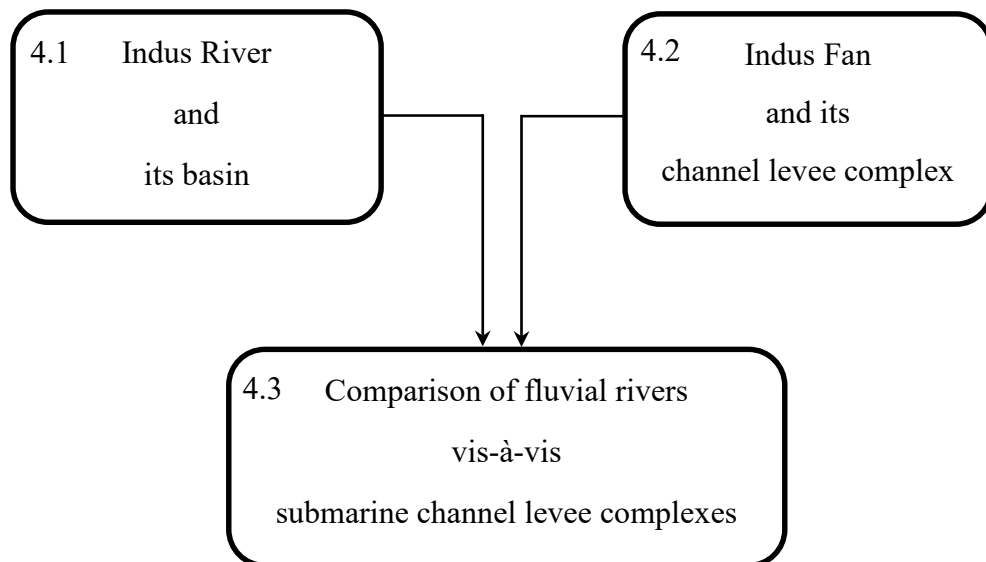
## **CHAPTER 4**

# **DATA ANALYSIS AND INTERPRETATION**

## CHAPTER 4

### DATA ANALYSIS AND INTERPRETATION

This research comprises of two kinds of data analysis—fluvial analysis using DEM data and submarine analysis using MBES data, followed by a parametric and stage-wise comparison of the two systems. The rationale behind using this two-way comparative approach is to identify the effects of the different processes that operate in each stage of river/channel development and also to control the extent of comparison. As mentioned earlier, parametric data from the upper basin are compared with the upper fan; data from middle basin with the middle fan; and data from lower basin with the lower fan. In this chapter of the thesis, the complete analysis and interpretations of the fluvial and submarine channel morphometry is discussed in depth, divided into three parts as shown below:



The first and second sections present a thorough morphometric account of the Indus Basin, and of the Indus Fan respectively, while the third section details the variations observed in the morphometric forms of fluvial rivers and submarine channels.

#### **4.1. Indus River and its basin**

The Indus Basin is one of the largest fluvial controlled landscapes of the world. Despite its large socio-economic relevance in South Asia, a detailed account of its morphometric variations for the entire course is still sketchy. A first-ever quantitative demarcation of the Upper, Middle and Lower Indus Basin is proposed, supported with geomorphometric analyses using five parameters, namely, longitudinal profiling, channel width, sinuosity, planform, slope and elevation-relief ratio (Prerna et al., 2018).

Analysis performed on DEM data, co-validated with other satellite data is efficient to extract the blueprint of the entire Indus River system and its tributaries. Mosaicking the entire data into a single dataset produces an extremely large file which albeit, useful for visual interpretation is unstable for modelling. Thus, each tile of the data is modelled separately to maintain accuracy and avoid data slivers. Once the data from all tiles are stitched together, calculation of geomorphometric parameters is performed. These parameters are (a) longitudinal profile; (b) channel width; (c) sinuosity; (d) planform and; (e) slope which are estimated for the Indus River. Elevation-relief ratio and hypsometric curve is calculated for the Indus Basin. Thence, a trend / profile of every parameter from river source to mouth is constructed. Association of each parameter with others is essential in order to identify and explain the sharp variations in morphometry. Based on an amalgamation of all parameters, the Indus Basin is divided into Upper, Middle and Lower Basin considering river behaviour, basin development, and anthropogenic effects. In further sections, each parameter/index used to build this morphometric account is detailed.

##### *4.1.1. Stream network identification*

The fundamental prerequisite for doing morphometric estimation of the Indus River was to extract the entire stream network, i.e. the river and tributaries and delineate the basin margins.

As explained in Section 3.2.1, several tools for automated extraction were run sequentially on DEM data tiles. The vector files generated from every tile were then coalesced to demarcate the main Indus River, its basin and contributing tributaries. Fig 4.1 shows the entire Indus network overlaid on the mosaicked DEM generated from CartoDEM and SRTM data (CartoDEM v-3 R1 2015; Jarvis et al. 2008). Geomorphometric parameters, in this study, are discussed only for the principal stream, i.e. the Indus River (marked as deep blue Fig 4.1).

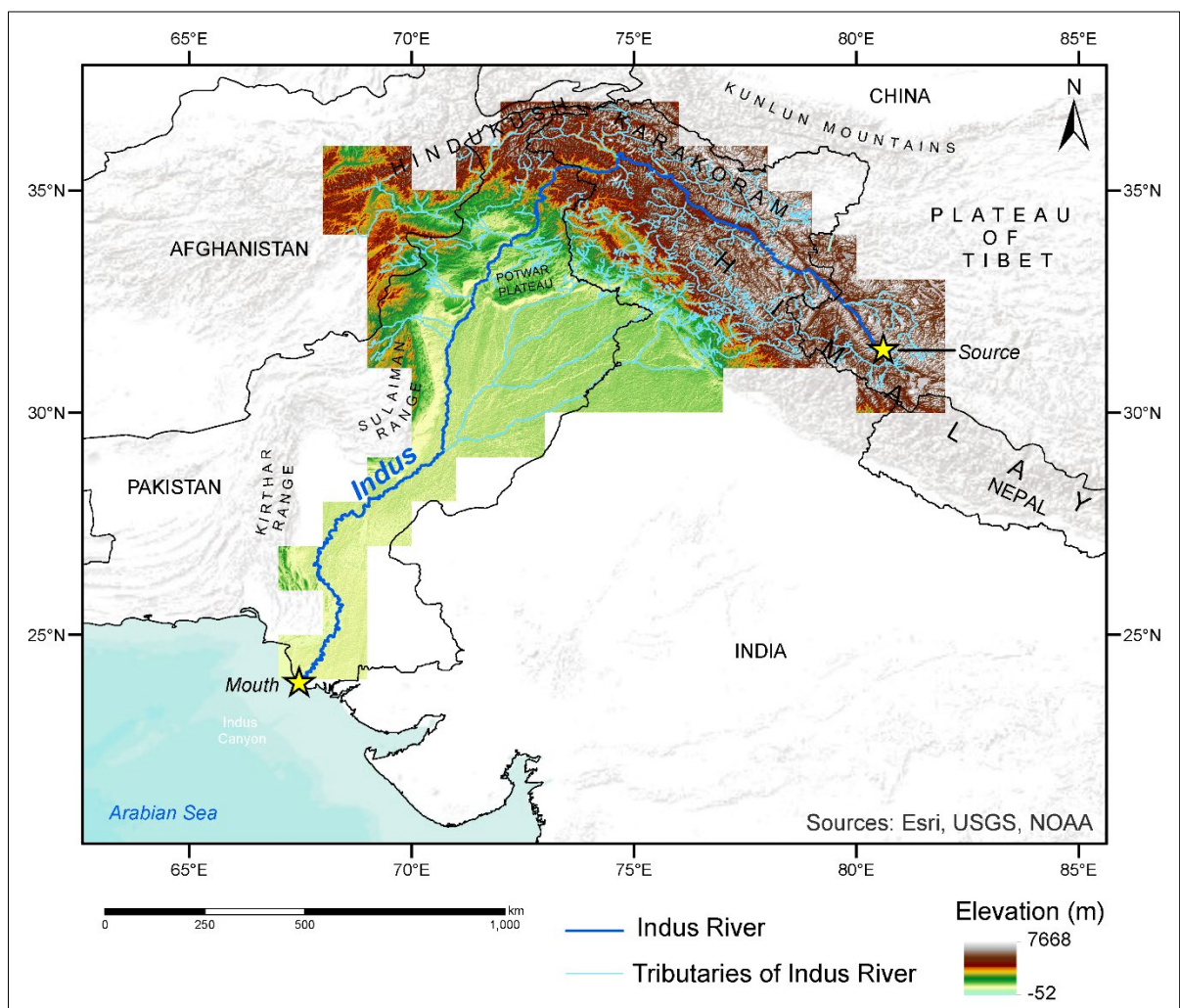


*Fig 4.1: Mosaicked grid from 78 tiles of DEM data superimposed with the extracted Indus drainage network. Bold blue line represents the Indus River, lighter blue lines represent tributaries, and yellow stars denote the river’s source and mouth. (Figure from Prerna et al., 2018)*

#### *4.1.2. Longitudinal profiling and channel width analysis*

The greatest benefit of a river's longitudinal profile is that it instantly delivers the morphological changes of a river from its source to the mouth. If accurately constructed, the profile is capable of representing every contrasting relief feature, because it is sensitive to elevation change. The profile of this 3000+ km long river is indeed quite interesting (Fig 4.2) Prerna et al. (2018) records the entire physiographic and tectonic record of the Indus River deduced from its longitudinal profile. The same account is produced below:

With the confluence of Gar Zangbo and Sênggê Zangbo flowing in the Gangdise Shan Range on the Tibetan plateau, the Indus originates north of the Indus Suture Zone (Clift, 2017). Gar Zangbo originates near a small lake Cuo Ma'erdeng (31°23'46"N, 80°32'25"E). At 4682 m above sea-level, this location has been considered as the source of the Indus River (Prerna et al., 2018). Following a steep gradient for the first 100 km of its course, the river widens into a lens shaped depositional valley with anastomosing channels. [Anastomosis occurs mostly under relatively low-energetic conditions near a (local) base level results causing partial diversion of flow from an existing channel onto the floodplain (Makaske, 2001)]. In this zone, Gar Zangbo gets united with the E-W flowing Sênggê Zangbo at 170 km from its origin (thereafter known as the Indus River) and roughly 30 km from there enter the Indian Territory.

Indus flows in a fairly SE-NW direction amidst the Ladakh and Zaskar ranges. A sharp rise in slope gradient is observed in the longitudinal profile of Indus at roughly 400 km, in Leh district, which continues till the Leh valley where the river widens marginally. This is typically attributed to the tectonically active Karakoram Fault (Fig 4.3) known to have caused substantive deformation in the region (Searle, 1996; Murphy et al., 2000). Vertical downcutting is dominantly observable in the longitudinal profile/cross-sections, till the Leh Valley. Indus is joined by the 138 km long Zaskar River from SW roughly 570 km away from its source.

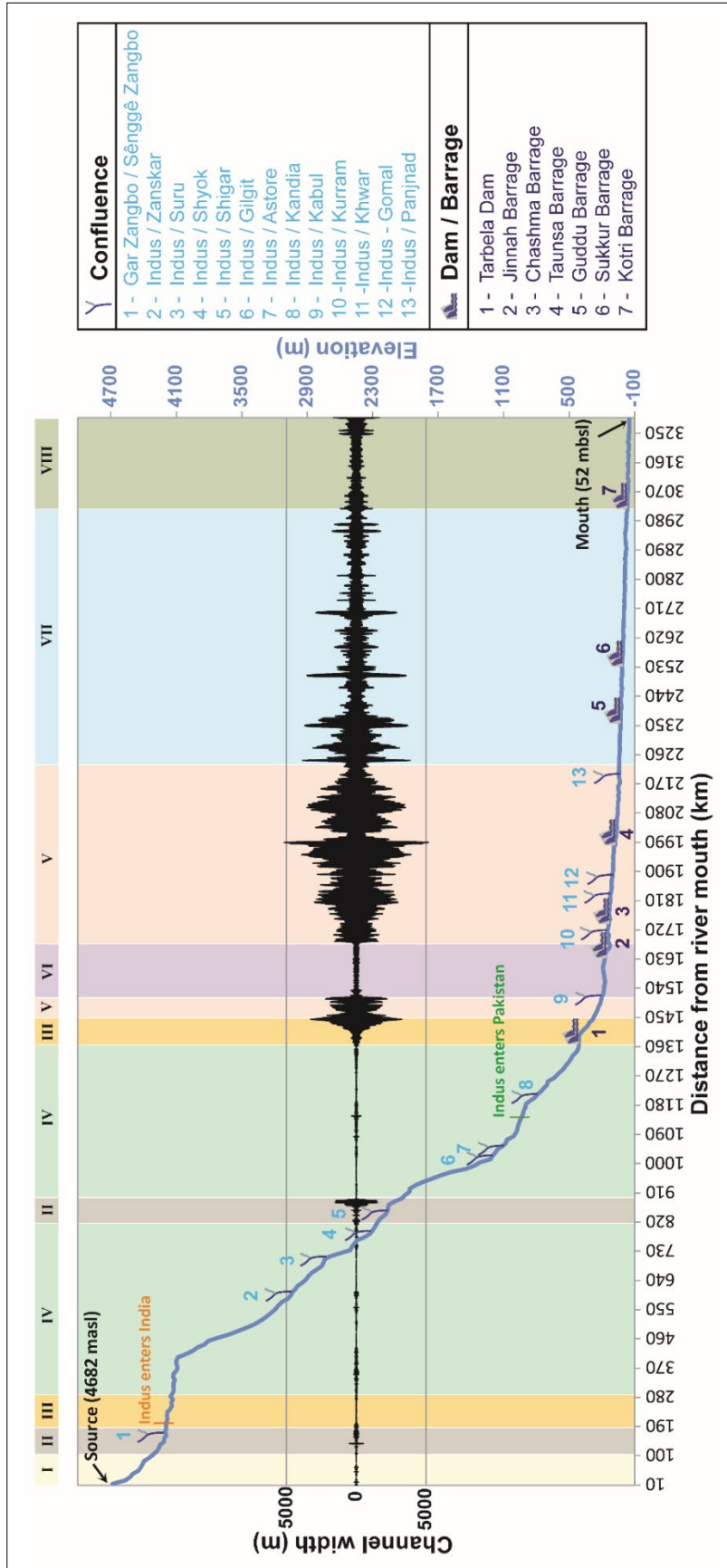
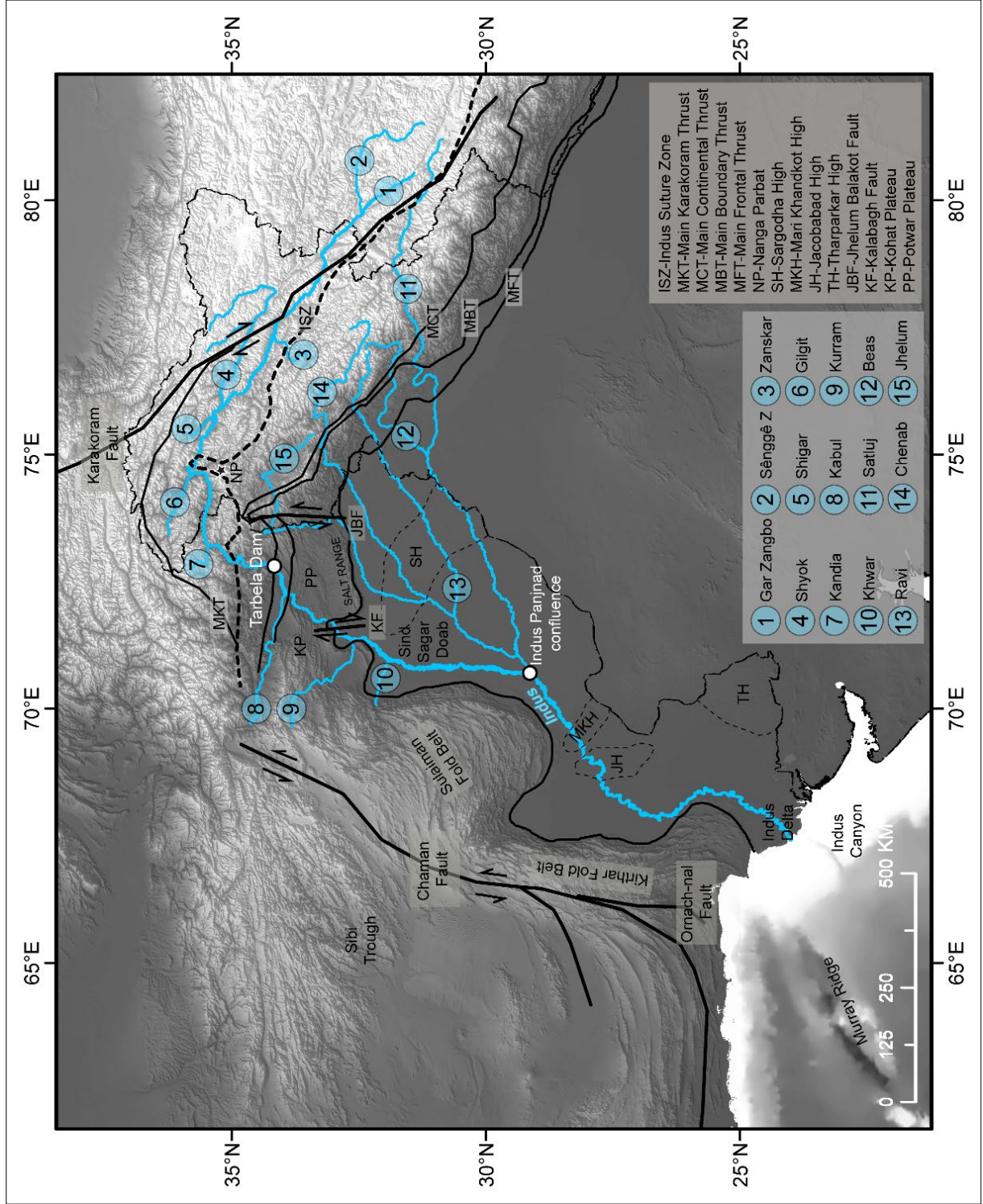


Fig 4.2: Longitudinal profile of the Indus River with channel width denoted at every 100 m. Channel width is represented as distance from channel axis to either bank, for e.g., if the width at a given point is 500 m, the graph would show 250 m on either side from 0 (primary ordinate). Different colour bands indicate the extent of each planform type (I to VIII) across the course of the river, discussed in Section 4.1.3 (Fig 4.6). Confluence points of Indus with its tributaries and major dams/barrages along its course are also marked. (Figure from Prerna et al., 2018)

Fig 4.3:  
 Tectonic map of  
 the Indus Basin  
 with major thrust  
 zones/faults  
 marked; modified  
 from Yin (2006),  
 Afzal et al. (2009),  
 Chen and Khan  
 (2010), Asim et al.  
 (2014), Mukherjee  
 (2015) and Prerna  
 et al. (2018). 15  
 major tributaries  
 of the Indus River  
 are plotted.



Suru River unites with Indus further 150 km downslope, and together they continue towards a major confluence at 850 km from the source in the Skardu valley district of Gilgit-Baltistan region of rivers Shyok and Shigar. This zone of channel widening and anastomosis is evident on the channel width profile (confluence 5, Fig 4.2). Near the Siachen glacier, Nubra River originates while the 525 km long Shyok River originates from the Rimo glacier. The confluence point of rivers Nubra and Shyok together form a major valley of the Ladakh district known as the Nubra valley. After Shyok joins Indus from the east and Shigar from the north at Skardu valley, the Indus River continues to incise through the Nanga Parbat massif with increased momentum (marked as NP, Fig 4.3). The Nanga Parbat massif is the northern outcrop termination of the Indian Plate as a gently northward plunging antiformal structure, and its tectonic contact with the overlying Kohistan island arc forms a ductile shear zone (Butler et al., 1992; Zeitler et al., 2001). It further acts as a demarcation between the plutonic rocks of the Kohistan-Ladakh Batholiths from the crystalline shield rocks of the Indian Plate (Dipietro et al., 2000; Ahmed, 2013). To flow around the impervious metamorphic rocks of the Indian shield, in northern Astore district, the river here makes a peculiarly evident U-shaped bend. Indus is then joined by its tributary from NW, the Gilgit River that flows for 245 km in a W-E direction originating from the Shandur Top Lake area. At the boundary of Skardu and Astore district of Gilgit-Baltistan region, the river forms a major gorge called the Rondu Canyon running for nearly 200 km between Sassi and Silbu (Butler et al., 1992; Kazmi and Jan, 1997). Due to the highly faulted structures and shear zones criss-crossing the area (Ahmed, 2013), the drainage pattern shows anomalies, evident in the longitudinal profile. Major whirlpools and enormous water masses causing rapids and waterfalls are witnessed in this belt. The sharp change in gradient in the longitudinal profile coeval with drastic drop in channel width between Skardu valley and confluence of rivers Indus and Gilgit represents this geomorphological zone (~1000 km from source).

Another 30 km further, Astore River from the west joins Indus. From this point, the river exits the Deosai mountain range resulting in a smoother longitudinal profile. The Indus River exits the Indian Territory and enters the Khyber Pakhtunkhwa Province of Pakistan at ~1150 km from its source (former North Western Frontier Province) (Fig 4.2).

After entering Pakistan, the first major tributary to join Indus from NW is the Kandia River. It originates from the Hindu Kush Mountains. Shortly before this confluence, a major drop in channel gradient is observed because it is here that the river forms the world's deepest gorge (6500 m from valley floor to ridge crest) in the Patan-Dasu region (Kazmi and Jan, 1997). The Kandia waterfalls near Kotgala region are known to be present in this area. Unfortunately, though, available literature is insufficient to identify the precise location of these falls. The Indus River further flows in a S-SW and soon exists from the undulating high relief of the Greater Himalayas, making its way into the Lesser Himalayans. A marked gradient fall facilitates a very strategic location for the Tarbela Dam Reservoir, world's largest earth-filled dam, built in 1974. This dam was served the purpose of irrigation and power generation, although, White (2001) projected the cessation of power generation and a decline in irrigation due to the heightened annual sediment inflow of over 200 million tonnes. It may not be inaccurate to expect this enormous human built dam to have caused a major transformation to the river's planform. Satellite imageries from certain locations presented in Section 4.1.6 are helpful in ascertaining the influence of the Tarbela Dam.

Beyond this point, one of the most significant right-bank tributaries of Indus, the Kabul River joins the Indus. Originating from the Panjshir province of Afghanistan, flowing eastward, it spans a distance of around 400 km before joining Indus near Attock in Pakistan. Its two tributaries from the Hindukush are Kunar and Swat. Haro River joins Indus from the east further 20 km after rivers Kabul and Indus unite. The confluence of Haro with Indus is yet another strategic location for hydropower generation, established as the Ghazi Barotha

hydropower project. As the river progresses south, it encounters a distinct geotectonic zone largely covered by Neogene Siwalik molasses (Kazmi and Jan, 1997) in Pakistan's Punjab Province, called the Kohat Potwar fold belt. The river cuts across the Kohat and Potwar Plateau (marked as KP, PP in Fig 4.3) before advancing through the Kalabagh gorges southward into the Salt Range. The western and north-western parts of the Salt Range are recorded as tectonically active ranges (Warwick, 2007). The entire system consists of residual hills from glacier debris (Encyclopædia Britannica, 2011) and is bound by Indus to the west and Jhelum to the east (Kazmi and Jan, 1997). The middle section of the plateau is associated with the structurally downwarped basin of Soan River that suggests tectonic movement in shaping the morphology (Prerna et al., 2018). The terrain mostly includes interlaced ravines, which are set deep in the soft Shiwalik beds composing the whole area (Ziring and Burki, 2019). The Salt Range—a highly upheaved block of the Indian Continental Shield is said to be one of the many structural-tectonic subdivisions of the Potwar Plateau (Khan et al., 1986; Gee and Gee, 1989). In this tectonically restricted basin, Indus is characterized by near vertical channel walls with minimal scope for lateral expansion, which results in the evidently reduced channel width. The Kalabagh fault (KF in Fig 4.3) forms the western margin of the Salt Range. It displaces the Salt Range Thrust (McDougall and Khan, 1990; Kazmi and Jan, 1997) and has also caused offset to the course of the Indus (Prerna et al., 2018). Once the river exists this geotectonic unit after the Kalabagh Fault, it flows through the Punjab Foreland. Here, the river is mostly characterized by broad channel widths, barring few locations which are anthropogenically controlled. No other significant variation in morphometry is observed. A doab is referred to the land between two confluent rivers. Sind Sagar Doab region is a wide and flat part of the Indus's course where it is joined by another major right-bank tributary, the Kurram River. It joins the Indus near Isa Khel town of Mianwali district in Pakistan after flowing ~300 km from the Spin Ghar Mountains of eastern Afghanistan. 20 km south of Kurram-Indus confluence is the

Chashma Barrage, which was constructed in 1971 to regulate the waters of the Indus. Two southern-most tributaries, namely, Khwar and Gomal, incise through the Sulaiman Range and join the Indus near Dera Ismail Khan, shortly after the Chashma Barrage. From here, until the Taunsa Barrage, that lies 2000 km down the course of Indus, the river attains maximum channel widening and braiding. After the Taunsa Barrage, the channel width, which includes sand bars/temporary islands, goes beyond 10 km. Finally, the river is conjoined by all its major left-bank tributaries draining the north western plains of India (rivers Satluj, Beas, Ravi, Chenab and Jhelum), which before joining Indus are collectively known as the Panjnad River. This major confluence occurs near Alipur town in Punjab district of Pakistan. The Indus Basin, after the confluence till its delta, is traversed by a number of basement highs like the Sargodha, Jacobabad etc., extending NW-SE for varying distances into uplifted regions (Khan and Clyde, 2013). Through the Guddu and Sukkur Barrages up till Mohanjo Daro, the river follows a NE-SW orientation, from where Indus flows southward, parallel to the Kirthar Range. The Kotri Barrage, last major construction on the Indus, is 300 km away from its delta. In its final reaches, the river roughly widens between 1 to 3 km, before draining into the Arabian Sea near Keti Bandar (23°59'33" N, 67°25'22"E). Completing a total distance of 3329 km from its source to the mouth, the river showcases several characteristic planform types, which are discussed in the following section.

#### *4.1.3. Sinuosity analysis and planform classification*

Using the value of Sinuosity Index (SI), streams can be classified as straight, meandering or braided (Prerna et al., 2018). Rosgen (1994) developed a river classification system wherein, SI was used as one of the parameters to differentiate among river types. Dey (2014) has presented a simpler classification into straight (<1.1), sinuous (1.1 – 1.5) and meandering

(>1.5). Makaske (2001) proposed the value of 1.3 as a distinction between straight and meandering streams.

The sinuosity plot of Indus River superimposed on its longitudinal profile shows a clear increase in sinuosity from source to mouth (Fig 4.4). SI ranges from 1.007 to 3.221. The first peak in the sinuosity profile coincides with the point where Indus makes a peculiar U-shaped bend in the Astore district between 900 and 1000 km. The second peak occurs at 1360 km from the source, shortly prior to the location of the Tarbela Dam. Thereafter, a zone of low sinuosity further downstream is due to impervious terrain of the Potwar plateau region, limiting the scope of the river to meander along its axis and controlling the river's overall morphometry.

At the point where Indus is conjoined with its five major left-bank tributaries, sinuosity can be seen to rise moderately at ~2170 km from source. After that, sinuosity sharply rises beyond Guddu Barrage at 2350 km (Fig 4.4), and follows an undulating form of sinuosity till it drains into the Arabian Sea. It can be ascertained through this analysis that geological formations control sinuosity in the upper and middle basin, however, heightened sinuosity in the lower basin occurs as a result of the dual effects of flatter topography and anthropogenic influences.

In terms of planform, Indus ideally follows a typical transition along its course, barring a few atypical forms, highlighting its uniqueness. Based on Rosgen (1994) and Makaske (2001), a distinction between anastomosed and braided channels is followed. An anastomosing river is a multi-channel river which is fundamentally different in form from a braided river. They have multiple channel belts, while braided rivers have a single channel belt but multiple thalwegs (Makaske, 2001) (Fig 4.5). Schumm (1985) defined anastomosing channels as true multi-channel systems, different from anabranching rivers which are essentially braided rivers with large exposed bars in relation to channel width. Anastomosing rivers are a composite form where individual channel belts may be braided/meandering/straight, resulting from in-channel processes such as lateral erosion and accretion or mid-channel bar formation (Makaske, 2001).

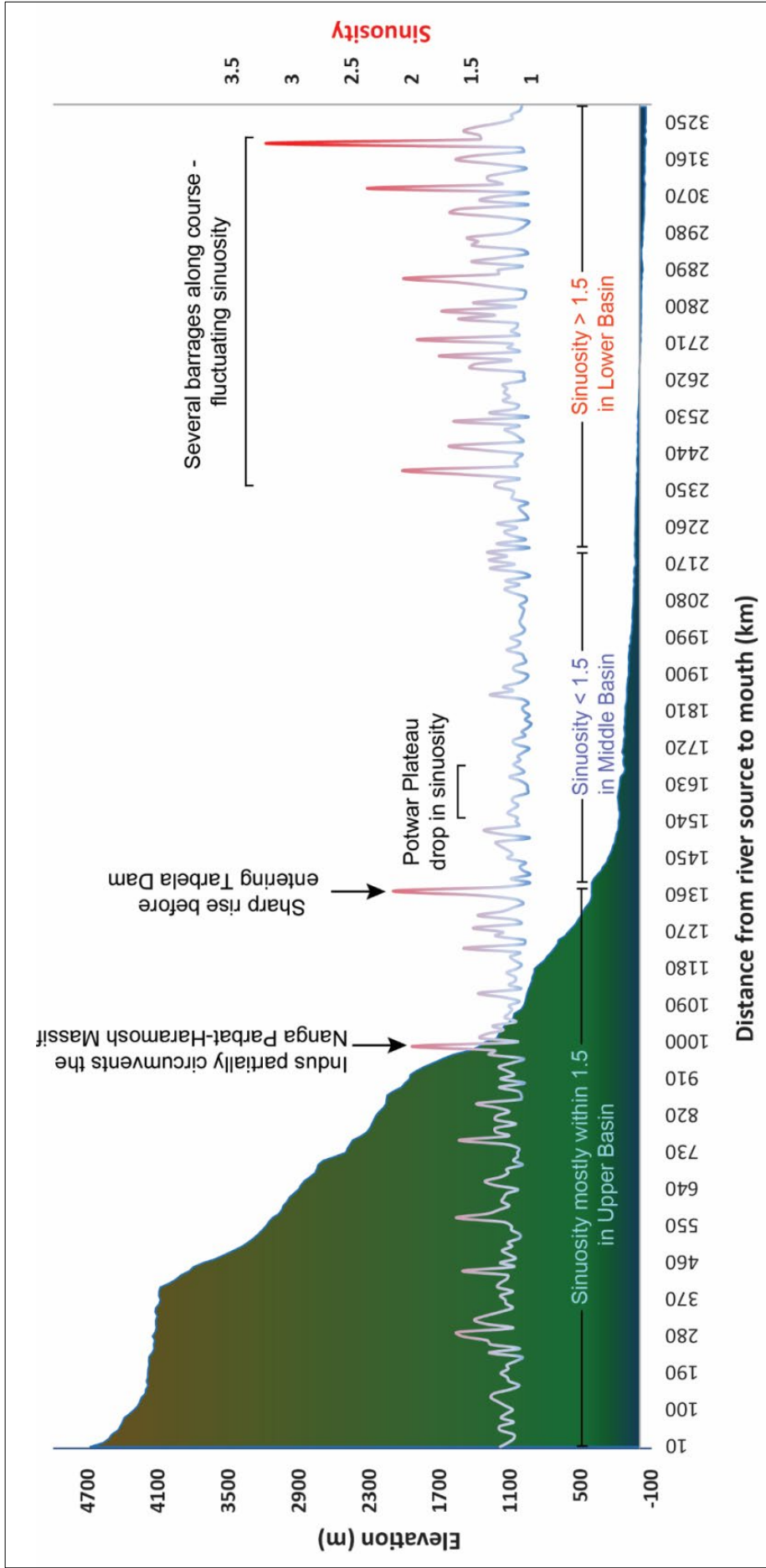


Fig 4.4: Plot of sinuosity values measured for every 10 km reach superimposed on the longitudinal profile of the Indus. SI ranges from 1.007 to 3.221. Demarcation of Upper, Middle, Lower Indus Basin shown here is discussed in Section 4.1.6. (Figure from Prerna et al., 2018)

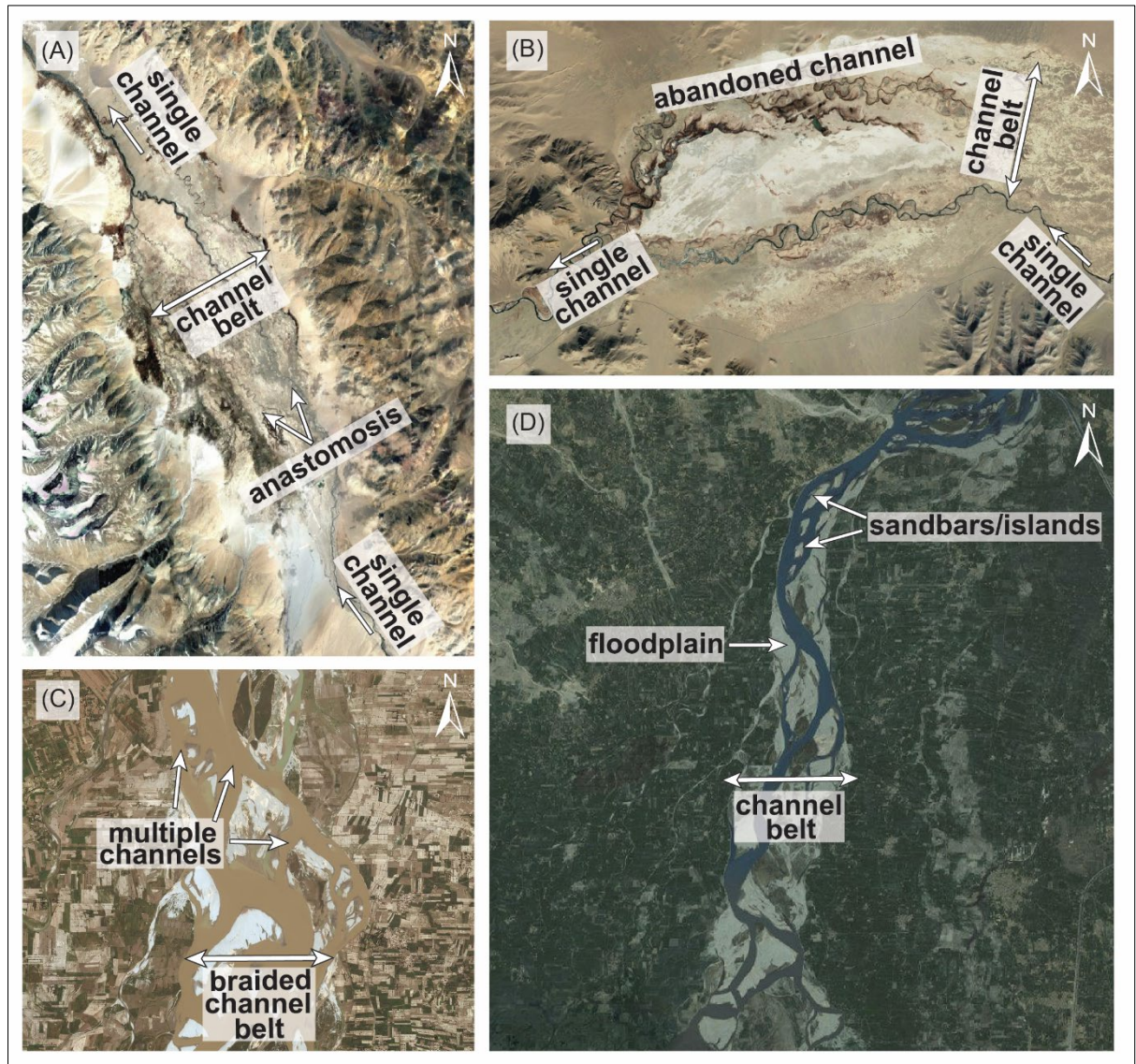


Fig 4.5: (A) Anastomosis of Gar Zangbo in the Tibetan plateau – channel splits from singular to multiple to single again due to drop in valley gradient causing loss of energy; (B) Sênggê Zangbo undergoes anastomosis – channel avulsion may have caused abandonment of one channel, broad channel belt indicates paleo-course; (C) Braided channel belt with multiple streams divided by depositional features; (D) Braided channel with exposed floodplains/sand bars etc. caused by lateral aggradation of the Indus River. (Source: Google Earth™). (Figure from Prerna et al., 2018)

Eight distinct planform types have been identified based on the cross-sectional and sinuosity behaviour of the Indus River. Fig 4.6 illustrates these planforms and characteristics.

- Type I – In this type, SI is less than or equal to 1.25. The channel planform is straight with dominant vertical downcutting (erosion) and limited lateral aggradation (deposition). This type is typical in the first 100 km near the source of Gar Zangbo in the Tibetan plateau from Lake Cuo Ma'erdeng.
- Type II – Anastomosing channels can include straight, meandering or braided channel belts within itself and sinuosity for each may be variable. For calculating SI of anastomosing channels, only the sinuosity of the main channel is measured. SI ranges between 1.25 - 1.5 in this planform type. Gar Zangbo undergoes anastomosis after transcending from the highlands towards an unnamed valley [Fig 4.5 (A)]; Indus River also experiences anastomosis in the Skardu valley where Shigar River joins the Indus.
- Type III – SI remains the same i.e. 1.25 - 1.5 as in Type II, but channel behaviour suggests a developing transition from youthful to mature stage of development. Combined vertical downcutting and lateral expansion are noticeable with greater sinuosity than Type I. Cross-sections represent smoother gradient across the channel axis. This characteristic type in the Indus's planform is witnessed after the confluence of Gar and Sênggê Zangbo where there is relatively smoother channel gradient, till about 300 km from the river source.
- Type IV – In this type, lateral aggradation overpowers vertical downcutting and meandering is markedly accentuated. Although vertical erosion is dominant, sedimentation of river load in the form of flood bank deposition starts to occur denoting typical mature stage channel behaviour. This type dominates a major part of the upper course of the Indus River till the Tarbela Dam, barring only the short extent where anastomosis is observed.

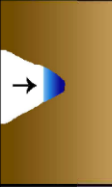
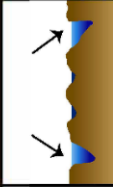
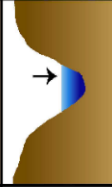
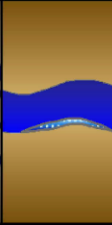
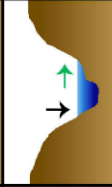
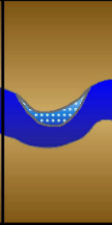
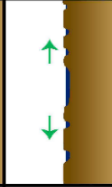
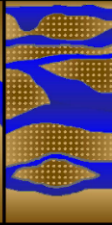
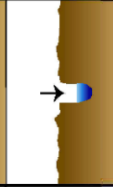
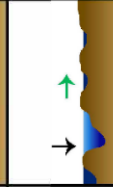
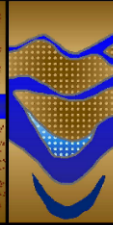
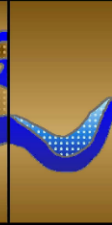
TYPE	CROSS SECTION	SINUOSITY	PLANFORM	DESCRIPTION
I		< 1.25		Vertical downcutting; low sinuosity; no lateral aggradation; typical youthful stage
II		1.25 - 1.5		Anastomosing channel; prime cause - drop in channel velocity/avulsion; sinuosity variable; typical mature stage
III		1.25 - 1.5		Vertical downcutting (non-centered); increased sinuosity than Type I; mild flood-bank deposition; youthful to mature stage
IV		> 1.5		Vertical downcutting and lateral aggradation; increased sinuosity than Type III; significant flood-bank deposition; typical mature stage
V		< 1.25		Braided channel; prime cause - drop in channel velocity/increased sediment load; multiple main channels; lower sinuosity than Type IV; large sand bars; typical mature stage
VI		< 1.25		Vertical downcutting; very low sinuosity; no lateral aggradation; structurally controlled; U-shaped valley
VII		> 1.5		Braided channel; single main channel; higher sinuosity than Type V; oxbow/scroll bars/sand bars; mature to senile stage
VIII		> 1.5		Single main channel; badland deposits on flood-banks; higher sinuosity than Type VI; oxbow, scroll bars; senile stage

Fig 4.6: Planform types identified along the course of the Indus River with their characteristics (refer Fig 4.2 for location). (Figure from Prema et al., 2018)

- Type V – A typically braided channel planform type with numerous streams flowing within the channel belt, often forming large elongated sand bars/islands is identified as Type V. Channel belts refer to the zone of activity of a straight/meandering/braided channel including bars and abandoned channel segments (Makaske, 2001). A primary channel may be present or absent with a possibility of channel load being equitably distributed. Because the channel belt is so wide that it appears to have a non-meandering planform, SI is restricted to 1.25. Once the river exits from the Tarbela Dam, excessive braiding can be observed. Again, whence the river exits the Potwar Plateau, it undergoes braiding [Fig 4.5 (C)] till its confluence with Panjnad River.
- Type VI – The Indus River portrays a characteristically distinct and unique planform which has been described as Type VI. Carving a peculiar U-shaped valley, the river flows through a structurally controlled and restricted path—in the region of the Potwar Plateau which causes a drastic change in the channel width profile of the river. Channel sinuosity is rather confined to a maximum of 1.25. Such a planform is typical of rivers in higher relief, but the Indus River flows through a U-shaped valley in the Middle Indus Basin. Right from Indus-Kabul confluence till the Jinnah Barrage, the river's cross-sections show U-shaped valleys with relatively straighter walls.
- Type VII – This type represents increased channel sinuosity of more than 1.5 with characteristics of mature to senile transition. Common features include ox-bow lakes, cut-offs, scroll bars, sand bars. Channel avulsion is also commonly observed. It is similar to Type V with respect to braiding behaviour, but increased sinuosity with the presence of a distinct primary channel differentiates this type from the others. Type VII is typical from the Indus-Panjnad confluence till the Kotri Barrage i.e. for most of the Lower Indus Basin.

- Type VIII – At this stage there is a singular active channel with remarkably reduced braiding. Sinuosity remains more than 1.5 with frequently forming ox-bows and scroll bars. As the river approaches in final stage nearing the delta, the system is deprived of sufficient water flow, and the river is able to transport only through one active channel. For the last ~300 km of its course (beyond Kotri Barrage), scroll bars are the only characteristic deposits noticeable along the banks of Indus River. A singular channel flowing alongside numerous abandoned channels and a drop in braiding is the typical planform till the Indus drains into the Arabian Sea.

The Indus River therefore exhibits 8 unique planform types from its source to the mouth, each formed under variable processes and with variable sinuosity. In Section 4.3, these planforms along with other morphometric indices will be compared with the planforms of the Indus Fan channel systems, to highlight their remarkable distinction.

#### *4.1.4. Slope analysis*

Sinuosity is the ratio between channel length and valley length; and as also a ratio between channel slope and valley slope (Flood and Damuth, 1987). For instance, a straight or non-meandering stream with sinuosity index value of 1 would also mean that its channel slope and the valley slope are same (Schumm et al., 2000). However, the relationship between sinuosity and slope is not simple. Schumm and Khan (1972) attempted to test correlation between sinuosity and slope by performing flume experiments, and demonstrated that certain threshold values of slope and/or sediment load exist, above which river patterns like sinuosity could get altered to a large extent. The channels remained straight in low gradient slopes and less sediment load, but as discharge increased, meandering forms developed i.e. higher the increase in gradient and sediment load, higher the sinuosity.

The notion that channel sinuosity and valley slope cannot be employed to predict the value of one another and are rather independent variables of stream morphology has been supported by other research works too. Flume model studies have been found difficult to extrapolate to natural river systems by Schumm and Khan (1972). They further concluded that the role of valley gradient in determining channel sinuosity does not show a strong relationship. Miller (1988) also supported this by mathematically establishing the lack of significance of valley gradient in explaining sinuosity.

Correlation and linear regression analyses of sinuosity and slope (Fig 4.7) indicate a very low positive correlation between the two variables [correlation coefficient ( $r = 0.02$ ), coefficient of determination ( $R^2 = 0.0004$ )]. Therefore, the morphological parameters of channel sinuosity and channel slope for the Indus River also support their mutual exclusivity.

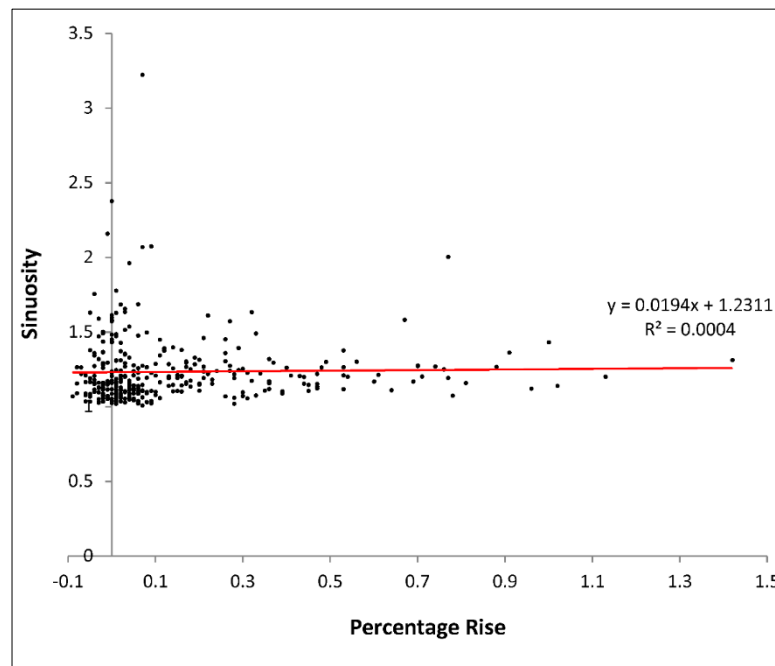


*Fig 4.7: Correlation and linear regression plot showing very low positive correlation between sinuosity and slope (percentage rise) in the Indus River system. (Figure from Prerna et al., 2018)*

It is ascertained that sinuosity and slope can neither be used to predict the value of one another nor are they mutual, but the independent influence of slope gradient on a river's morphometry cannot be ignored. Channel gradient is a key condition that helps a river in maintaining equilibrium and provide efficient conditions for erosion, transportation and deposition. Therefore, in this study, slope or channel gradient has been considered as an important geomorphometric parameter.

The concept of a graded river as defined by Mackin (1948) is a river "...in which, over a period of years, slope is delicately adjusted to provide, with available discharge and with prevailing channel characteristics, just the velocity required for the transportation of the load supplied from the drainage basin". Although, Miller and Miller (2007) believed that Mackin's definition overstates the role of slope, the concept of a graded river is highly valuable in understanding fluvial mechanics. The peaks in the slope profile correlate well with the longitudinal profile of the Indus River (Fig 4.8).

In the first 100 km of the river's course steep gradient exists which is reflected in the percentage rise graph. Thereafter, gentler profile can be observed through the confluence valley of Gar and Sênggê Zangbo. From ~400 km till around 1360 km near Tarbela Dam, sharp change in gradient is evident. The Upper Indus's course is dominated by vertical downcutting and increased gradient till this point. Where Indus River nearly circumvents the northern flanks of the Nanga Parbat-Haramosh Massif (Inam et al., 2008) and joins Gilgit River, the sharpest jump in slope occurs at ~1000 km from river source in the Astore district. This point also coincides with high sinuosity shown in Fig 4.4. The tectonic effects active in this part of the river's course cause knick-points in the longitudinal profile which coincide with numerous peaks in the slope profile. Once the river exits the Upper Indus Basin, smoother slope gradient can be seen in the slope gradient profile till the river's delta.

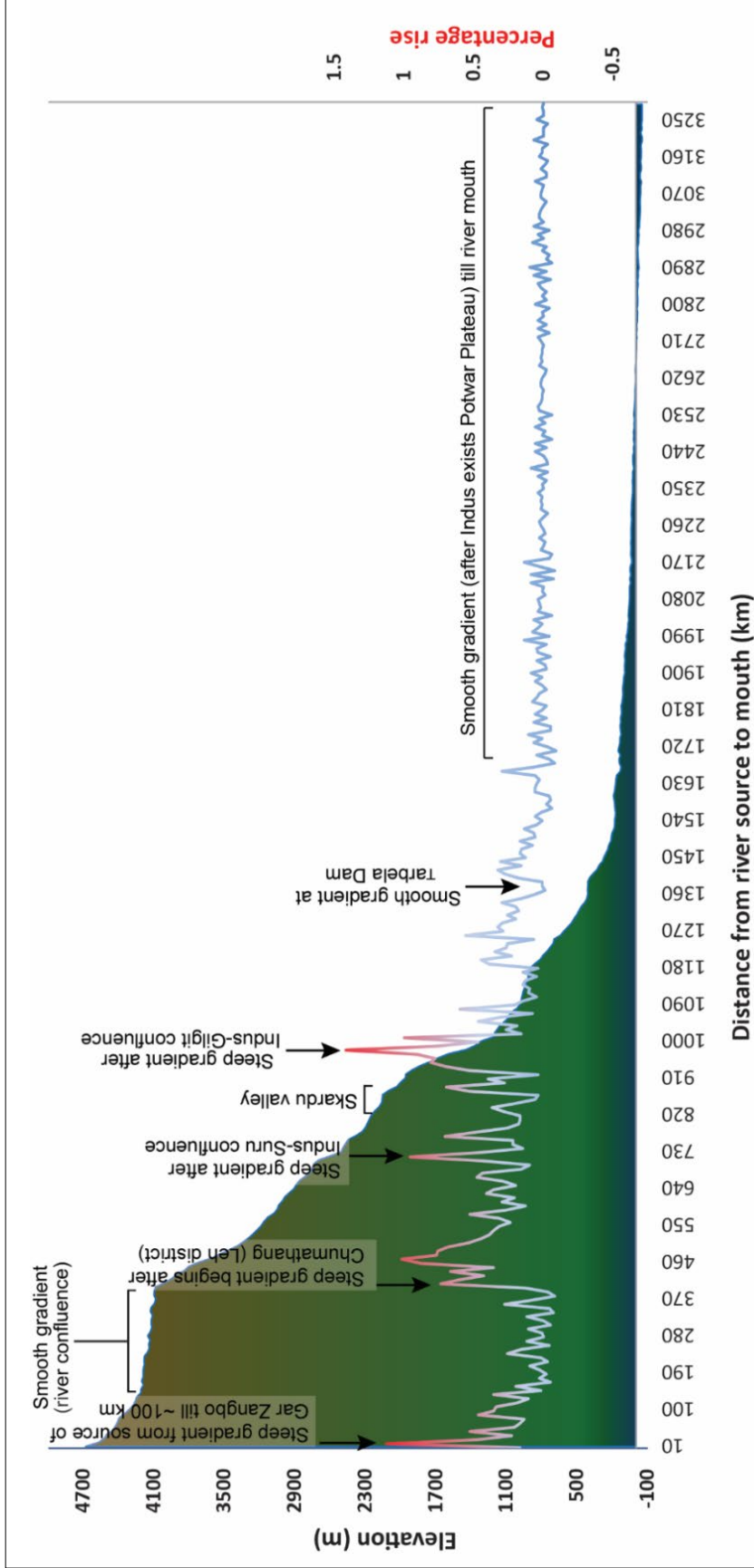


Fig 4.8: Plot of percentage rise measured for every 10 km reach superimposed on the longitudinal profile of Indus River. Slope (percentage rise) varies from  $-0.09$  to  $1.42\%$ . (Figure from Prerna et al., 2018)

#### 4.1.5. Elevation-relief (E) analysis

E can also be expressed as a percentage—an indicator of the remnant of the present volume as compared to the original volume of the basin (Ritter et al., 2002). The approximation of E to HI is discussed previously in Section 3.1.3. There are several inferences pertaining to the interpretation of value of HI or E, summarized in Table 4.1. Strahler (1952) studied three different watersheds, each belonging to a unique stage of the geomorphic cycle. The first drainage basin represented early youth/inequilibrium stage with an integral value of 79.5%; the second basin with a fully mature topography had a value of 43%, and the third basin with old topography had an integral value of 17.6%. The low HI values of old stage basins were mostly associated with the presence of monadnocks—isolated hill/range of hills standing above the general level of a peneplain resulting from the erosion of the surrounding terrain.

Table 4.1: Interpretations of HI/E values (Source – Prerna et al., 2018)

Value of HI or E	Description	Author(s)
> 60%	Inequilibrium (youthful) stage	Strahler (1952)
35 – 60%	Equilibrium (mature) stage	
< 35%	Monadnock stage	
15-40%	Isolated relief features on extensive level surface	Wood and Snell (1960); Pike (1963)
40-80%	Broad level surface broken by occasional depressions	
> 50%	Dominant diffusive/hill-slope processes	Willgoose and Hancock (1998)
~50%	Relatively stable, developing landscape	
< 50%	Dominant fluvial processes	
> 50%	Approaching youthful stage	Singh and Sarangi (2008)
< 50%	Approaching monadnock stage	

Complimentary to the E or HI is the Hypsometric curve (HC). It is related to the volume of the rock in the basin; and the amount of erosion that had occurred in a basin vs. what still remains (Hurtrez et al., 1999). It also allows comparison of forms of basins of different sizes and elevations (Strahler, 1952).

The HC of the Indus Basin [(Fig 4.9 (A))] is complex and challenging to interpret because it shows a combination of stages as per Strahler's model [(Fig 4.9 (B))]. In Strahler's three watershed study, a distinct curve shape is suggested for each stage of landform development, wherein, young basins in inequilibrium follow a convex upward curve, mature basins upon attaining equilibrium follow a typical S-shaped curve and older basins in the monadnock phase have a concave downward trend.

The value of E is 0.31 for the Indus Basin implies that ~31% of the original rock mass is still present within the basin. Interpreting this value of 31% along with HC of the Indus Basin, suggests that a major segment from the middle relief is still experiencing inequilibrium while the remaining basin has attained tectonic stability.

Indus Basin's HC starts with a sharply descending concave curve owing to the small percentage of high relief in its upper reaches. As the percentage area starts to rise, the HC starts to bulge in a convex form in the middle sector, followed by a distinctly concave downward trend, attributable to the high proportion of landmass belonging to lower elevation slabs. Quantitatively, 20% of the area in Indus's drainage basin lies in the highest 40% of relief, 40% of area belongs to the middle 7-60% of relief, and remaining 40% of the area lies within the lowest 7% of relief (Table 4.2, Fig 4.10).

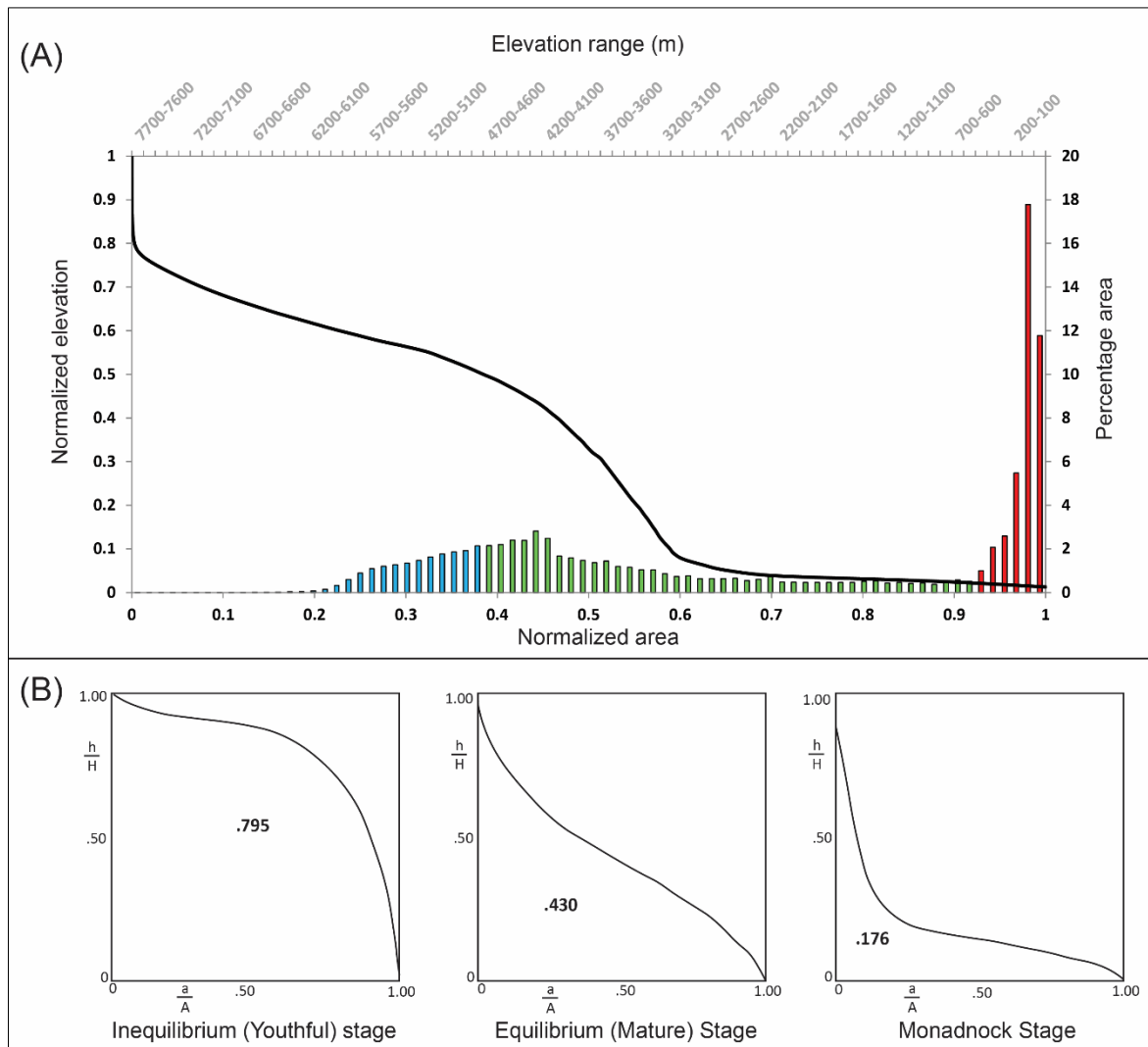


Fig 4.9: (A) Hypsometric curve for the Indus Basin. Normalized area (primary abscissa) is plotted against normalized elevation (primary ordinate) and the secondary axes show percentage areas within each elevation slab (of 100 m interval); (B) shapes of hypsometric curves belonging to youthful stage, mature stage and monadnock Stage with HI of 79.5%, 43% and 17.6% respectively (Strahler, 1952). (Figure from Prerna et al., 2018)

Table 4.2: Stages of development within the Indus Basin based on Hypsometric Curve (Source - Prerna et al., 2018)

Sector	Basin Area (%)	Relief (%)	Elevation (m)	Stage (as per Strahler, 1952)
Blue	20	Highest 40	7700 to 4600 m	Equilibrium - mature stage
Green	40	Middle 53	4600 to 400 m	Inequilibrium - youthful stage
Red	40	Lowest 7	400 to -100 m	Equilibrium - mature stage

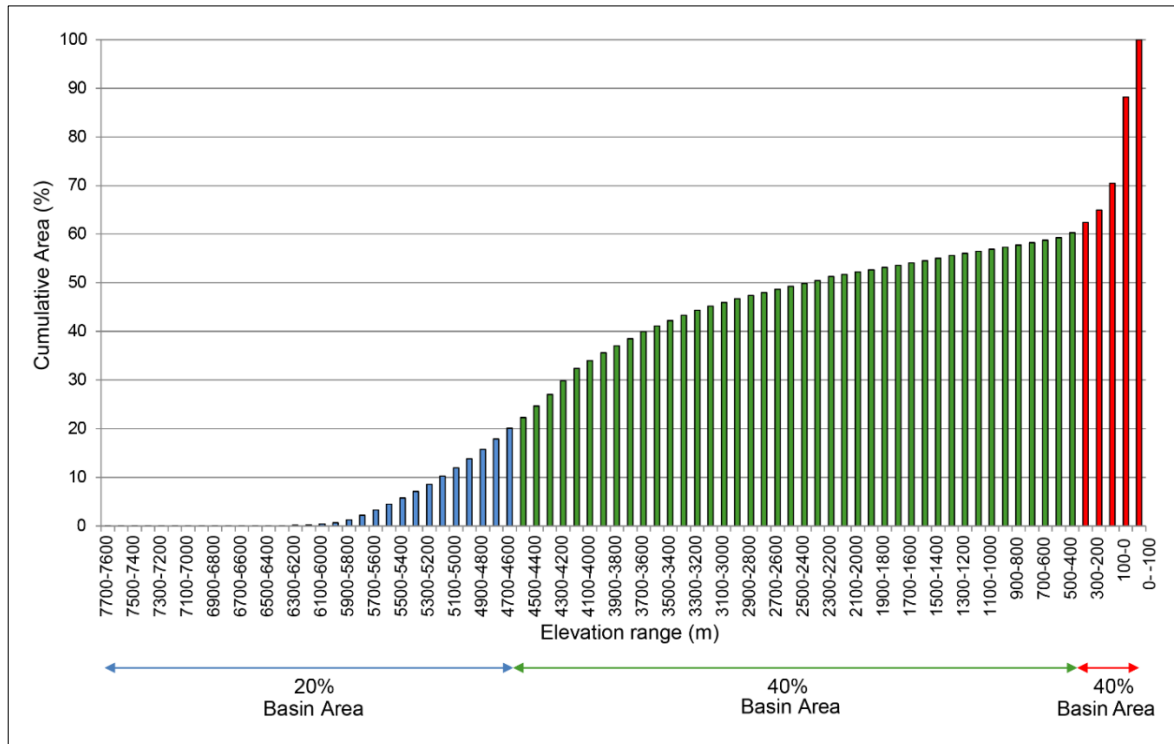


Fig 4.10: Hypsometric curve for the Indus Basin with cumulative percentage area. (Figure from Prerna et al., 2018)

The interpretation of the HC supports that the basin may be undergoing geomorphic transformation in the mid-relief sector, covering 40% of its area (marked in green, Fig 4.10). It is similar in form to the inequilibrium stage given by Strahler (1952). This sector of the Indus Basin has greater proportion of its remnant rock still remaining, therefore, it is inferred that the elevation slab between ~4600 m to ~400 m is yet to attain erosional stability and the denudational processes are still active. The prominent convex bulge in the HC of the Indus River is attributed to this mid-relief sector of the Indus Basin.

#### 4.1.6. Demarcation of Upper, Middle, Lower Indus Basin

Combining the morphometric analyses discussed in Sections 4.1.1. – 4.1.5., it becomes possible to divide the Indus Basin into Upper, Middle and Lower basins. However, in a system such as the Indus, immense exposure to fluvial mechanics, climatic variations and tectonic undulations

with anthropogenic effects cannot be ignored as they give rise to rather interesting structural variations, making the interpretation of the morphometry of this river more challenging. As discussed in previous sections, the tectonic and geological influences in certain parts of the Indus Basin are so vivid that they have steered the evolution of the river course and its adjoining basins. Therefore, a multifaceted approach is essential to quantify down-course physio-morphological variations along the Indus.

Prerna et al., (2018) elucidate the reasons which could be attributable to the complex morphometric trends of the Indus river and its basin. In the past, the river and the basin have undergone and are perhaps still undergoing substantial dynamic changes over a long period of time. River metamorphosis is defined by Schumm (1969) as the complete alteration of river morphology occurring as a result of climate change or anthropogenic causes. Disturbances, both natural or anthropogenic or both, often influence the interactions between driving and resisting forces of landform development, to an extent that the system is stressed beyond the limits of stability and equilibrium (Miller and Miller, 2007). Disequilibrium may lead to an altered or metamorphosed form that continuously strives to attain equilibrium by coping with the modified conditions. A river system like Indus, which has witnessed severe anthropogenic adjustment in the recent decades, along with climatic and tectonic upsurges in geologic time is bound to undergo metamorphosis. Satellite imageries are excellent sources which can be effective to observe such adjustments (Fig 4.11 - 4.13). The imageries exemplify the modified planform of the river with records of pre and post construction of barrages/dams. Major course alteration, ox-bow formations, disappearance of smaller channels etc. are evidences of metamorphosis.

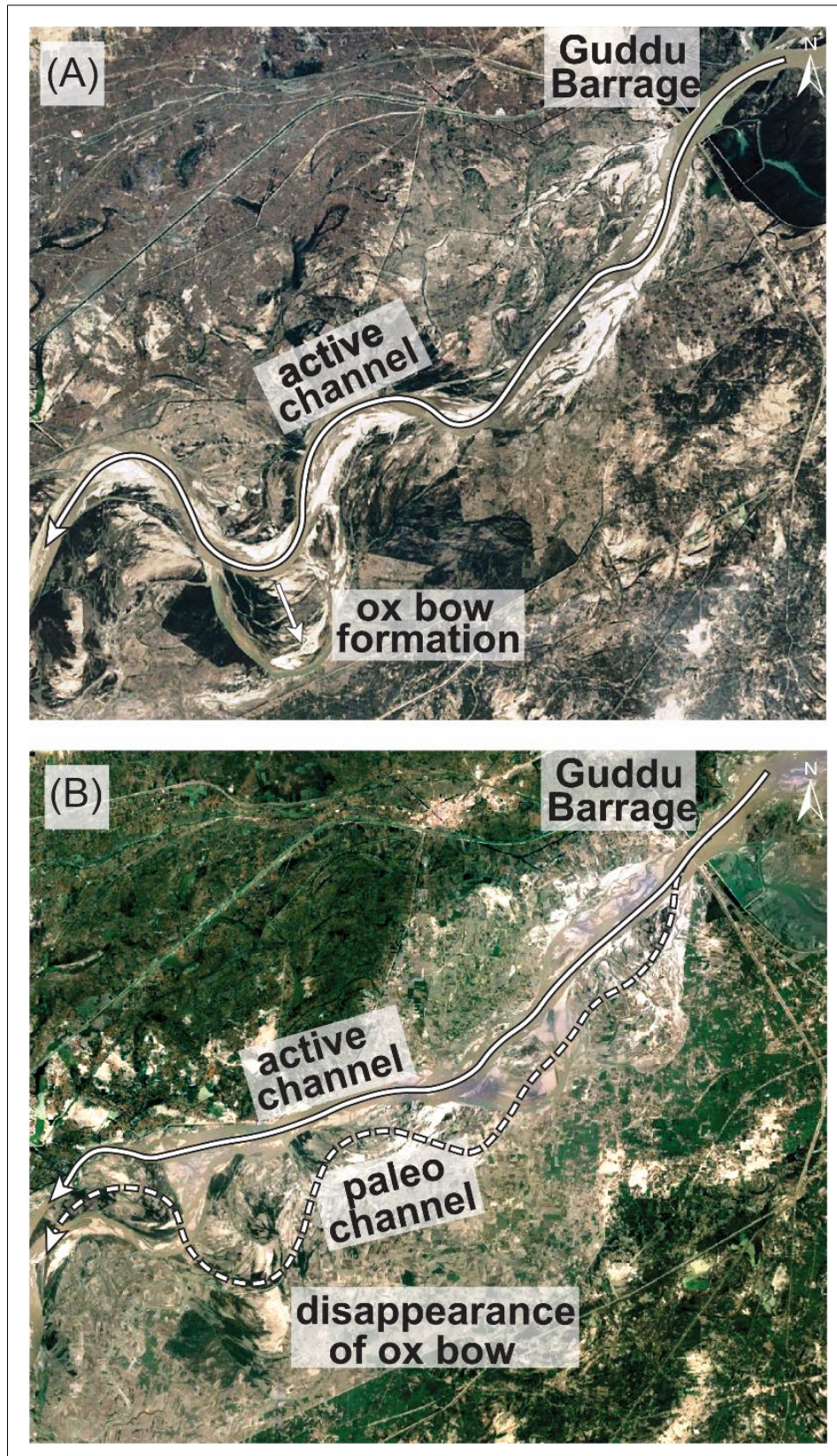
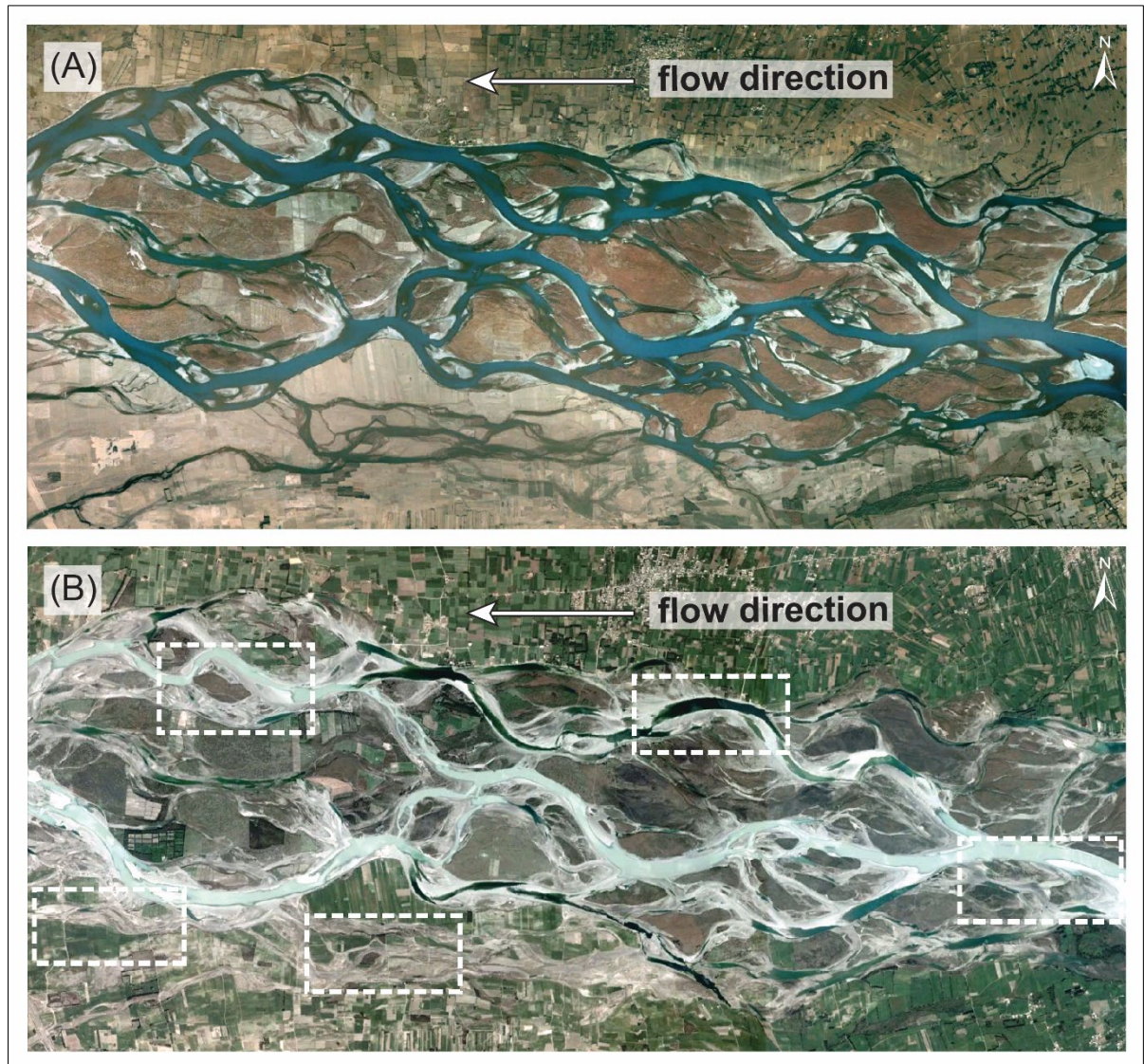


Fig 4.11:

(A) Satellite imagery of 1984, Guddu Barrage in Pakistan shows the then active channel with ox-bow formation developing towards the lower reach; (B) Satellite imagery of 2017 shows severe lateral migration of active channel, disappearance of ox-bow and remarkable change of channel belt planform. (Source: Google Earth™)

[Completed in 1962, the influence of the barrage on the river course is phenomenal but due to data limits, images are restricted to 1984]. (Figure from Prerna et al., 2018)



*Fig 4.12: (A) Satellite imagery of 2001, Indus River after Tarbela Dam - shows a highly braided reach of the river with well-developed depositional features; (B) Satellite imagery of 2017 - shows visible difference in channel width (marked in boxes) at several locations within and beyond the channel belt, caused either by climatic or anthropogenic influences. (Source: Google Earth<sup>TM</sup>). (Figure from Prerna et al., 2018)*

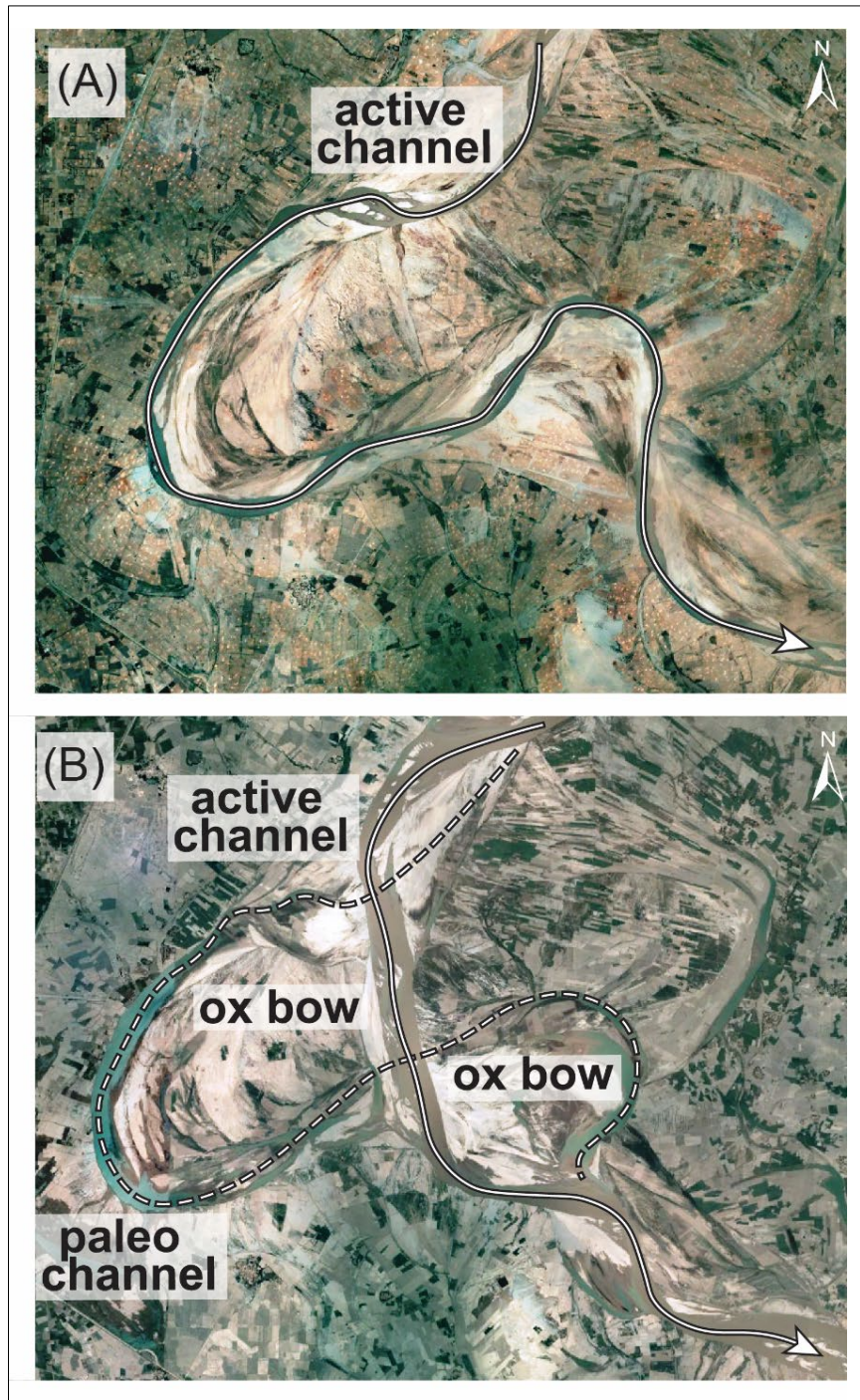


*Fig 4.13:*  
 (A) Satellite imagery of 2010, near Manchhar Lake, Pakistan - shows a highly sinuous channel of Indus; (B) Satellite imagery of 2017 - shows one fully and two nearly developed ox-bows on either side of the active channel which has undergone major lateral migration. (Source: Google Earth<sup>TM</sup>). (Figure from Prerna et al., 2018)

These records of planform variations indicate that the Indus River system is still undergoing river metamorphosis and is evolving with time. This is corroborated by the hypsometric curve and longitudinal profile which differ from the theoretical patterns of landform development, and could be influenced by the evolving Middle Indus Basin. Normally these measures help in demarcation of upper-middle-lower basins or youth-mature-senile stage

of river development, but in case of the Indus system, limited research on this demarcation makes it furthermore arbitrary. Previous studies propose division of the basin into upper and lower basin—either without a boundary or at a physical location e.g. at a barrage or dam. However, a demarcation based on transformation of the basin and river in terms of morphometry provide stronger grounds to demarcate basin boundaries. This demarcation is essential to support extensive research in each of these characteristically distinct basins. Each geomorphometric parameter (viz. the longitudinal profile, channel width, sinuosity, planform, and slope) is an indicator of stage of river development, which are effective to build a morphometric account. E and HC further corroborate the overall tectonic/geologic state of the Indus. After a consolidation of all these indicators, a morphometric demarcation of the Indus Basin has been proposed.

The first major physiographic knick-point on the Indus's course is the peculiar elevation drop within 400 km from its source seen on the longitudinal profile, which as previously stated could be attributed to the tectonically active Karakoram Fault. Precisely after Chumathang village of Leh district, the river follows a steeper gradient and continues so till the Skardu valley. The next major contrast in relief occurs after the exit of the Indus River from Deosai mountain range in Khyber Pakhtunkhwa province of Pakistan and into the smoothly grading plains around Peshawar and Rawalpindi. This is where the Tarbela Dam is present, acting as a reservoir for all the water draining the high-relief sector of Upper Indus Basin. This point of contrasting relief is proposed as the margin of the Upper and Middle Indus Basin (Fig 4.14). Until this point, the basin is associated with higher relief and the channel type shows youthful to mature characteristics (Prerna et al., 2018).

Further downslope, the river progresses through the Potwar Plateau towards the Jinnah and Chashma Barrages. The plateau, as previously explained, causes a remarkable change in channel behaviour—restricting it from following a typically mature pattern [i.e. sinuosity >1

with depositional features]. It is only after the river opens out into the plains of Sind Sagar Doab that it exhibits mature characteristics with distinct depositional lobes and braided stream flow. From there on till the confluence of Indus and Panjnad, Type V of channel behaviour prevails. Since the channel behaviour is remarkably different after this confluence point—it is proposed as the Middle-Lower Indus Basin margin (Prerna et al., 2018).

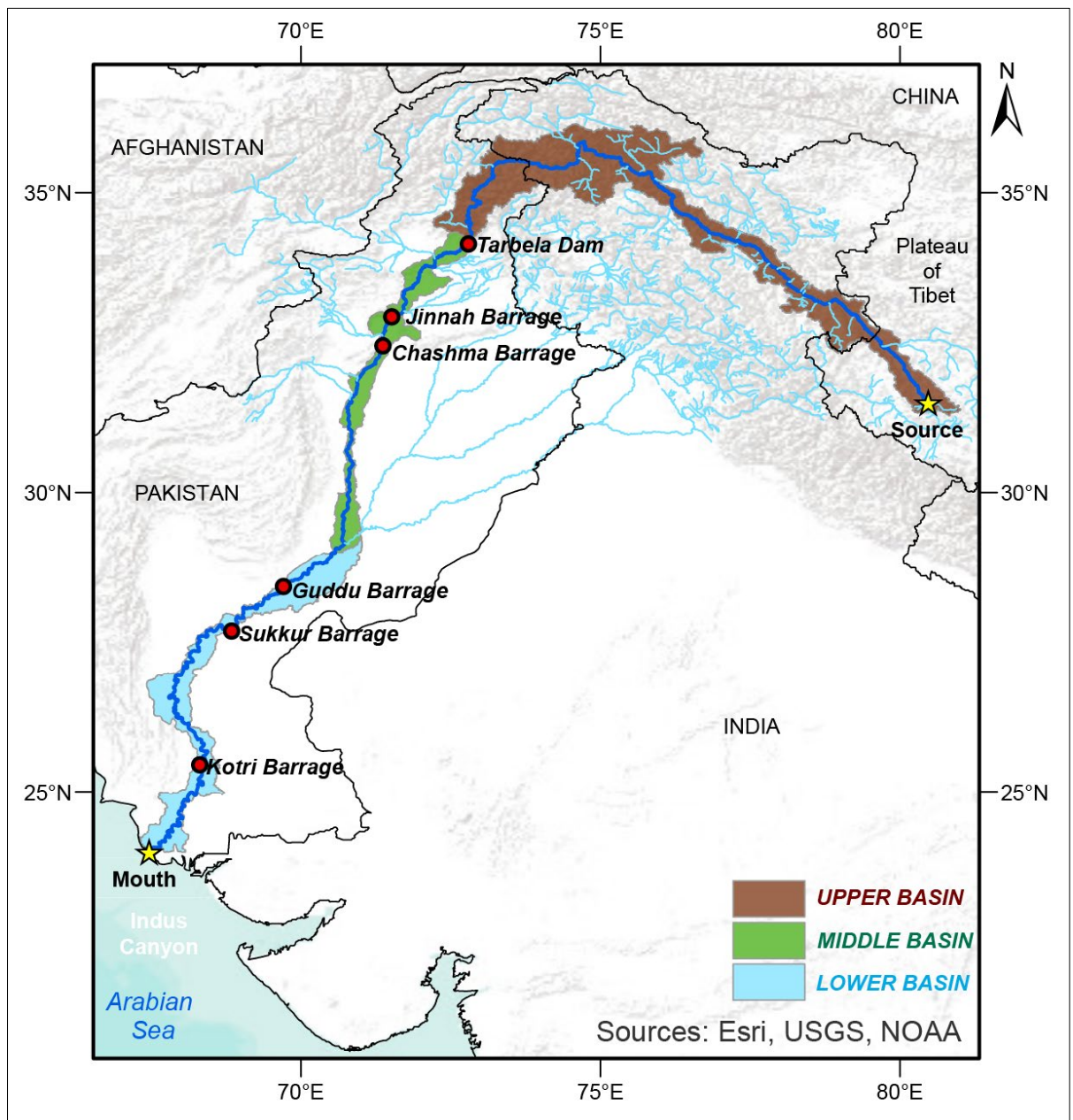


Fig 4.14: Indus Basin divided into Upper, Middle and Lower Basin; locations of major dams/barrages are marked along the river. (Figure from Prerna et al., 2018)

The marked rise in sinuosity, reduction in braiding, and dominance of a single master channel are characteristics of the Lower Indus Basin. The haphazard pattern of channel width seems to be mostly attributable to the construction of several barrages en route. Guddu, Sukkur and Kotri barrages greatly influence the channel planform in this part. River sinuosity is accentuated in the Lower Indus Basin with a declivity in channel width. Khan and Akbar (2012) stated that the overall impacts of anthropogenic effects in the fluvial Indus system are best observed downstream after Kotri Barrage. In the pre-Kotri period (1956-1961), there was not a single day with a zero flow downstream from this barrage which increased progressively following the commissioning of the Kotri and Guddu barrages and Mangla Dam on the Jhelum River. Inam et al. (2008) found zero flow days downstream from Kotri Barrage to cross 250 days per annum post 2001 (data recorded from 1956-2004). Such research signifies the human influence to explain the currently active river metamorphosis of the Indus system. The demarcation based on key geomorphometric parameters provides a thrust to encourage research as extended scope, and could hence become a roadmap for further analyses to form a synthesized climatic, geological, or anthropogenic approach.

#### *4.1.7. Gist of fluvial analysis*

In order to compare the morphometry of fluvial rivers and submarine channels within the extent of corresponding stages, it was essential to first demarcate the fluvial basin into Upper, Middle and Lower Indus Basin. Since information for this was not readily available, a quantitative demarcation had to be generated based on critical geomorphometric parameters (viz. longitudinal profiling, channel width, sinuosity, slope and elevation/relief ratio). Geostatistical and hydrological operations performed on DEM data, suggest that the highest and lowest relief sectors are tectonically more stable than the middle relief sector, which is inferred from a convex hypsometric curve. Elevation-relief ratio of ~31% for the basin indicates tectonic

stability of remnant rock. Cross-sectional profiles demonstrate anomalous patterns that deviate from expected and typical characteristics of youthful, mature and senile stages of river development. All parameters are spatially coalesced to provide a first-ever holistic morphometric account of the Indus basin while describing fine-scale planform variations of the spectacular dynamics of this enormous river basin.

#### **4.2. Indus Fan and its channel levee complex**

The Indus Fan with its elaborate channel levee complexes have been studied and discussed since the 1970-80s and perhaps even earlier. Pioneering works by Naini and Kolla (1982), McHargue and Webb (1986), Kenyon et al. (1987) and many others were major contributors behind our present-day understanding of the fan and the distributary network of its channels. Over time, with the addition of more surveys in the region, detailed knowledge on the internal architecture and evolution is being resolved. This study also attempts to add to the understanding of submarine channel systems, especially with respect to the Indus system.

Data for the Indus Fan is not as expansive as for the Indus Basin. As discussed previously, blocks of available data ensonifying the channel levee complex of the Indus Fan with published literature is used here to present a well constrained channel network. For this reason, each dataset is discussed individually in this section to describe the morphometric behaviour and evolution of channel systems from shelf to sink. This approach, though constrained by the limited offshore data, provides an effective morphometric snapshot of the channel system.

Prerna and Kotha (2020) elucidate the details of the morphometric behaviour and evolution of channel systems in the submarine Indus Fan which are reproduced in the following sections.

#### 4.2.1. *Upper Indus Fan*

The present-day active Indus Canyon along with two other paleo canyons forms an extensive erosional zone, namely, the Indus Trough (Kolla and Coumes, 1987). Less than 40 km SSE from the delta, the canyon head is evident as a bathymetric incision. Known to have originated as a result of mass wasting and slumping near the river mouth during Pleistocene, it further developed by retrograde slumping during high sea-level stand (Kolla and Coumes, 1987). The Indus Canyon is hence the source point of the elaborate channel levee complexes of the Indus Fan. In the upper reaches of the Indus Canyon, where the canyon incises the shelf, slumping was recorded by (Naini and Kolla, 1982), which is further corroborated by MBES data (Fig 4.15). On the other hand, the lower section is dominant by multiple coherently-spaced terraces, each separated by near vertical boundaries (Fig 4.15), implicative of erosion and deposition without being disrupted by slumping (Clift et al., 2014). Terraces are defined as topographically flat areas above the channel thalweg but within the channel belt (Hansen et al., 2017). They have also been noted in the Indus Canyon by von Rad and Tahir (1997) and closely resemble the planform of the Benin-Major channel levee complex offshore Niger Delta (Deptuck et al., 2003). These terraces—defined as topographically flat areas above the channel thalweg but within the channel belt (Hansen et al., 2017), also suggest sequent lateral accretion and vertical erosion, frequently observed in submarine channel levee complexes (Peakall et al., 2000; Deptuck et al., 2003; Heiniö and Davies 2007; Kane et al., 2007; Kolla et al., 2007, Babonneau et al., 2010, Qin et al., 2016). Subrahmanyam et al. (2008) and Kolla et al. (2012) reported sinuous channels in the Upper Bengal Fan flanked by several terraces resulting from overbank spilling and lateral cutting. Hansen et al. (2015) summarize several ways of terrace formation considering studies from the Indus, Bengal Fan, Amazon Fan, La Jolla Canyon, Zaire Canyon etc., all of which confirm that terraces are common features of submarine morphology. Levee formations are lacking through the canyon, but once the turbidity channels cross the foot

of the continental slope, they form large aggradational channel levee complexes with several hundred meters' relief (Kolla and Coumes, 1987). Fig 4.15 and Fig 4.16 show bathymetric data from the Indus canyon (Block S1) and Upper Indus Fan (Block S2) with cross-sections representing the transformation in channel morphometry.

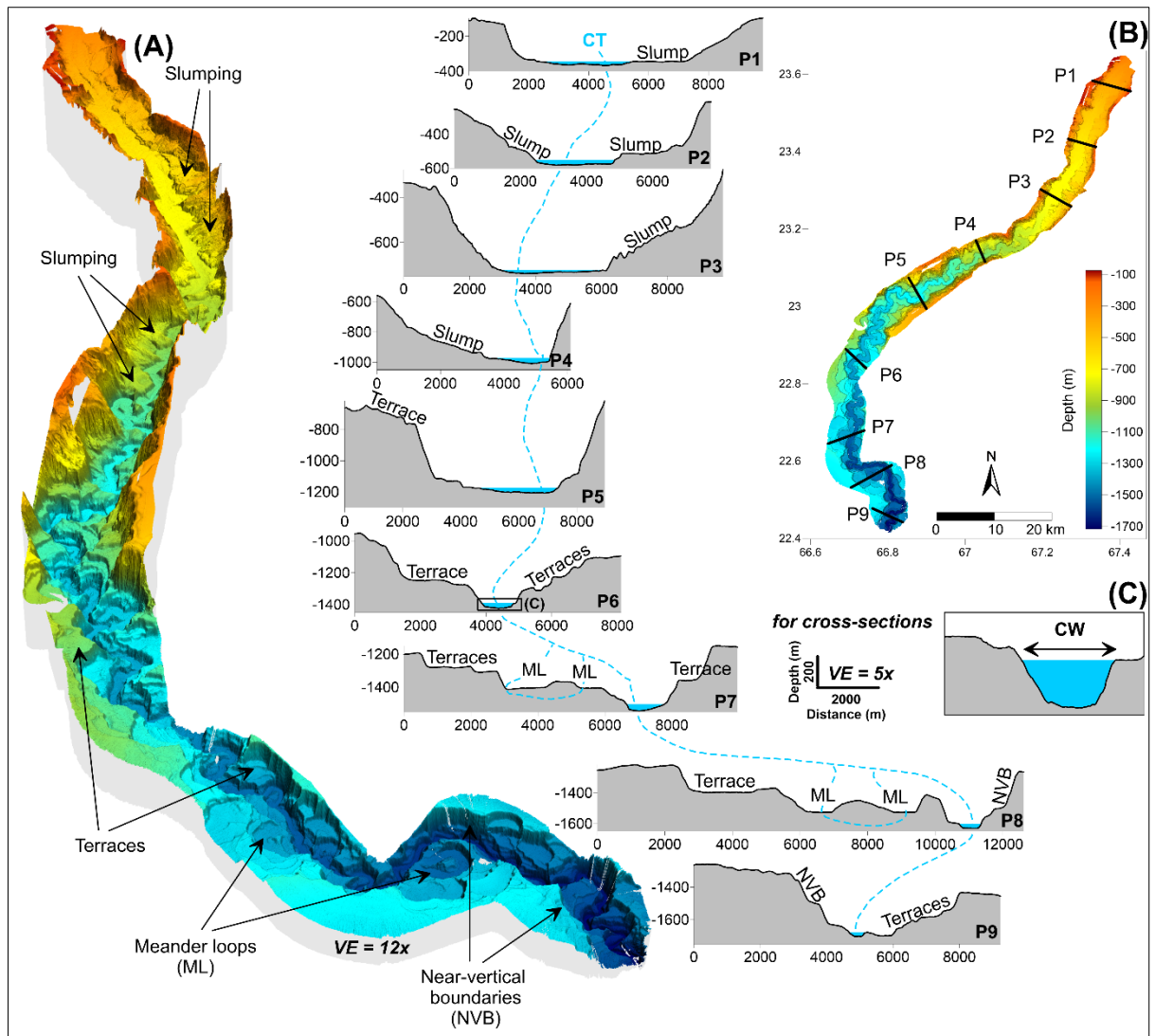


Fig 4.15: (A) 3D surface map of the Indus Canyon (Block S1, refer Fig 2 for location). Vertical exaggeration (VE) is 12x. (B) 2D surface map of the Indus Canyon showing location of cross-sections P1 to P9. Note transition from side wall slumping to flat terraces and near-vertical boundaries along the channel thalweg. (C) Enlarged representation of box drawn on P6 showing how channel width is estimated. [CT: channel thalweg; CW: channel width; ML: meander loop; NVB: near-vertical boundary] (Figure from Prerna and Kotha, 2020)

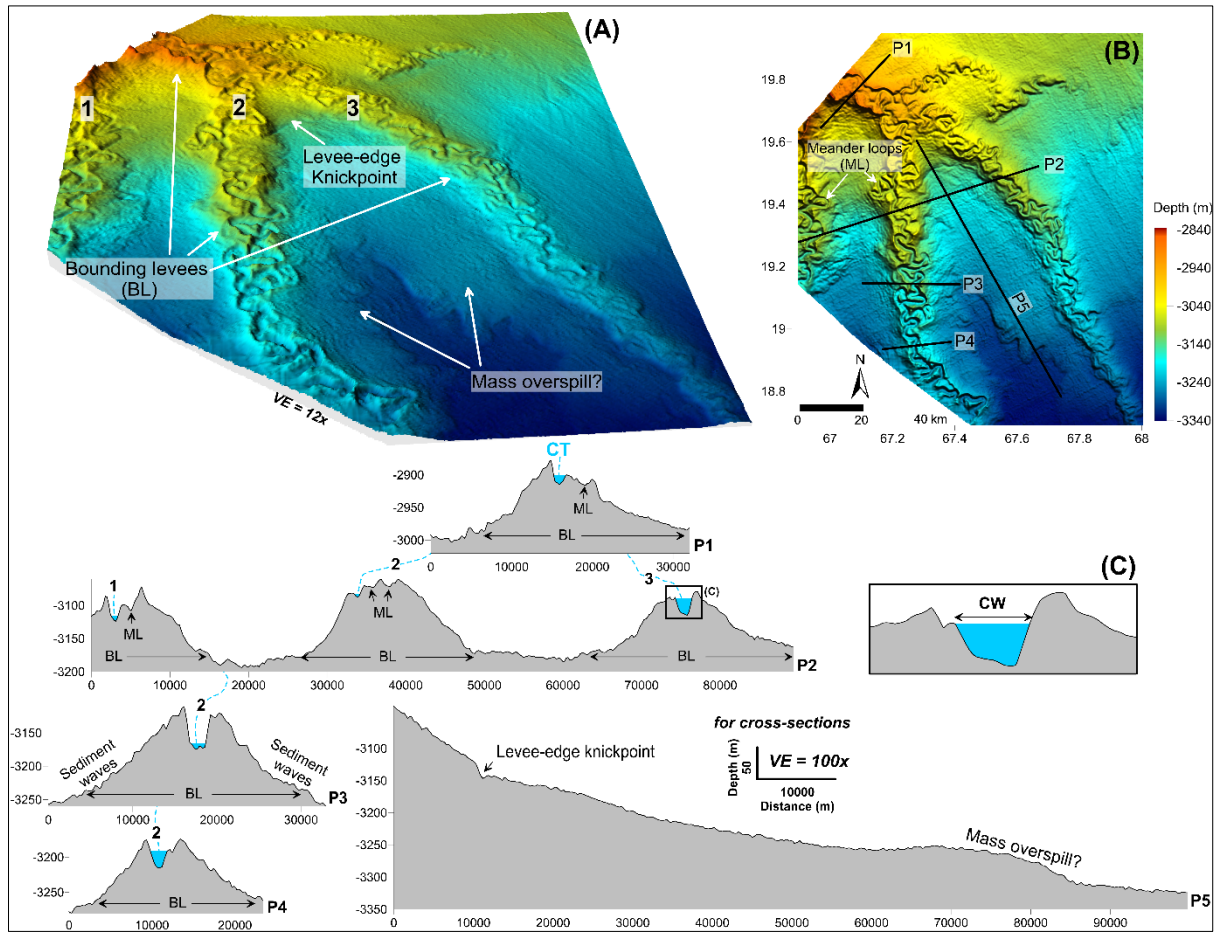


Fig 4.16: (A) 3D surface map of channel levee complex in the Upper Indus Fan (Block S2, refer Fig 2 for location). Vertical exaggeration (VE) is 12x. (B) 2D surface map of channel levee complex in the Upper Indus Fan showing location of cross-sections P1 to P5. Note transition in levee height down-fan along the channel thalweg. (C) Enlarged representation of box drawn on P2 showing how channel width is estimated. [CT: channel thalweg; CW: channel width; BL: Bounding levees; ML: meander loop] (Figure from Prerna and Kotha, 2020)

In the Upper Indus Fan, beyond the Indus Canyon, data from Block S2 shown channels dissipating into smaller channel levee complexes whilst maintaining the high sinuosity and lateral aggradation. Meandering channels with loops and cut-offs are easily discernible. The concept of master bounding-levees (Posamentier, 2003; Kolla et al., 2007) is adopted here to describe the high relief levee deposits (Fig 4.16). At about 20°N latitude (3000 m isobath), they start to split as finger-like projections emanating from a larger amalgamated channel levee complex in different directions, spreading tens of kilometers away from one another. The inner channels are far more sinuous than these master bounding-levees, which are products of

overspill from several channel loops within their confines. The levees reach maximum height (+100 m) in the Upper Indus Fan between 1500 to 3000 m isobaths, and develop concomitantly on both flanks of the channel with sediment waves on the outer edges, similar to those observed by Amir et al. (1996). The cross-sectional views of channels corroborate these findings and help to discern variations as they evolve down-fan (P1-P4, Fig 4.16). From the confined terrace-flanked structure in the canyon, they alter morphometrically within the Upper Indus Fan to form elevated master bounding-levee type structure.

#### *4.2.2. Middle Indus Fan*

The most recent scientific drilling result from IODP Expedition 355 from the Middle Indus Fan affirmed the direct link between Indus River and the fan sediments based on provenance (Pandey et al., 2016). MBES data from the Middle Indus Fan show extremely sinuous channels (Fig 4.17), with SI values  $>4$  at certain locations but with reduced channel width (discussed further, Fig 4.19). Clark et al. (1992) in their multi-fan study classified Indus Fan as an end-member with high sinuosity developing at relatively lesser gradients (1:400). The Amazon Fan channels also undergo highest sinuosity in the middle fan (Flood and Damuth, 1987). Average slope gradient as per the data observed is 1:650 in this zone. The sinuosity measured here is of the channels per se and not of the bounding master levees, which are much less sinuous. In this way, they are similar to the fluvial river planform of the Middle Indus Basin. There also, the braided channel belt is less sinuous but individual channel belts are sinuous.

In the Middle Indus Fan, channels continue to vertical incise and form considerable levees, though smaller in dimension compared to the Upper Indus Fan. Cross-sections constructed along the Middle Indus Fan channels suggest continuity of bifurcated individual channel levee systems, as observed in the Upper Indus Fan. The diminishing height of the

channel levees are indicative of reduced turbidity current flow and sediment concentration (Fig 4.17). Channel avulsions are very frequent in this part of the fan (Amir et al., 1996).

Here, a distinction is made between the relatively low-lying levees observed along the flanks of incisional channel 1 and the bounding levees rising 20-40 meters above the seafloor formed by aggradational channels 2 and 3 (Fig 4.17). Compared to the other channels, the starkly sinuous planform of the western-most channel 1 appears to be devoid of bounding levees creating only faint imprints on the seafloor and forming a clear incised valley in the substrate (P1-P2, Fig 4.17). The pronounced incision of channel 1 suggests higher erosive capacity, perhaps with greater turbidite flux, but without sediment waves and bounding levees. On the other hand, channels 2 and 3 (P3 to P7, Fig 4.17) have bounding levees, albeit, channel 2 plausibly ceases due to its encounter with a geological barrier—the Laxmi Ridge. The levee height of channel 3 is close to 40 m in the north reducing to 20 m downfan above the channel thalweg (P5 to P7, Fig 4.17). Significant reduction in levee size is seen as a characteristic trait of middle-to-lower fan transition, first observed by Flood and Damuth (1987) in the Middle Amazon Fan. Evidences of sheet-sands or unchanneled turbidity currents in Lower Indus Fan were reported by Kolla and Coumes (1987) and Shanmugam and Moiola (1988). Perhaps, the middle segment of channel 3 is buried by such sheet-sands flowing from the north-east. Within a span of ~150 km from west to east, variable channel levee forms indicate differential erosional/depositional signatures.

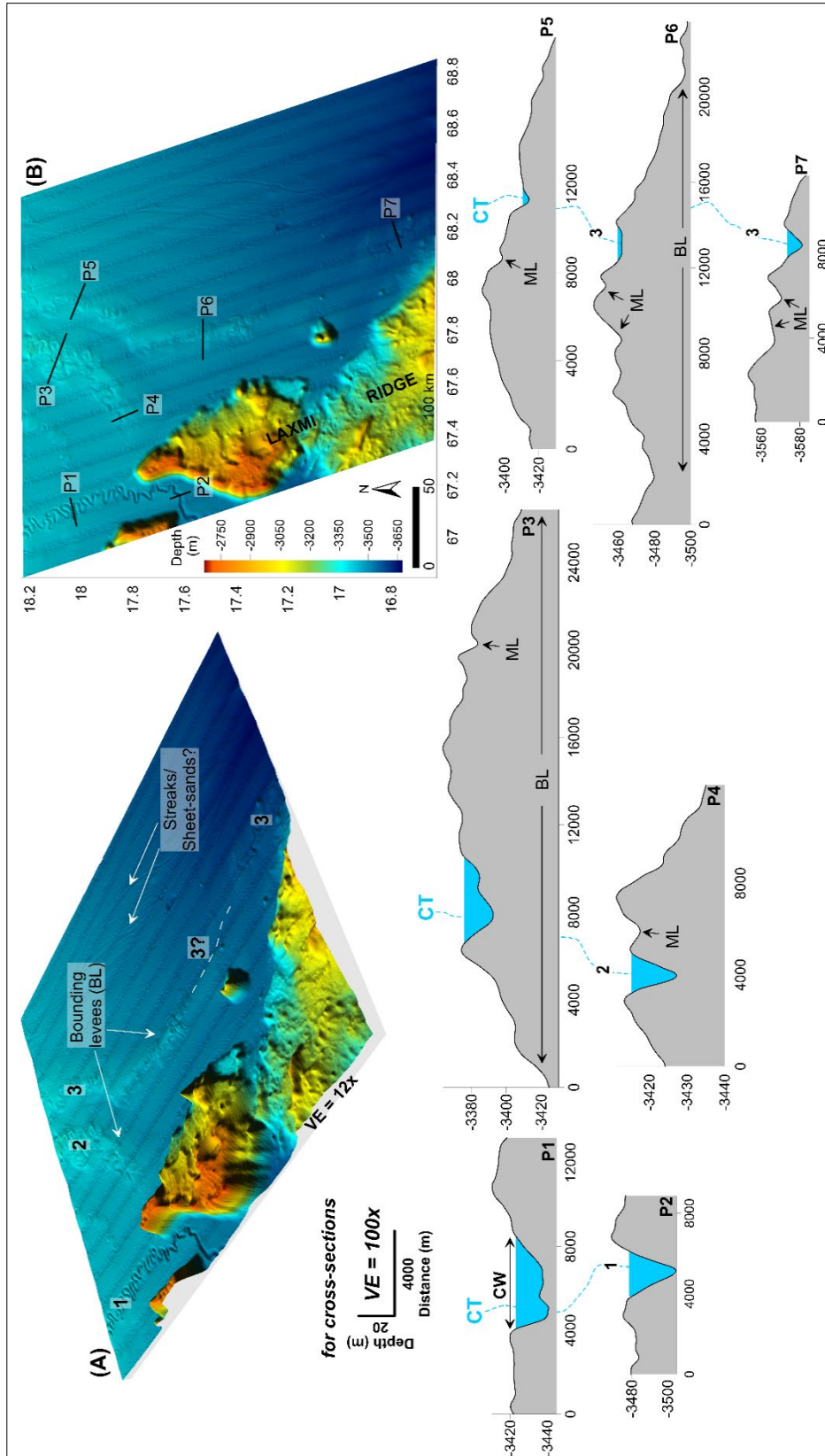


Fig 4.17: (A) 3D surface map of channel levee complex in the Middle Indus Fan (Block S3, refer Fig 2 for location) showing three channels numbered 1 to 3. Vertical exaggeration (VE) is 12x. Channel 3 does not show surface impressions in the middle segment denoted by white dashed line. (B) 2D surface map of channel levee complex in the Middle Indus Fan showing location of cross-sections P1 to P7. Note distinction between incisional channel 1 without bounding levees and aggradational channels 2 and 3 with bounding levees. The positive relief feature is the Laxmi Ridge. [CT: channel thalweg; CW: channel width; BL: Bounding levees; ML: meander loop]. (Figure from Prerna and Kotha, 2020)

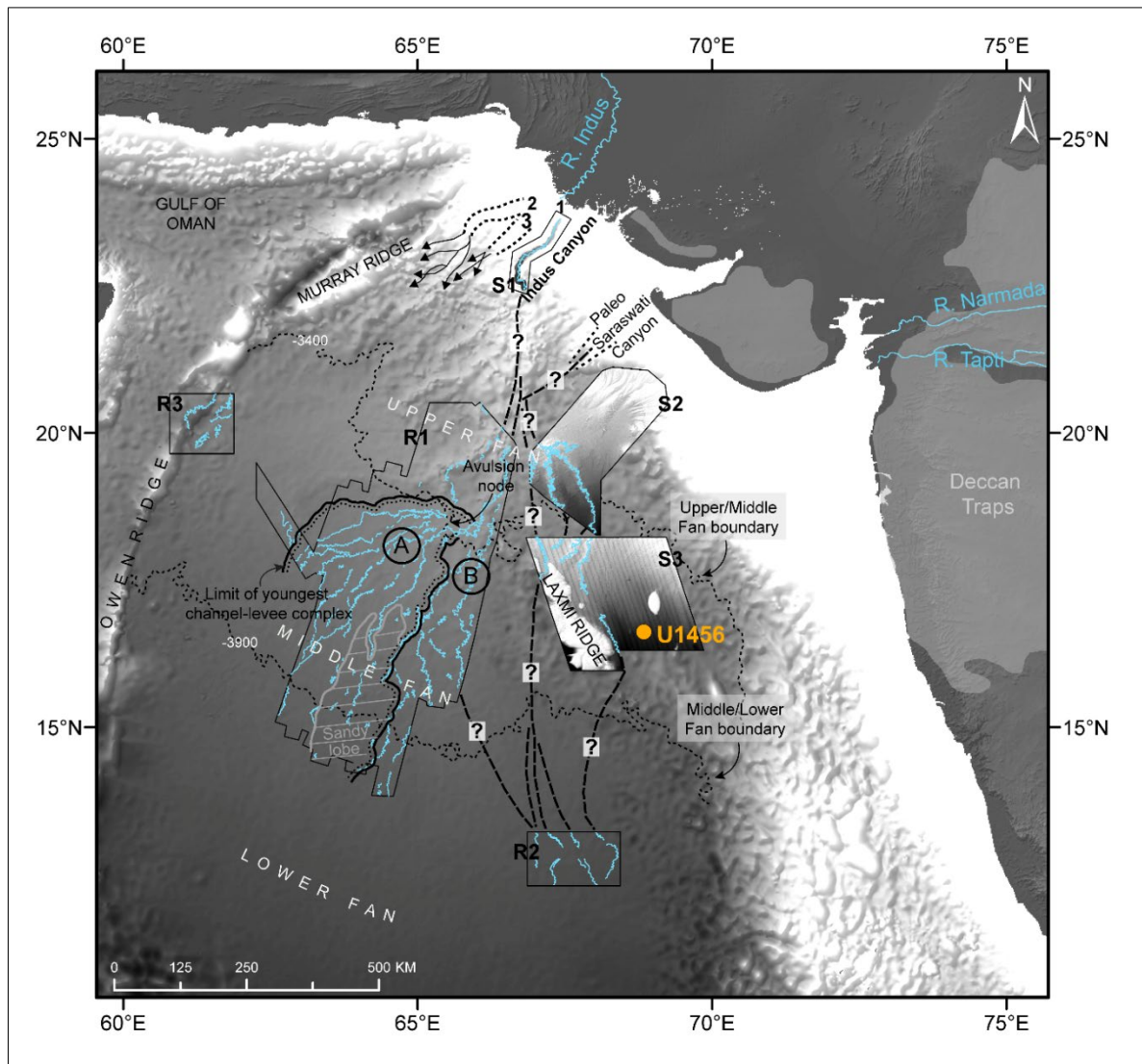


Fig 4.18: Channel network in the Indus Fan with canyon complexes 1-3 (youngest to oldest, modified from McHargue and Webb, 1986; Amir et al., 1996). Blue lines represent channels identified from study Blocks [S1, S2, S3] and reference Blocks [R1, R2, R3] modified from Kenyon et al. (1995), Kodagali and Jauhari (1999) and Bourget et al. (2013) respectively. Fan boundaries are modified from Kolla and Coumes (1987), black dashed lines indicate probable channel network and orange circle represents the location of Site U1456 in Laxmi Basin. (Figure from Prerna and Kotha, 2020)

A pioneering geophysical survey in the Middle Indus Fan—primarily using GLORIA sidescan sonar, seismic profiles and coring operations, reported a distributary complex of large sinuous channel levee complexes forming radial patterns (Kenyon et al., 1995). The channel levee complex resolved by the sidescan sonar data was noted to avulse in the Upper Indus Fan creating two distinct bifurcating systems (marked as A and B, Fig 4.18). Channel-width is

difficult to extract but the main feeder is wider pre-avulsion than the younger order channels of system A and B (Kenyon et al., 1995). System B was suggested to be arising from another proximal canyon linked to the ancient Saraswati River (Fig 4.18) in north-eastern Arabian Sea (Kolla and Coumes, 1987; Kenyon et al., 1995).

On studying the spatial behaviour of the channels curving onward into the Middle Indus Fan, the direct association of system B with the paleo Saraswati River and its offshore canyon seems doubtful, but the possibility of Saraswati-led channels joining the Indus channel levee complex cannot be ruled out. In the Laxmi Basin region of the Middle Indus Fan, IODP drill results from Site U1456 (Fig 4.18) have established the influx of sediments originating from Narmada and/or Tapti River using provenance (Khim et al., 2018, Kumar et al., 2019). With more geophysical data in the future, both present-day and paleo channel impressions from these auxiliary sources in the Indus Fan could be verified.

Combined inferences from datasets R1 and S3 confirm high sinuosity throughout the Middle Indus Fan. Channels on the east of Laxmi Ridge were first identified by Mishra et al. (2015). This clarified that the positive relief feature does not obstruct the continuation of channels eastward or southward in the Indus Fan, but can certainly impede individual channels, as seen in Channel 2 (Fig 4.17). A relatively flat region spread between higher ground formed by older channel levees is suggested as a sand-rich lobe of younger system A (Fig 4.18), based on backscatter behaviour and down-fan trending streaks that resemble pattern of channel mouth lobes (Kenyon et al., 1995; Kenyon and Millington, 1995). Streaks observed in dataset S3 could be similar to what Kenyon et al. (1995) suggested, but are insufficient to confirm lobe formation in the Middle Indus Fan.

The ancient Indus canyons and their associated channel levee complexes studied by McHargue and Webb (1986); Kolla and Coumes (1987); Clift et al. (2002); Berlin (2014) could have been the paleo source feeders of the channels observed in the far west of the Middle Indus

Fan from block R3 (Bourget et al., 2013), and their connection can be further corroborated with additional geophysical data. However, for the purpose of comparing their morphometry with channels from the eastern Middle Indus Fan, their sinuous planform suggests similarity.

#### 4.2.3. *Lower Indus Fan*

Inferences from the Lower Indus Fan are limited as it is relatively the least studied section of the Indus Fan. Even so, the continuity of turbidite channels carrying characteristic terrigenous sediments is well established through geophysical observations and drill operations (Whitmarsh et al., 1974a, 1974b; Naini and Kolla, 1982; Kolla and Coumes, 1987; Prell et al., 1989; Govil and Naidu, 2008; Shareef et al., 2018). Another pioneering bathymetric study by Kodagali and Jauhari (1999) affirmed the presence of sinuous channels extending till the Lower Indus Fan.

From the available data in the Lower Indus Fan, average channel width recorded is 900 m with moderate sinuosity. With a flat surface gradient of 1:1200, channels extend down-fan with reduced sinuosity bound by smaller levees roughly 20 m high with ox-bows (Kodagali and Jauhari, 1999). The Mississippi Fan portrays a similar reduction in levee size with reduced sinuosity in its lower fan (Bouma et al., 1985b). Kolla and Coumes (1987) suggested the presence of unchanneled currents in the Lower Indus Fan which spread as sand-rich turbidity sheet-flows (or sheet-sands) that dominate in front of the terminated channels. Submarine channel levee systems of Amazon Fan, off East Corsica, La Jolla system, Congo Fan and many others are seen to culminate as lobes (Jégou et al., 2008; Deptuck et al., 2008; Covault et al., 2012, Picot et al., 2016). Deptuck and Sylvester (2018) reasoned their development to the stage when turbidity currents exit channel confinement and lose sediment carrying capacity. Formation of lobes can vary significantly from system to system. In the example of Wilmington channel, lobes are formed immediately after the shelf break due to change in gradient (Deptuck

and Sylvester, 2018). But in the case of the Indus Fan, lobe formation is debatable due to the absence of mounding characteristic on seismic sections (Kolla and Coumes, 1987). Shanmugam and Moiola (1988) also pointed that sheet-sands of the Lower Indus Fan must not always be considered analogous to depositional lobes. Hence additional geophysical evidence is required to confirm the presence of lobes or absence thereof in the Lower Indus Fan.

#### *4.2.4. Gist of submarine analysis*

The analysis of the Indus Fan's elaborate channel system elucidates the variant morphometry of the channels from canyon source to sink. Bathymetric data from three blocks in the Upper and Middle Indus Fan are combined with previous literature to build the potential channel network of the Indus Fan. Subsequently, morphometry is assessed based on the parameters: (a) longitudinal profile, (b) channel width, (c) sinuosity, (d) planform and (e) slope, similar to the fluvial Indus Basin analysis.

The deeply incising, highly sinuous, terrace flanked morphometry of a singular channel in the Canyon, transforms into multiple bifurcating levee systems. Within the Upper Indus Fan, maximum variation in channel planform is witnessed attributed to the change in gradient from slope to plain. Sinuosity observed in this region is far more than the entire course of the Indus River on land. The most vivid features of the Upper Indus Fan are the elaborate sediment levee deposits tapering up to 100 m relief. In the Middle Indus Fan, sinuosity is at its peak with channel levees continuing to form, albeit, in smaller dimensions. Data from the Lower Indus Fan is scanty; however, previous literature confirms channels with minimum 1 km width and negligible levees. Presence of lobe formation however, could not be confirmed.

The following section builds a two-way comparison between the morphometric form of fluvial rivers and submarine channels. Quantified indices derived from the subaerial-submarine morphometric assessment form the basis for this comparison.

### **4.3. Comparison of fluvial rivers vis-à-vis submarine channel levee complexes**

#### *4.3.1. Upper Indus Basin vs. Upper Indus Fan*

Both these regions represent the most erosive sections of the river and channel, respectively. Topography and sediment flux play a key role in controlling the velocity of the river/channel, thereby, shaping the planform. Closest to the source, river dynamics are unstable because equilibrium between sediment load and carrying capacity is not fully attained. But, the morphometric patterns indicate huge disparity in river and channel planform. They showcase the variable role played by the agents of erosion and deposition and the resultant morphometric variation.

A moderately convex shaped longitudinal profile represents the high-relief segment of the Upper Indus Basin. Here the Indus River is predominantly erosive with marginal lateral aggradation. It is a zone of rapid incision, downcutting and gorges, resulting from exceptionally high denudation and tectonic uplift (Kazmi and Jan, 1997; Ahmed, 2013). The river typically forms a v-shaped section, with channel width averaging to 250 m throughout the Upper Indus Basin. The spikes in channel-width plot [Fig 4.19 (A1)] indicate areas of river confluences. The Upper Indus Basin in the Himalayan complex is structurally confined which restricts sinuosity, hence Sinuosity Index (SI) rarely exceeds the value of 2 [Fig 4.19 (A2)]. Valley slope gradient is most accentuated in the Upper Indus Basin, given the undulating terrain of the high-relief. Evident jumps in the slope gradient plot signify this throughout the Upper Indus Basin [Fig 4.19 (A3)]. In all, it is a structurally confined zone of high relief, dominant erosion, vertical downcutting and moderate sinuosity.

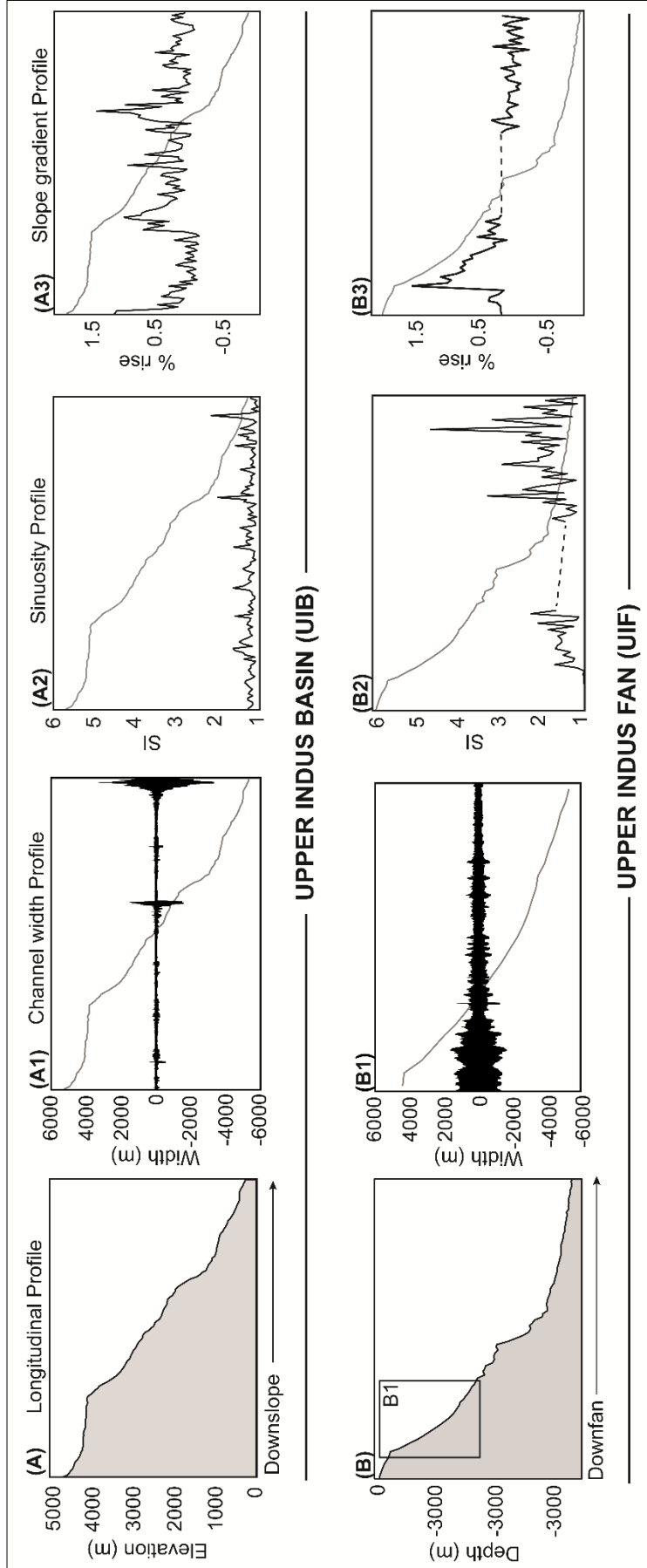


Fig 4.19: Geomorphometric comparison of Upper Indus Basin [UIB] and Upper Indus Fan [UIF]. (A) Longitudinal profile of UIB; (A1) Channel-width profile of UIB; (A2) Sinuosity profile of UIB; (A3) Slope gradient (in percentage rise) of UIB; (B) Longitudinal profile of UIF; (B1) Channel-width profile of UIF, data extent marked on B; (B2) Sinuosity profile of UIF; (B3) Slope gradient represented (in percentage rise) of UIF. Dotted lines represent data gap.

The differing erosive/depositional nature of the channels in the Upper Indus Fan is well preserved in their channel width and sinuosity profiles. Channel width, which barely averages beyond 250 m in the Upper Indus Basin, goes as high as 3 km in the canyon-part of the Upper Indus Fan with an average of 1 km [Fig 4.19 (B1)]. Width could not be measured throughout the extent of Upper Indus Fan due to data constraint but from what best could be inferred, channel width is > 1 km throughout. Coming to sinuosity, submarine channels may seem to meander similar to fluvial channels (Brice, 1974; Kolla et al., 2001), but the precise mode of sinuosity evolution in deep-water systems may differ (Kolla et al., 2001). Also, the intensity of sinuosity and stage of development are seen to vary. In this study of the Indus, SI values in the Upper Indus Fan are accentuated right from the beginning (> 4) and continue so well into the Middle Indus Fan [Fig 4.19 (B2)].

Sinuosity in both environments is a gradual process, involving interaction of flows, sediments and underlying topography—in an attempt to establish equilibrium (Kolla et al., 2001, 2007). However, the fairly common trend of low to high sinuosity in fluvial environments is seen to be diametric in the submarine system. Relief gradient is found to be similar in the Upper Indus Basin and Upper Indus Fan mostly within -0.5 to 1.5% rise. These variations are attributed to the completely disparate morphology of the Upper Indus Fan, portrayed by a concave-down longitudinal profile denoting sharper gradient change than the Upper Indus Basin [Fig 4.19 (A) and (B)].

The cross-sectional views of channels in the fluvial and submarine systems are interesting and help in discerning the variations within. Along the Upper Indus Basin, cross-sectional views remain consistent, with typical narrow v-shaped valley forms. However, cross-sections from the Upper Indus Fan are rather different and tend to evolve drastically down-fan (Fig 4.20). As the channel progresses from the upper canyon and into the large channel levee

complex, it alters morphometrically from the terrace flanked/confined wall structure to the master bounding-levee structure.

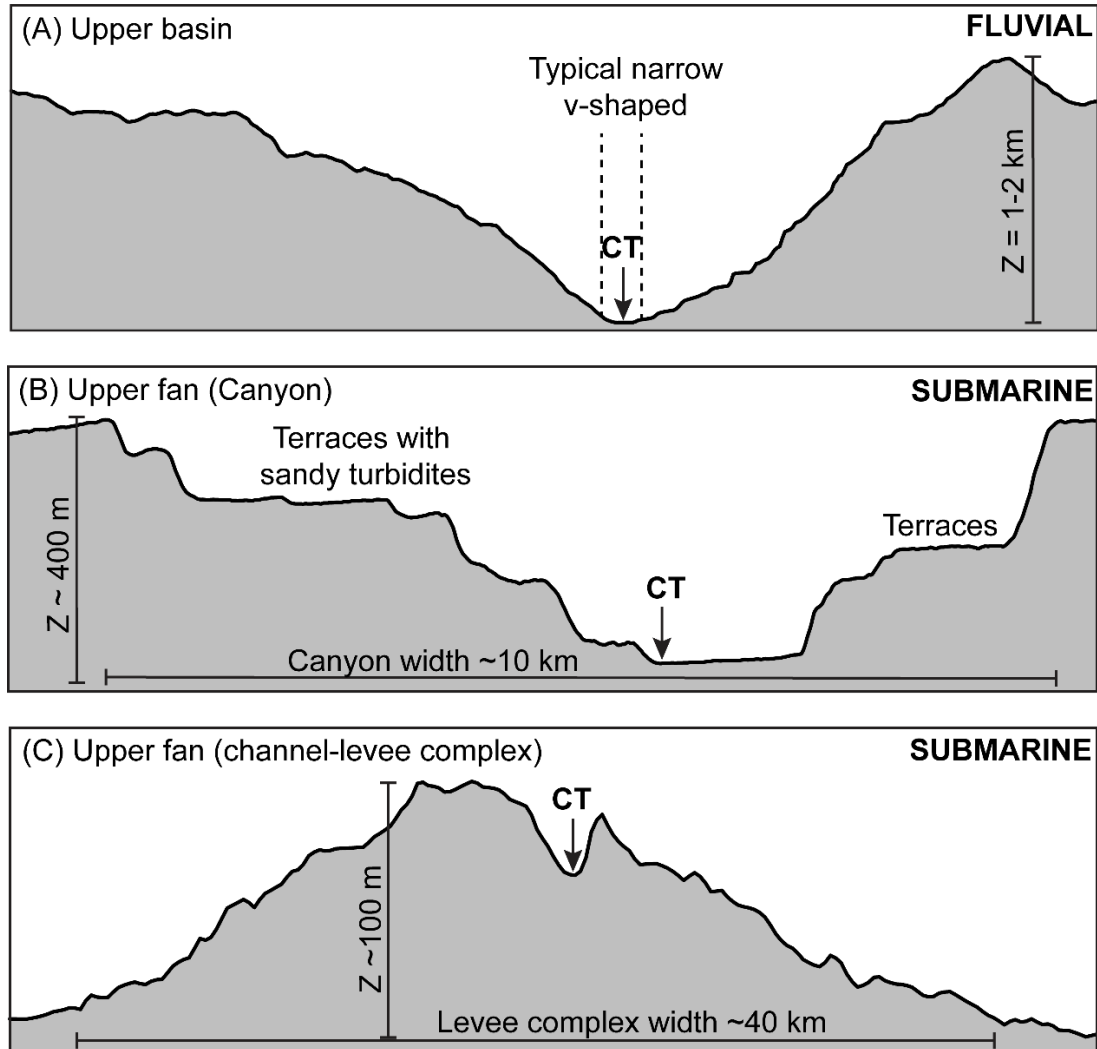


Fig 4.20: Representative channel cross-section showing transformation from (A) Upper Indus Basin; (B) Upper Indus Fan (canyon); and (C) Upper Indus Fan (channel levee) [CT: channel thalweg, Z: depth].

Another contrasting element in the fluvial/submarine debate is the phenomenon of channel avulsion, largely more common in submarine systems (Kolla et al., 2001). Avulsion, although existent in both environments, could be triggered by different causes, with varying frequency and mechanism. Some studies from the fluvial Indus Basin supplement the fact that avulsion occurs in fluvial systems too (Gaurav et al., 2011; Syvitski and Brakenridge, 2013;

Singh et al., 2017). But in most cases, avulsion is caused by stochastic events like excessive rainfall-led flooding, embankment breach or structural failures of built reservoirs; and anthropogenic effects like water diversion. Kolla (2007) identified evidence of avulsion resulting from long-term episodic eustatic or climatic changes in the Zaire Fan, however, avulsion-threshold causing conditions like—channel sinuosity increase, lengthening, slumping, channel plugging etc. also cause avulsion in deep-water systems. Prins et al. (2000) observed avulsion at two locations in the Upper and Middle Indus Fan, controlled by abrupt decrease in down-slope gradient caused by reactivation of buried normal faults and marked reduction in channel dimensions. Hence, avulsion may not be alien to either system but the controlling factors differ significantly.

#### *4.3.2. Middle Indus Basin vs. Middle Indus Fan*

The peculiarity of these two regions is that they both indicate zones of maximum deposition in the fluvial and the submarine system. In most physiographic environments, a sudden drop in relief corresponds to reduced erosion and accentuated sediment deposition—typically identified as the middle section of a basin. The same holds true for submarine fans, as they too undergo relief drop and disintegrate into lesser order channels. However, the morphometry and pattern of the depositional planform is quite contrasting.

The Middle Indus Basin extends from the Tarbela Dam in the Lesser Himalayas up to the confluence of Indus and Panjnad Rivers. This segment of the river's course encounters tremendous drop in channel relief, leading to increased lateral aggradation and heavy deposition with reduced vertical incision. Characteristically mature by its stage of development, the Indus River is predominantly braided with large sandbar deposits in the channel belt. Leaving the part where the river flows through the topographically restricted Kohat Potwar fold belt (Prerna et al., 2018), channel width in the Middle Indus Basin is at its

maxima [Fig 4.21 (A1)]. Heavy braiding is majorly attributable to the construction of dams/barrages along its course, but also due to reduced relief and excessive deposition. A braided river consists of a single main channel belt with multiple thalwegs (Makaske, 2001) which although may be sinuous by themselves, do not affect the sinuosity of the river. This limits the SI values of Indus River to  $< 1.5$  in the Middle Indus Basin [Fig 4.21 (A2)]. Channels of the Middle Indus Fan showcase narrower planform yet are extremely sinuous with SI values  $> 4$  at certain points [Fig 4.21 (B1) and (B2)]. The longitudinal profiles of the Middle Indus Basin and Middle Indus Fan only appear similar but their morphology does differ. Average gradient in the Middle Indus Basin is 1:3600 as opposed to 1:650 in the submarine Middle Indus Fan. On land, the low-relief basin experiences lateral aggradation with braiding, scroll bars/islands and channel width averaging at  $\sim 3$  km.

Another important aspect is the phenomenon of braiding in fluvial rivers. Braiding is found to be rare in submarine environments (Damuth and Flood, 1985; Wynn et al., 2007) partly due to the unfavourable conditions required for formation and the lack of well constrained data from truly sinuous channel systems, which can offer insights about the process. Foreman et al. (2015) performed experiments of subaqueous channel formation to produce a braided planform from flow aspect ratios of depth and width that are similar to those that produce river braiding. They explained the rarity of braiding in submarine channels due to a combination of factors that induce greater levee deposition and limit channel widening. Lack of evidence of braiding from the Indus Fan led us to opine that fluvial-like braiding is absent from the submarine system of the Indus.

River behaviour in the Middle Indus Basin is found to be categorically different from the channels of the Middle Indus Fan. Although, the morphometry is topographically controlled, their depositional structures are profoundly disparate ranging from the dominantly braided less sinuous low-lying river vis-à-vis the steep levees of highly sinuous channels.

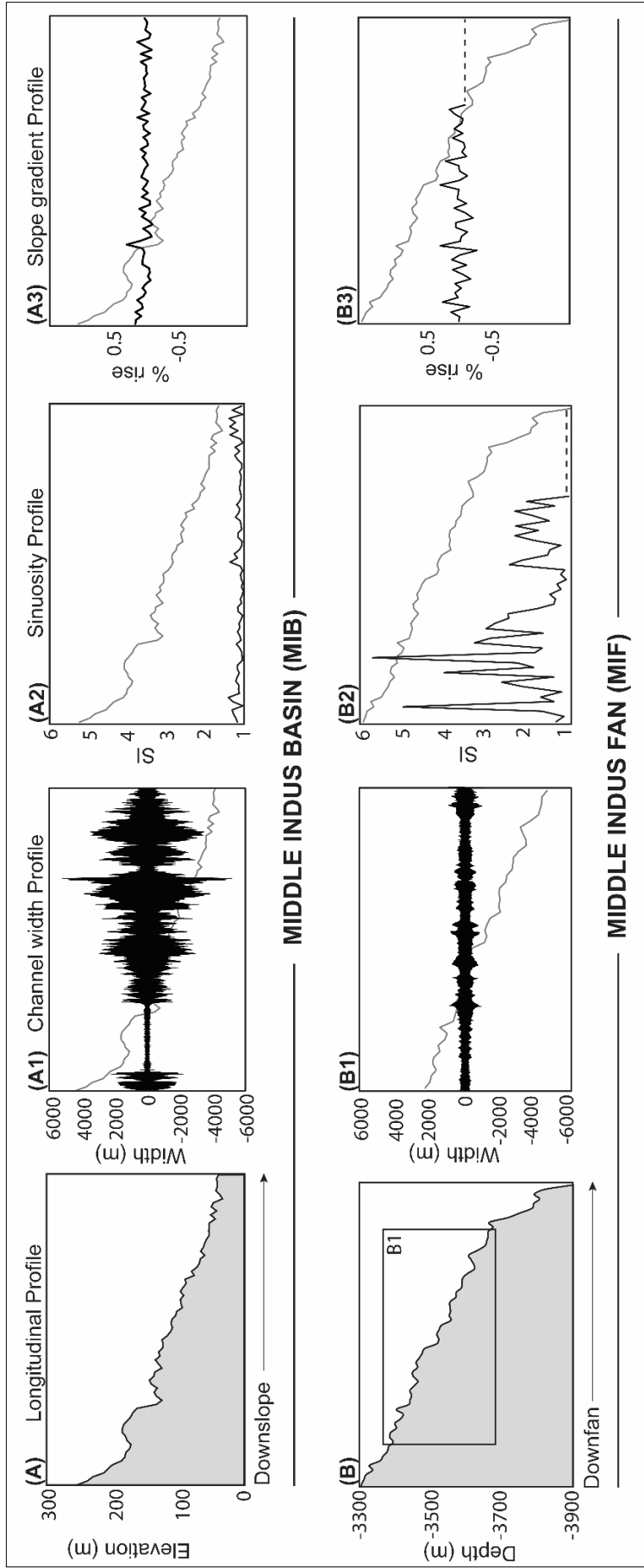


Fig 4.21: Geomorphometric comparison of Middle Indus Basin [MIB] and Middle Indus Fan [MIF] (A) Longitudinal profile of MIB; (A1) Channel-width profile of MIB; (A2) Sinuosity profile of MIB; (A3) Slope gradient (in percentage rise) of MIB; (B) Longitudinal profile of MIF; (B1) Channel-width profile of MIF, data extent marked on B; (B2) Sinuosity profile of MIF; (B3) Slope gradient (in percentage rise) of MIF. Dotted lines represent data gap. All profiles superimposed on longitudinal profile A and B.

#### 4.3.3. *Lower Indus Basin vs. Lower Indus Fan*

Towards the finality of a river/channel's course, depositional features usually dominate the planform. A typical deltaic form on land can thus be compared to terminal lobes in the ocean, as both indicate the incapacity of the river or channel to transport sediments due to reduced flow velocity—leading to deposition of the abundant sediment load. Yet, the planform in both regions shows much difference with respect to morphometry.

In the Lower Indus Basin, the river undergoes braiding due to losing large amount of its transportation capacity at dam sites with accentuated deposition, widening considerably and forming ox-bows/scroll bars (Prerna et al., 2018). Highly sinuous in its planform, the river continues to drain as a single channel till its delta, with channel width averaging at 1300 m. Much variation is not witnessed in the river planform of the Indus River in the Lower Indus Basin. The channels continue with a width of at least 1 km and minimal levee formation. Presence of lobes cannot be ascertained with available data.

Fig 4.22 represents river/channel planforms from Indus Basin (A-C) vis-à-vis Indus Fan (D-F), as observed on satellite imageries/MBES data. The Indus River transforms from a moderately sinuous, narrow belted stream that undergoes heavy braiding and meandering in the Middle Indus Basin on encountering drop in relief, and thereafter into a highly sinuous single channel belt with evident meanders, scroll bars and ox-bows. On the contrary, planform variation in the submarine Indus Fan follows a different course. Starting as a highly sinuous channel in the upper reaches of the Indus Canyon, the channel belt is flanked by terraces and meander loops. After exiting the canyon, the single channel complex gets distributed into multiple systems with their own composite levee built-up. Continuing so in the Middle Indus Fan, the channels form evident levees but gradually lose sediment flux in the far reaches of the Lower Indus Fan with negligible levee built-up.

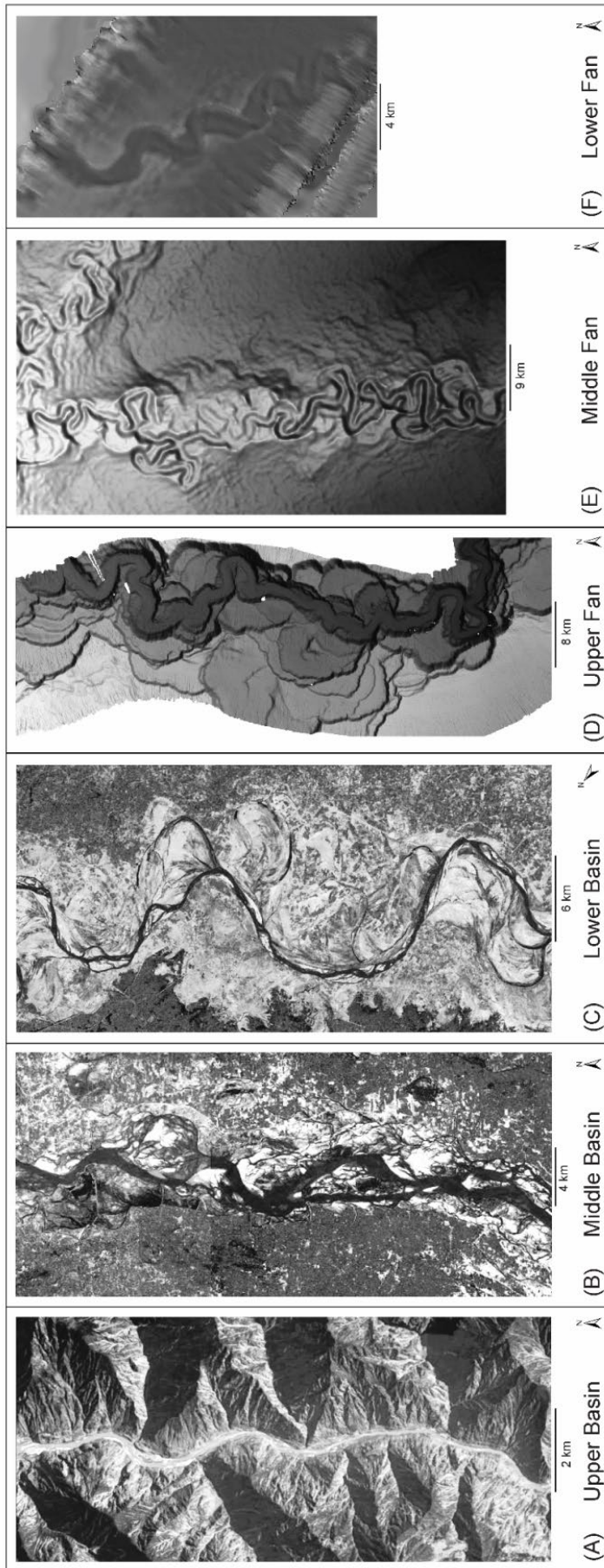


Fig 4.22: Representative planforms from Upper, Middle, Lower Indus Basin and Upper, Middle, Lower Indus Fan. [Data source: (A-C) ESRI™ World Imagery (WGS84); (D) Clift and Henstock, (2015); (E) NCPOR (n.d.); (F) Ward (2007)].

## **CHAPTER 5**

### **DISCUSSION AND CONCLUSION**

## CHAPTER 5

### DISCUSSION AND CONCLUSION

A simple analogy between fluvial rivers and submarine channels has existed for long, especially on the basis of planform and morphometry. Despite the fact that a broad resemblance does occur, what often go unnoticed are the disparate causative phenomena that shape and control these systems. Here, we present a first-ever morphometric investigation of one single river system by comparing the onshore part of the river with its submarine fan-channel system. To recapitulate the analysis performed in this work, the primary objectives are listed below:

- To understand the architecture and evolution of the submarine Indus Fan and its associated channel system. This includes (a) mapping the existent channel structure using available data; (b) studying the variation of channel morphology from shelf to abyssal plains; (c) examining variations in the channel form through the various stages and processes of development.
- To compare the morphology of Indus Fan and its submarine channels vis-à-vis Indus Basin and its river. This involves (a) identification of river flow pattern in the fluvial Indus Basin; (b) morphometric measurements across various stages of river development; (c) stage-wise comparison of submarine and fluvial channel behaviour with respect to each geomorphometric parameter.

The entire Indus River is analysed in coherence with the offshore channel levee complexes of the Indus Fan, segment by segment i.e. upper basin with the upper fan, middle basin with the middle fan and lower basin with the lower fan, to ascertain the differences in function and form. Using the exhaustive geophysical data from the river basin and part data

from the submarine fan, key geomorphometric parameters like longitudinal profile, channel width, sinuosity, and planform are calculated to build morphometric accounts of the two systems with optimized precision. Absolute values, as extracted, from the DEM and MBES data have been presented for comparison.

After the morphometric accounts are built, one-to-one comparison is done between fluvial and submarine channels. Based on collective considerations, we conclude that the rivers and channels differ on the very same grounds on which they are considered similar—planform and morphometry. Due to the differences in intensity of erosional and depositional processes active in the subaerial and submarine environments, longitudinal profiles of the river basin/submarine fan show unconformity. Coeval erosion and deposition as witnessed in the submarine fan are unlikely in this river basin, where mostly one dominant process is found to be active per stage (Kolla et al., 2007). On the other hand, channel width invariably goes from high to low in submarine systems; and from low to high in fluvial. We attribute such differences to the effect of a single-point/canyon-fed distributary flow and multi-point/tributary-fed cumulative flow source system. The depositional features, particular to each system, are mutually exclusive. Braided river planform dominate fluvial systems, whereas, high-relief bounding levees are found only in submarine systems. With evidence of channel width, depth and sinuosity uniformly reducing in submarine channels and increasing in fluvial rivers, this study attempts to persuade the dilution of the analogy between fluvial rivers and submarine channels.

### **5.1. Holistic observations**

Planform of every river or channel system transforms from source to sink, given the modulations in topography, flow velocities and the sediment flux etc. The idea of comparing a fluvial basin and its counterpart—a submarine fan of a single river system, in this case the

Indus, was to quantify the existing variability and possibly attribute them to causative phenomena. The Indus Basin approximates its submarine fan in terms of area (Section 2.2); but the trends of morphometric indices calculated for the fluvial river and submarine channels do not conform morphometrically.

For a river flowing ~3300 km on land and thenceforth as sediment carrying channel levee complexes for at least another 2500 km, Indus shows remarkable variability in stream/channel planform from source to sink. The transformation of the Indus from land-to-deep sea, represented as a single longitudinal profile helps in quantifying the variability between the fluvial and the submarine environment (Fig 5.1). As previously seen, cross-sections are also crucial to understand the effects of erosional and depositional processes applying within and along the channel belt. Planforms and cross-sections compared in Fig 5.2 imply a simple-to-complex form development on land vis-à-vis a complex-to-simple form in the submarine sphere. Each zone is characterized by a set of unique channel features which only result from the variable processes acting upon them. A summarized description of the Indus Basin and Indus Fan follows.

A smoothly meandering, narrow channel planform with  $SI < 2$  is characteristic of the erosion-dominant high-relief Upper Indus Basin (Fig 5.1). The convex-shaped longitudinal profile of this zone of the Indus Basin is useful to identify knick-points where sharp change in gradient is encountered. For most of this region, the river forms a v-shaped valley as erosion is stronger than deposition (A1, Fig 5.2). As a result, channel width is also confined (average 250 m) with infrequent channel widening that represent locations of river confluence in the Upper Indus Basin (Fig 5.1). The graph of channel gradient is jagged for most of this zone. Further downstream, the erosive component of river progression gets downplayed by deposition and lateral aggradation is witnessed along cross-sections (A2-A3, Fig 5.2).

In the Middle Indus Basin, encountering a drop in relief, channel width rises. In Fig 5.1, the transition zone of the Upper-Middle Indus Basin represents this zone of increasing channel width, however, shortly after crossing the Tarbela Dam (location of Upper-Middle Basin boundary), channel width is again restricted as it traverses through the Potwar Plateau. Other than that, the river has an average width of 2700 m in the Middle Indus Basin. Braiding is the dominant planform in this zone with large sand-bars and islands (Fig 5.1 and A4, Fig 5.2), which is attributable to the construction of dams/barrages along course, and also due to reduced relief causing abrupt deposition. A braided river consists of a single main channel belt with multiple thalwegs (Makaske, 2001), which although may be sinuous by themselves, do not affect the sinuosity of the river. This limits the SI values of the Indus River to  $<1.5$  (Fig 5.1).

In the Lower Indus Basin, average channel width is 1300 m with increasing sinuosity going up to 3 (Fig 5.1). Meanders and ox-bows are commonly observed in this zone (A5-A6, Fig 5.2). A depositional form with one major channel represents the dominant planform. In all, the channel form grows from a simple-to-complex planform in the fluvial Indus Basin with typical characteristic features of an erosive river with v-shaped valley in the upper basin, braided and depositional form in the middle basin, and finally culminating as a single channel sinuous river with ox-bows and meanders in the lower basin (A6, Fig 5.2).

Coming to the submarine fan, a highly complex channel planform is witnessed inside the Indus Canyon and in the Upper Indus Fan (Fig 5.1). In the upper reaches, slumping is dominant (B1, Fig 5.2) and further down, flat terraces and near vertical boundaries flank the highly sinuous channel belt. Meander loops denote lateral aggradation and vertical downcutting (B2, Fig 5.2). The concave-down longitudinal profile of the submarine Indus Fan, especially in the upper reaches, is representative of accentuated erosion that scour the shelfal regions causing sharper gradient change; and channels are at least a km wide throughout the Upper Indus Fan (Fig 5.1). Within the Canyon where the channel is already sinuous, on exiting it,

channel sinuosity further rises up to 4 in the bifurcating channel levee systems of the Upper Indus Fan (Fig 5.1). As seen previously, high tapering levees (+100 m) rising above seafloor are typical in this zone (B3, Fig 5.2).

In the Middle Indus Fan, most of these characteristic attributes of channel planform are seen to continue. Meanders are also evident in the bathymetric data from both Upper and Middle Indus Fan. Channel sinuosity is at its maximum in this region, however, further downfan a reduction is recorded (Fig 5.1). Levee heights are reduced and mostly range between 40 to 20 m above the channel thalweg (B4, Fig 5.2) and are very faint along incisional channels making only marginal imprints on cross-sections (B5, Fig 5.2). The complex dominant planform of the canyon and upper fan gradually evolves into a smoother planform in the Middle Indus Fan (Fig 5.1).

The Lower Indus Basin channel planform is studied from Kodagali and Jauhari (1999) and Ward (2007). As discussed, channels are on average 900 m wide with moderate sinuosity and smaller dimension levees rising around 20 m from the seafloor with evident ox-bows. Therefore, a complex-to-simple planform development is witnessed in the submarine fan. As the distance between the source-point canyon and channel levee systems increases, channel dimensions reduce and surface deposits become fainter. To summarize:

1. SI values range from 1 to 3.2 in the Indus Basin (Prerna et al., 2018) and from 1 to 5.7 in the Indus Fan (Fig 5.1). Maximum channel width on land is observed in the Lower Indus Basin (5-7 km) and in the Upper Indus Fan part of the submarine fan (3-4 km) (as detailed in Section 4.3). These values confirm that the fairly common trend of increasing sinuosity and channel width from source to mouth in fluvial environments is diametric in the submarine system.

2. Meandering planform, meander loops and ox-bows are symbolic of the mature stage of channel development. Based on the findings, these are present in the submarine environments right from the canyon until the Middle Indus Fan (B2 to B4 Fig 5.2). On land however, they develop only in the Middle/Lower Indus Basin (A5-A6 Fig 5.2). Also, fluvial and submarine planforms in the middle sections of basin/fan are profoundly disparate, ranging from the dominantly braided and wide river to the deep-incising sinuous channels.
3. Instead of the broad, smoothly tapering floodplains on land (A4 to A6 Fig 5.2), large levees rising >100 m from the seafloor are seen in the Indus's submarine channel levee complexes, stacked along the flanks of the channels (B3-B4, Fig 5.2). Both features result from overspill but their dimensions are contrasting.
4. Terrace formations are observed in both systems, but their dimensions vary which further suggests that they were formed under different processes/conditions. Evidence of filled and strath terraces on land (A2, Fig 5.2) in the Upper Indus Basin are present (Kumar and Srivastava, 2018) but the relatively smaller coherently spaced submarine terraces (B2, Fig 5.2) probably indicate a higher frequency of vertical erosion and lateral aggradation.
5. Braiding is rarely observed in submarine environments (Damuth and Flood, 1985; Wynn et al., 2007). Foreman et al. (2015) explained the rarity of braiding in submarine channels due to a combination of factors that induce greater levee deposition and limit channel widening. Nevertheless, lack of evidences of braiding from the Indus Fan led us to infer that fluvial-like braiding (as observed in A4, Fig 5.2) is absent from the submarine system of the Indus. The comparative observations are summarized in Table 5.1.

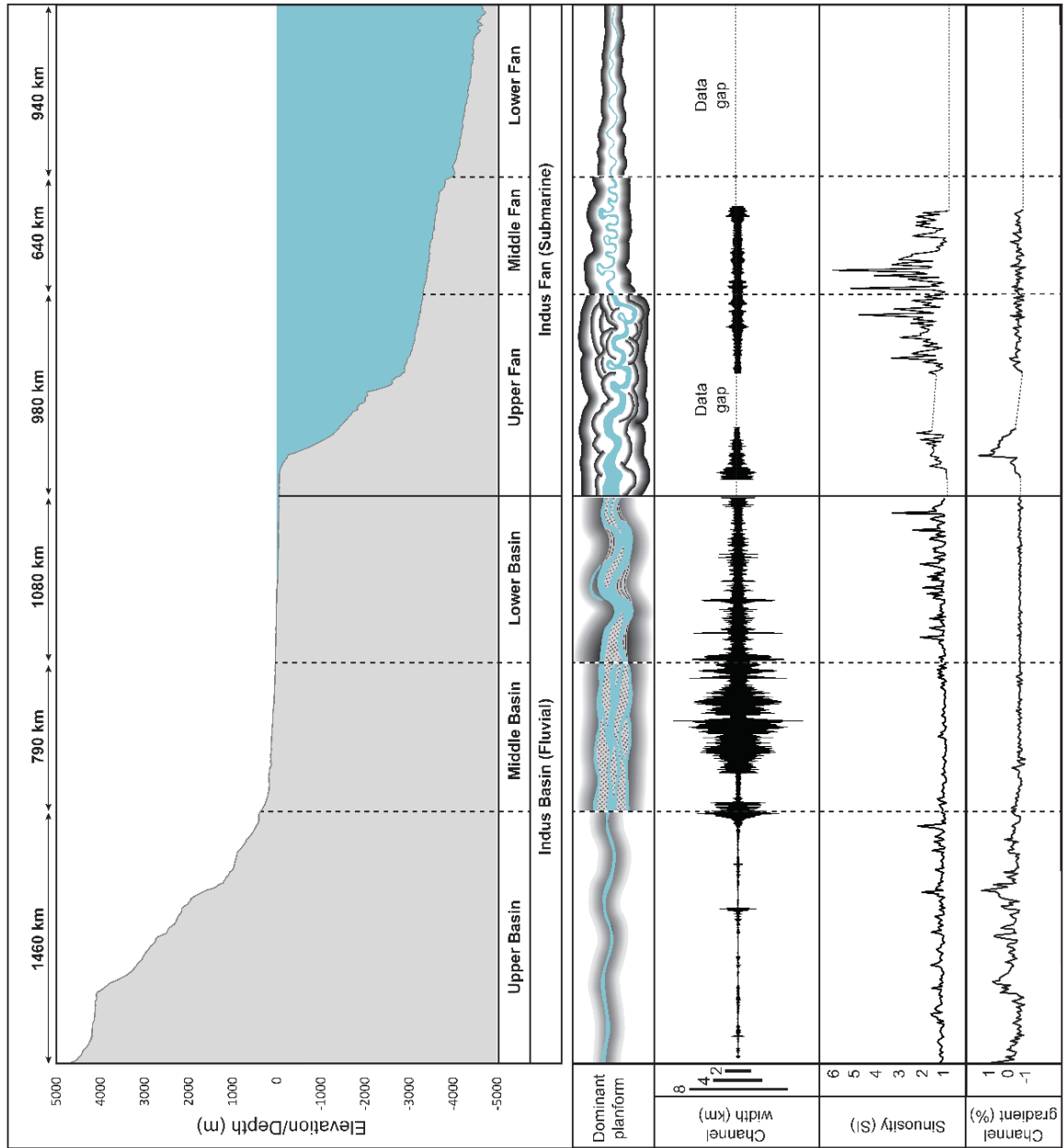


Fig 5.1: Combined longitudinal profile with Upper, Middle, Lower boundaries of the fluvial Indus Basin and the submarine Indus Fan. Dominant planform type, channel width, sinuosity and channel gradient through each zone of the Indus Basin and Indus Fan denote the transformation of a land-to-deep sea system. (Figure from Prerna and Kotha, 2020)

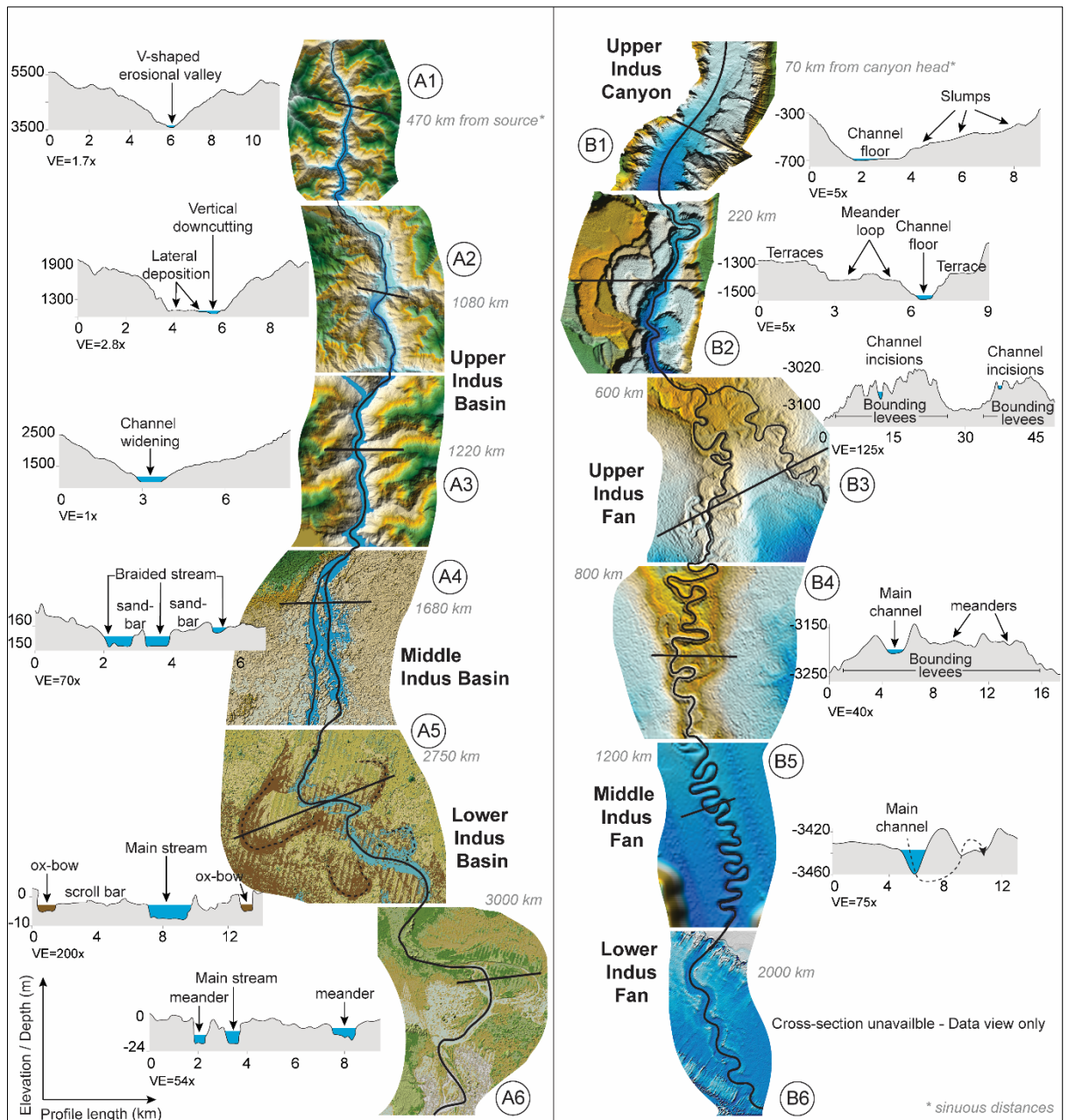


Fig 5.2: Dominant planforms and representative cross-section from the Indus River (A1 to A6) and the Indus Fan channels (B1 to B6). Blue polygons on every cross-section denote channel width. [Data source: Indus Basin (Block F1); Upper Indus Canyon (Block S1); Upper Indus Fan (Block S2); Middle Indus Fan (Block S3); Lower Indus Fan (Ward, 2007)]. (Figure from Prerna and Kotha, 2020)

Table 5.1: Summarized observations on comparison of fluvial and submarine channels  
(Source – Prerna and Kotha, 2020)

Aspect	Parameters considered	Region	Fluvial Basin	Submarine Fan
Channel process	Longitudinal profile; channel width; SI profile	Upper	Dominantly erosive	Erosive and depositional
		Middle	Dominantly depositional	Erosive and depositional
		Lower	Dominantly depositional	Dominantly depositional
Lateral expansion	Channel width;  <i>[considering width: ≤ 1 km—Low ≥ 1 km—High]</i>	Upper	Low (avg. 250 m)	High (avg. 1000 m)
		Middle	High (avg. 2700 m)	High (avg. 1000 m)
		Lower	High (avg. 1300 m)	Low (avg. 900 m)
Sinuosity	SI profile  <i>[considering SI: ≤ 2—Low 2 to 3—Moderate ≥ 3—High]</i>	Upper	Moderate (1 to 2.15)	High (1 to 4.62)
		Middle	Low (1 to 1.39)	High (1 to 5.71)
		Lower	High (1 to 3.22)	Moderate (1 to 2.24)
Meander loops/ cut-offs	Planform; Cross-sections	Upper	Absent	Present
		Middle	Present	Present
		Lower	Present	Present
Levee height	Cross-sections	Mostly in Middle Basin/Middle Fan	Moderate	Significant
Terrace formation	Cross-sections; Planform	Only in Upper Basin/Upper Fan	Present (mostly fluvio-glacially driven; and over-bank spilling)	Evident (driven by sequential lateral and vertical aggradation; and overbank spilling)
Braiding	Planform	Mostly in Middle Basin	Present	Absent

## 5.2. Causative factors

There is substantial morphometric evidence from the fluvial Indus basin and submarine Indus fan clearly showing nonconformity. Both systems are complex in their own ways with a multitude of factors interplaying. We infer that variance in morphometry is primarily an indicator of the different processes active in fluvial and submarine systems. The major dissimilarities introduced in Section 1.3.2. were found to be equally applicable in this analysis of the fluvial Indus Basin and submarine Indus Fan. Those and a few other crucial factors are discussed in this section.

- The source system:

A river system develops as a multi-point source system, whereas a submarine fan system is a single-point source system (Fig 5.3). Rivers are almost always joined by tributaries i.e. multi-point, making the main river a cumulative higher-order stream with increasing erosive potential. Submarine channel systems have a diametric mechanism. A single conduit (for e.g. through a canyon head) carrying turbidites gets distributed into several lower order channels with diminishing erosive potential. Deptuck and Sylvester (2018) found submarine and fluvial rivers to be fundamentally different due to the lack of tributaries in a single-point canyon system; and because the size of submarine channels reduced down-fan. In the Indus system too, this factor is considered to be the most vital in causing morphometric variation.

Channel width and channel depth are often studied to assess the erosive and depositional potential of a river system. Flood and Damuth (1987) while comparing the Amazon Fan channels to fluvial rivers concluded that channel width, depth, levee size and cross-sectional area reduced down-fan, which was in contrast to subaerial rivers where the sediment discharge increases downstream with more tributaries adding into the main stream.

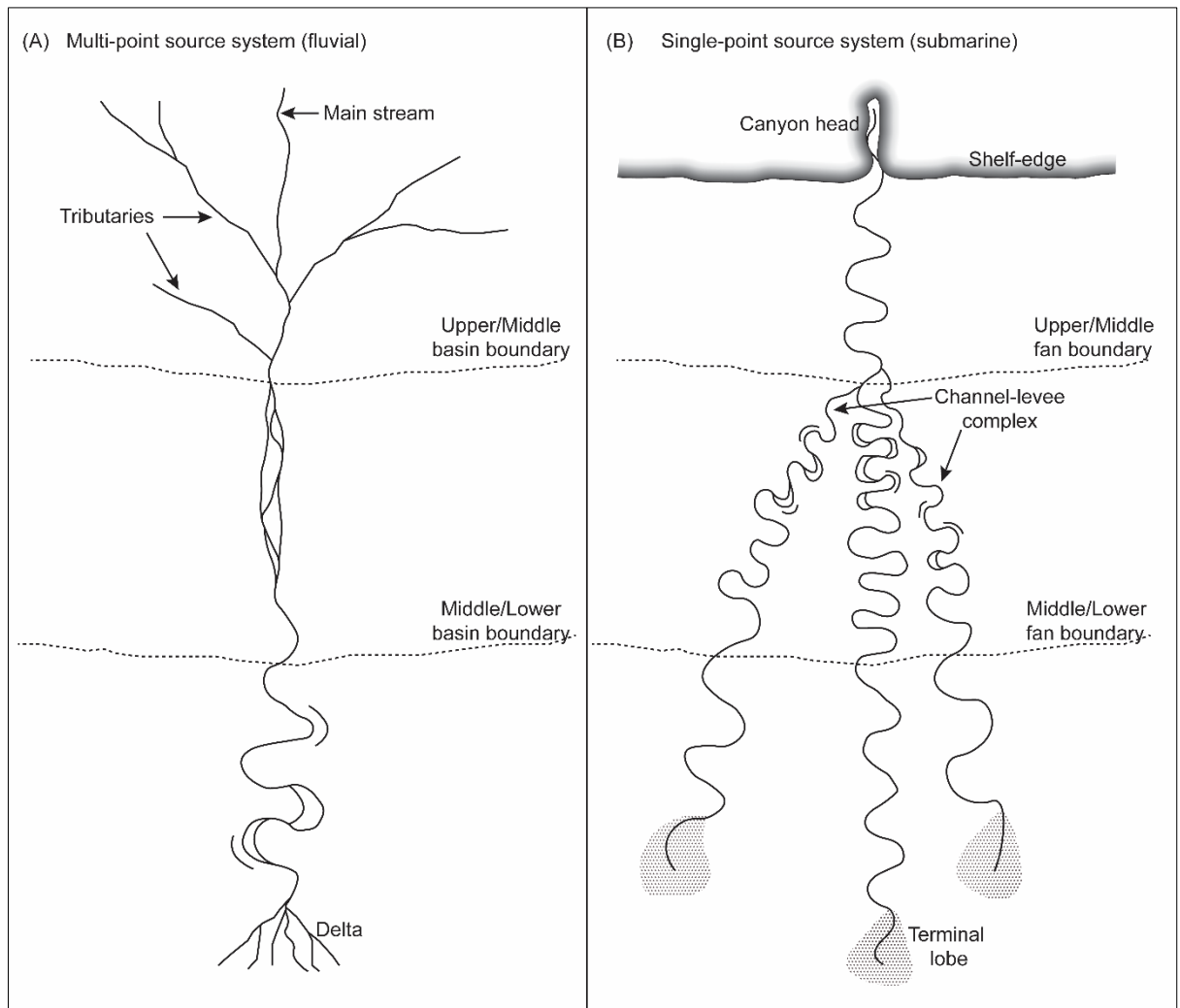


*Fig 5.3: Schematic comparison of a typical (A) multi-point source system and (B) single-point source system.*

Konsoer et al. (2013) concluded that submarine channels have cross-sectional dimensions that can exceed the dimensions of the largest rivers on earth by an order of magnitude. In our analysis of the Indus Basin and Fan, we find that channel width increases in the former (though highest widths are recorded in the Middle Indus Basin as the Lower Basin is anthropogenically controlled) and reduces in the latter. Cross sections from the Upper, Middle and Lower Indus Fans confirm a downward trend of channel depth as well. The major controller for this distinction could be (a) the influence of a single-point and a multi-point source of flow and (b) density contrasts between turbidity currents and river flow. Single point-source channel-fan systems such as the Indus, Amazon (Flood and Damuth, 1987) or Zaire

(Babonneau et al., 2002) have one and only one point of turbidite influx, and as the distance from the source point increases, the erosive strength of the channels and the thickness of turbidity currents reduces, thereby making the channels' cross-section smaller, and levees thinner. To conclude:

- ✓ Morphometry varies between distributary vs. cumulative flow
- ✓ erosive potential rises in fluvial systems
- ✓ channel dimensions decrease in submarine systems

- Density contrasts:

Running water and turbidity currents are known to have variable densities and therefore, they (a) erode differently, and (b) deposit differently. Thicker and dense turbidity currents in submarine systems, especially in the canyon and shelfal regions, are able to scour the sediments more strongly. Also, as discussed previously, density contrasts between river/channel flow and ambient flow also cause variation in morphometry. As opined by Kolla et al. (2007), these contrasts cause major differences in the internal architecture and modes of evolution of fluvial and submarine environments and Konsoer et al. (2013) suggested that the added friction between turbidity and ambient flows cause steeper channel gradients in submarine systems. Another aspect is greater superelevation, i.e. difference in the water surface level between the inside and outside wall of a river/channel bend (Ghahfarokhi et al., 2008), noted in submarine systems, attributed to flow density contrasts (Imran et al., 2009).

These density contrasts also control depositional products of rivers/channels. Fluvial flood-bank deposits result from overbank flooding; just as submarine levees are created by turbidity currents over spilling the channel flanks, but the submarine channel levees are typically greater in thickness than in fluvial rivers (Amir et al., 1996). Kolla et al. (2007) believed that it is the coalescence of sediment-gravity flows with the entrained ambient water

that makes the flow thicker and denser causing the deposition of thick channel levees. As has been confirmed in our analysis of the Indus as well, high relief levees are exclusive to submarine systems only. Wynn et al. (2007) considered these hundred meters plus high aggradational levees as the most spectacular distinction in submarine and fluvial systems. As per Peakall et al. (2000), continuous overbank spilling in submarine channels causes large levees to be formed as opposed to piecemeal levee build-up seen in fluvial rivers. The thicker turbidity currents act as a triggering force for channel plugging and frequent avulsions in submarine channels. Also, braiding is restricted in submarine systems due to high relief levees and higher channel gradient. To conclude:

- ✓ steeper channel gradient exists in submarine systems
- ✓ greater superelevation exists in submarine system
- ✓ levees of submarine channels are thicker than fluvial rivers
- ✓ continuous vs. piecemeal levee built-up in submarine and fluvial system respectively
- ✓ high variation in relief of flood-bank levees and submarine channel levees
- ✓ thicker turbidity flows trigger channel plugging and avulsion
- ✓ high relief levees restrict braiding in submarine systems

- Sinuosity development:

Sinuosity on land can be a function of several factors—slope and resistance (Lazarus and Constantine, 2013), sediment load (Schumm and Khan, 1972), discharge, tectonic instability, proximity to faults (Timár, 2003, Zámolyi et al. 2010) etc. In submarine systems, sinuosity is controlled by initial erosive base, lateral stacking, lateral accretion and seafloor topography (Mayall et al., 2006). Peakall et al. (2000) and Kolla et al. (2007) held that channel evolution and sinuosity models differ between fluvial and submarine systems. In the fluvial Indus Basin, sinuosity is largely controlled by topography in the Upper Indus Basin and high sediment load,

accentuated by damming, in the Lower Indus Basin (Prerna et al., 2018). Kolla et al. (2001) studied sinuous channels from Congo Fan to point that high sinuosity in submarine channels arises from repeated vertical aggradation and lateral migration instead of only lateral migration as observed in fluvial systems. In the Indus Fan too, we believe high sinuosity to result from episodic lateral migration and vertical aggradation, although initial seafloor topography would have played a major role. Again, the velocity profile of turbidity currents is known to have implications on sinuosity in submarine channels (Deptuck and Sylvester, 2018) which are found to be far more complex and contrasting to rivers (Peakall and Sumner, 2015). To conclude:

- ✓ Different factors control sinuosity in submarine and fluvial systems
  - ✓ Variation in velocity profiles of river flows and gravity flows effect sinuosity
- 
- Channel development:  
Lateral accretion and vertical erosion can be coeval in submarine systems. Kolla et al. (2007) summarized the differences in migratory patterns of submarine and fluvial systems by studying seismic amplitude trends. He opined that lateral migration and vertical aggradation could occur in a variety of forms, either continuous, or discrete or in combinations thereof. Jobe et al. (2016) in their study concluded that vertical aggradation is stronger in submarine systems with lateral accretion being more dominant in fluvial systems after comparing stratigraphic patterns of numerous fluvial and submarine channel systems, and Kolla et al. (2001) stated that vertical aggradation always accompanies lateral migration in deep-water channels. High incidence of lateral migration is also noted only in the fluvial Indus Basin due to low valley entrenchment, which is contrastingly high in the submarine extent—obstructing channel widening. Migration in submarine could also be more episodic if the strength of turbidity currents is discontinuous.

Hence the functioning of erosive/depositional elements during channel development could differ significantly in the two systems. To conclude:

- ✓ Lateral and vertical growth/migration operate in different forms
- ✓ Lateral aggradation is more dominant in fluvial systems
- ✓ High valley entrenchment in submarine systems

Other controlling factors like effects of Coriolis and centrifugal forces, base-level attainment, steady flows and catastrophic flows, vertical and horizontal density gradients, helical flow behaviour are believed to have a diametric influence on shaping the geometry of fluvial and submarine channels (Imran et al., 1999; Kolla et al., 2001, 2007; Corney et al., 2006; Keevil et al., 2006, 2007; Peakall and Sumner, 2015) and must be explored further in the context of the Indus system.

### **5.3. Conclusion**

This morphometric investigation aims to (a) quantify the variation between fluvial river and submarine channel morphometry with comparative data from the Indus system; and (b) to identify the causative factors behind the observed differences.

Beginning as a narrow, erosive and low sinuosity stream, the Indus River in the Upper Indus Basin shows typical characteristics of a youthful river. Contrastingly, internal structure of the Upper Indus Canyon shows near-vertical walls and terrace formations indicating inner-levée deposition, vertical aggradation and lateral migration. The channel diverges into several radially spreading lower-order channels in the Upper Indus Fan, on encountering drop in relief, which are also incisive and depositional at the same time. Over-bank deposits like the bounding-levees are characteristic features in this part of the Indus Fan. The high sinuosity of

the Upper Indus Fan continues in the Middle Fan as well. Such high sinuosity ( $SI >4$ ) is nowhere witnessed in the entire fluvial Indus Basin.

The Indus River in the low-relief Middle Basin tends to spread laterally in a braided form, yet within low SI values. Excessive channel widening is witnessed here. The Middle Indus Fan channels do not show any similar traits. They continue to flow within bounding-levees or outer-levees (smaller in dimension than bounding-levees) with very high sinuosity and reducing valley depth down-fan—indicating reduced erosion/accretion. However, there is a significant reduction in levee size. This was seen as a characteristic trait of middle-to-lower fan transition, observed by Flood and Damuth (1987) in Middle Amazon Fan.

Although data from the Lower Indus Fan is scanty, it does suggest that the channel behaviour is opposed to the Lower Indus Basin. On land, the river develops from a braided (less sinuous) planform to a single channel (more sinuous) river, with several scrollbars and ox-bows in its vicinity, and continues so till it meets the sea, forming a depositional delta. A delta is of course absent from the dictionary of submarine features; the closest approximation made to a lobe. But as discussed, lobe formation in the Lower Indus Fan is not confirmed. The lesser sinuous narrow channels with low-lying outer-levees and very shallow thalwegs are characteristic of the Lower Indus Fan.

The Indus Fan channel systems follow divergent morphometry. In the Upper Indus Canyon near-vertical walls and terrace formations indicate inner-levee deposition, vertical aggradation and lateral migration. After exiting the canyon in the Upper Indus Fan, the highly sinuous channel diverges into several radially spreading lower-order channels which also demonstrate coeval incision and deposition creating high-relief bounding-levees—characteristic of the region. In the Middle Indus Fan, they continue to flow creating bounding-levees or outer-levees (smaller in dimension than bounding-levees) with significant sinuosity. Reduced valley depth down-fan is indicative of reduced sediment flux and overspill. Narrow

channels with low sinuosity, weak outer-levees and very shallow thalwegs are characteristic of the Lower Indus Fan.

Principal causative factors for morphometric variations in fluvial rivers and submarine channels are (a) multi-point versus single-point source system i.e. presence and absence of tributaries respectively; (b) increasing sediment flux in fluvial systems downstream versus distributary-like division in submarine systems; (c) density contrasts between turbidity/sediment-gravity flows and river flows causing differential patterns of sinuosity and aggradation; (d) difference in characteristic depositional features and their dimension e.g. flat-wide floodplains vs. high-tapering bounding levees; (e) differences in functioning of erosional/depositional elements during channel development; and (f) progressively increasing and decreasing channel dimensions in fluvial rivers and submarine channels, respectively.

The Indus Fan and its associated channel levee systems is one of the most expansive and tectonically complex submarine fan systems of the world (Section 2.2). The presence of another proximal ancient canyon complex with its own recorded history of channel levee development makes it all the more intriguing. We believe that a thorough analysis of this system could entail a wider picture of the entire canyon-fed channel-levee-lobe system. The comparison presented here between the fluvial and submarine channel behaviour, from the composite system of the Indus is a first-ever.

A brief account of the most noteworthy submarine-fluvial comparative studies is provided here to coalesce this study with other examples worldwide. One of the pioneering long-range side-scan sonar surveys of the Amazon Fan led to the study by Flood and Damuth (1987) where channels were observed and compared with fluvial rivers on the basis of morphometry. Significant similarities were found but further scope of comparing hydrodynamic relations was suggested in order to estimate submarine channel behaviour from fluvial observations. Later, Clark et al. (1992) after measuring channel parameters from 16

submarine fans, with a focus to formulate a quantitative classification of fan systems worldwide, found some submarine channels comparable with fluvial channels. Two end-members—high-sinuosity, low-gradient and low-sinuosity, high-gradient were identified to classify submarine fans, and variations from these were attributed to tectonic controls or flow-type variations. Kolla et al. (2001) first attempted comparison of Congo Fan submarine channels with fluvial data sets from other sources to summarize a series of similarities and dissimilarities. Subsequently, results from Kolla et al. (2007) were more skewed towards the dissimilarities identified between fluvial and submarine channels. Wynn et al. (2007) exhaustively studied fan system across the globe and opined against that the long-held notion of similarities between fluvial river systems and submarine channel systems solely based on observable planform morphology. With more and more scientific advancement, flume-based/laboratory and numerical simulation based studies like Imran et al. (1999); Corney et al. (2006); Keevil et al. (2006); Kane et al. (2008); Lajeunesse et al. (2010); Darby and Peakall (2012); Foreman et al. (2015) were possible, which contributed significantly towards comparing fluvial-submarine channel forms. Data-rich comparative accounts discussed by Konsoer et al. (2013) and Jobe et al. (2016) also recorded differences in channel geometry, discharge, evolution, stratigraphic records etc. Two more rigorous studies by Sømme et al., (2009) and Nyberg et al., (2018) are worth mentioning for their source-to-sink data extensive approach describing morphological and sedimentological parameters to predict subsurface system behaviour and applicability to ancient systems.

Needless to say that every system is unique in its own form, with variable tectonic and topographic conditions, sediment flux, flow velocity etc.—a generalized model can be built if the system is studied in its entirety. Deptuck and Sylvester (2018) rightly stated that research on submarine fans and their channel systems is still far limited compared to our knowledge of fluvial systems, suggesting the need for more source-to-sink studies to bridge the gap. Several

other aspects for making a dichotomy of fluvial and submarine systems can be included like—role of base level, Coriolis and centrifugal forces, latitudinal controls, grain size variation, in-channel circulations etc. Our analysis here is limited to planform and morphometry but we do showcase the opposing trends inherent in both systems which are equally crucial to conclude that submarine channels and fluvial rivers are similar only superficially and must not be considered similar in *function* and *form*.

Two research papers emanating from this research are detailed below:

**Paper 1:** Prerna, R., Pandey, D.K., and Mahender, K. (2018) *Longitudinal Profiling and Elevation-Relief Analysis of the Indus*. *Arabian Journal of Geosciences, Springer*. Vol 11:343. DOI 10.1007/s12517-018-3657-5

**Paper 2:** Prerna, R., and Mahender K. (2020) *Geomorphometric comparison of submarine channel-levee complexes with fluvial river systems: observations from the Indus*. *Geo-Marine Letters, Springer*. DOI 10.1007/s00367-020-00654-8

#### **5.4. Scope for further research**

Elevation and bathymetric data are the core components in our study. Although extremely potent for deciphering surface processes, their applicability for sub-surface profiling can be limited at times. High-resolution seismic data are considered to be far more effective for understanding temporal and spatial modulations in channel forms. Significant headway—covering a plethora of aspects relevant to submarine fans and channel levee complexes using seismic reflection or sub-bottom profiling has been performed (Kolla et al., 2001; Babonneau et al., 2002; Posamentier, 2003; Abreu et al., 2003; Clift et al., 2002; Deptuck et al., 2003; Jégou et al., 2008). Such studies have refined the working knowledge of these marvellous geomorphic features of the deep sea environment. Ocean core sampling have already affirmed

the continuity of channels in the Indus Fan and their linkage with the Indus River by establishing provenance (Whitmarsh et al., 1974a, 1974b; Kolla and Coumes, 1987; Prell et al., 1989; Pandey et al. 2016; Kumar et al., 2019; Lu et al., 2020), however, establishment of a complete climatic/stratigraphic record since the onset of sedimentation would ameliorate our understanding of the history of fan development. Further scope lies in the integration of seismic reflection or sub-bottom profile data and sediment core samples with bathymetric data to better describe the evolution of channel levee systems. Similarly, on land, due to the high distortion of natural morphometry by anthropogenic influence, alternate geophysical data sources can provide better constraints to allow paleo-reconstruction of river pathways.

In this study, the best available data sources have been utilised, but the inherent limitations must be discussed. The main concerns faced were pertaining to the data gaps, especially in the Indus Fan and to the quality of MBES data in certain blocks. Previously mentioned in Section 3.3, seamless data, as available for the Indus Basin's subaerial analysis, is currently unavailable for the submarine fan. Due to variable data sources for the Indus Fan, with inconsistent spatial resolutions, it was a challenge to accurately decipher channel morphometry in certain pockets. Nevertheless, a segmented yet exhaustive account of channel patterns from shelf-to-abyssal plains was successfully obtained. With technological advancement, wider coverage of the submarine systems and access to improved data seems imminent. As a result of that, higher number of parameters can be estimated with greater accuracy. It would be our endeavour to pursue greater research by addressing the limitations faced in this research and come forth with improved research outcomes.

## **5.5. Epilogue**

All in all, this thesis presents a quantified comparison of the morphometric behaviour of fluvial rivers on land with submarine channel levee systems from one single river system—the Indus.

Our attempt to dissuade the long-standing analogy of onshore rivers and offshore channels stands successful using DEM and MBES data. It not only brings out the obvious differences that are expected to exist in a fluvial and submarine environment, but also quantifies the not so obvious *range* of these differences. Indices and parameters discussed here affix a range for such variations. The very idea behind presenting a complete source-to-sink depiction of an onshore river and its consequent submarine channel system is to capture the inherent variations in terms of morphometry. The values discussed in this study are indispensable components rather than merely representative. Geomorphometric parameters help discern the minuteness of changing forms and functions. Needless to say that there are many other aspects of hydrology, geomorphology with a variety of exogenic influences which must be incorporated in a fluvial-submarine debate. It is our understanding that morphometric comparison plays a key role by delivering an impactful impetus to investigate further. With similar research for different fan systems across the globe, a more vivid understanding of onshore river systems and their associated submarine channel forms can be explored. As a parallel implication, such a comparative study also emphasises the caution required before assuming similarity in fluvial-submarine processes and features. In modern times where deep sea submarine reservoirs are seen as the future of resource exploration, in-depth details about their depositional mechanism and associated processes are vital. Modelling of submarine processes based on laboratory experiments and visible fluvial impressions are not uncommon (Section 1.2.1). Complementary to that, assessing the degree of variation is of equal importance in order to avoid erroneous interpretations. A tiered approach beginning with mapping the system, understanding it and then proposing a comparison attempts to cover the wide gamut of factors that influence the system as a whole. With more and more data in the future, we sincerely hope that this study along with many others would help bridge the lacuna of our understanding of fluvial and submarine systems.

## **REFERENCES**

## References

- Abreu, V., Sullivan, M., Pirmez, C., Mohrig, D. (2003). Lateral accretion packages (LAPs): an important reservoir element in deep water sinuous channels. *Marine and Petroleum Geology*. 20(6-8), 631-648. <http://doi.org/10.1016/j.marpetgeo.2003.08.003>
- Afzal, J., Williams, M., Aldridge, R.J. (2009). Revised stratigraphy of the lower Cenozoic succession of the Greater Indus Basin in Pakistan. *Journal of Micropalaeontology*. 28(1), 7–23. <https://doi.org/10.1144/jm.28.1.7>
- Ahmed, M.F. (2013). A regional study of landslide hazards and related features in the Upper Indus River Basin, northern Pakistan (Doctoral Dissertations). Paper 2109. USA: Missouri University of Science and Technology. [http://scholarsmine.mst.edu/doctoral\\_dissertations/2109/](http://scholarsmine.mst.edu/doctoral_dissertations/2109/)
- Amir, A., Kenyon, N.H., Cramp, A., Kidd, R.B. (1996). Morphology of channel-levee systems on the Indus deep-sea fan, Arabian Sea. *Pakistan Journal of Hydrocarbon Research*. 8(1), 43-53. <https://pjhr.org.pk/index.php/pjhr/article/download/97/89/>
- Antobreh, A.A., Krastel, S. (2006). Morphology, seismic characteristics and development of Cap Timiris Canyon, offshore Mauritania: a newly discovered canyon preserved-off a major arid climatic region. *Marine and Petroleum Geology*. 23(1), 37-59. <https://doi.org/10.1016/j.marpetgeo.2005.06.003>
- Asim, S., Qureshi, S., Asif, S., Abbasi, S., Solangi, S., Mirza, M. (2014). Structural and stratigraphical correlation of seismic profiles between Drigri Anticline and Bahawalpur High in Central Indus Basin of Pakistan. *International Journal of Geosciences*. 5(11), 1231-1240. <https://doi.org/10.4236/ijg.2014.511102>
- Awasthi, K.D., Sitaula, B.K., Singh, B.R., Bajacharaya, R.M. (2002). Land-use change in two Nepalese Watersheds: GIS and Geomorphic Analysis. *Land Degradation & Development*. 13(6), 495-513. <https://doi.org/10.1002/ldr.538>
- Babar, Md. (Ed.). (2005). Hydrogeomorphology of landforms. In: *Hydrogeomorphology: fundamentals, applications and techniques*. New India, India: New Delhi Publishing Agency. Retrieved from [https://books.google.co.in/books?id=HetiC6uWB2kC&prints\\_ec=frontcover&source=gbs\\_ge\\_summary\\_r&cad=0#v=onepage&q&f=false](https://books.google.co.in/books?id=HetiC6uWB2kC&prints_ec=frontcover&source=gbs_ge_summary_r&cad=0#v=onepage&q&f=false)
- Babel, M.S., Wahid, S.M. (2008). Freshwater under threat: South Asia. United Nations Environment Programme. Nairobi, Kenya. Retrieved from [https://www.preventionweb.net/files/7989\\_southasiareport1.pdf](https://www.preventionweb.net/files/7989_southasiareport1.pdf)
- Babonneau, N., Savoye, B., Cremer, M., Klein, B. (2002). Morphology and architecture of the present canyon and channel system of the Zaire deep-sea fan. *Marine and Petroleum Geology*. 19(4), 445-467. [https://doi.org/10.1016/S0264-8172\(02\)00009-0](https://doi.org/10.1016/S0264-8172(02)00009-0)
- Babonneau, N., Savoye, B., Cremer, M., Bez, M. (2010). Sedimentary Architecture in meanders of a submarine channel: detailed study of the present Congo Turbidite Channel (Zaiango Project). *Journal of Sedimentary Research*. 80(10), 852-866. <http://doi.org/10.2110/jsr.2010.078>
- Bea, R.G., Wright, S.G., Sircar, P., Niedoroda, A.W. (1983). Wave induced slides in South Pass Block 70, Mississippi Delta. *Journal of Geotechnical Engineering*. 109, 619–644. [https://doi.org/10.1061/\(ASCE\)0733-9410\(1983\)109:4\(619\)](https://doi.org/10.1061/(ASCE)0733-9410(1983)109:4(619))
- Bastia, R., Radhakrishna, M. (Eds.). (2012). *Basin evolution and petroleum prospectivity of the continental margins of India*. (Vol 59, 1<sup>st</sup> ed.). Developments in Petroleum Science.

- Oxford, UK: Elsevier. Retrieved from <https://www.sciencedirect.com/bookseries/developments-in-petroleum-science/vol/59>
- Berlin, T.L. (2014). Channel-levee complexes and sediment flux of the Upper Indus Fan (Master's Thesis). 1236. USA: Louisiana State University. [https://digitalcommons.lsu.edu/gradschool\\_theses/1236](https://digitalcommons.lsu.edu/gradschool_theses/1236)
- Bouma, A.H., Normark, W.R., Barnes, N.E. (Eds.). (1985a) *Submarine fans and related turbidite systems*. (1<sup>st</sup> ed.). Frontiers in Sedimentary Geology. New York, USA: Springer. [http://doi.org/10.1007/978-1-4612-5114-9\\_21](http://doi.org/10.1007/978-1-4612-5114-9_21)
- Bouma, A.H., Stelling, C.E., Coleman, J.M. (1985b). Mississippi Fan: Gulf of Mexico. In: A.H., Bouma, W.R., Normark, N.E., Barnes (Eds.), *Submarine fans and related turbidite systems*. (1<sup>st</sup> ed.). Frontiers in Sedimentary Geology. New York, USA: Springer. [http://doi.org/10.1007/978-1-4612-5114-9\\_21](http://doi.org/10.1007/978-1-4612-5114-9_21)
- Bourget, J., Zaragosi, S., Rodriguez, M., Fournier, M., Garlan, T., Chamot-Rooke, N. (2013). Late Quaternary megaturbidites of the Indus Fan: origin and stratigraphic significance. *Marine Geology*. 336, 10-23. <http://doi.org/10.1016/j.margeo.2012.11.011>
- Brice, J.C. (1974). Evolution of meander loops. *Geological Society of America Bulletin*. 85, 581-586. [https://doi.org/10.1130/0016-7606\(1974\)85<581:EOML>2.0.CO;2](https://doi.org/10.1130/0016-7606(1974)85<581:EOML>2.0.CO;2)
- Burbank, D.W., Beck, R.A. (1991). Models of aggradation versus progradation in the Himalayan Foreland. *Geologische Rundschau*. 80(3), 623-638. <https://doi.org/10.1007/BF01803690>
- Butler, R.W.H., George, M., Harris, N.B.W., Jones, C., Prior, D.J., Treloar, P.J., Wheeler, J. (1992). Geology of the northern part of the Nanga Parbat massif, northern Pakistan, and its implications for Himalayan tectonics. *Journal of the Geological Society*. 149(4), 557-567. <https://doi.org/10.1144/gsjgs.149.4.0557>
- Calvès, G., Huuse, M., Clift, P.D., Brusset, S. (2015). Giant fossil mass wasting off the coast of West India: The Nataraja submarine slide. *Earth and Planetary Science Letters*. 432, 265-272. <https://doi.org/10.1016/j.epsl.2015.10.022>
- Carmichael, S.M., Akhter, S., Bennett, J.K., Fatimi, M.A., Hosein, K., Jones, R.W., & Tozer, R.S.J. (2009). Geology and hydrocarbon potential of the offshore Indus Basin, Pakistan. *Petroleum Geoscience*. 15, 107-116. <https://doi.org/10.1144/1354-079309-826>
- CartoDEM v-3 R1. (2015). *NRSC Open EO Data Archive (NOEDA)*. National Remote Sensing Centre. Retrieved from <http://bhuvan.nrsc.gov.in/data/download/index.php>
- Chen, L., Khan, S. (2010). InSAR observation of the strike-slip faults in the northwest Himalayan Frontal Thrust system. *Geosphere*. 6(5), 731-736. <https://doi.org/10.1130/GES00518.1>
- Clark, J.D., Kenyon, N.H., Pickering, K.T. (1992). Quantitative analysis of the geometry of submarine channels: Implications for the classification of submarine fans. *Geology*. 20(7), 633-636. [https://doi.org/10.1130/0091-7613\(1992\)020<0633:QAOTGO>2.3.CO;2](https://doi.org/10.1130/0091-7613(1992)020<0633:QAOTGO>2.3.CO;2)
- Clift, P.D., Shimizu, N., Layne, G. D., Gaedicke, C., Schlüter, H.-U., Clark, M., & Amado, S. (2001). Development of the Indus Fan and its significance for the erosional history of the Western Himalaya and Karakoram. *Geological Society of America Bulletin*, 113(8), 1039-1051. [https://doi.org/10.1130/0016-7606\(2001\)113<1039:DOTIFA>2.0.CO;2](https://doi.org/10.1130/0016-7606(2001)113<1039:DOTIFA>2.0.CO;2)
- Clift, P.D. (2002). A brief history of the Indus River. In: P.D., Clift, D., Kroon, C., Gaedicke, J., Craig (Eds.), *The tectonic and climatic evolution of the Arabian Sea region*. Special

- Publications No. 195. London, UK: The Geological Society. 237-258. <https://doi.org/10.1144/GSL.SP.2002.195.01.13>
- Clift, P.D., Gaedicke, C., Edwards, R., Lee, J.I., Hildebrand, P., Amjad, S., White, R.S., Schlüter, H.-U. (2002). The stratigraphic evolution of the Indus Fan and the history of sedimentation in the Arabian Sea. *Marine Geophysical Researches*. 23(3), 223-245. <http://doi.org/10.1023/A:1023627123093>
- Clift, P.D., Blusztajn, J., (2005). Reorganization of the western Himalayan river system after five million years ago. *Nature*. 438. 1001-1003. <https://doi.org/10.1038/nature04379>
- Clift, P.D., Carter, A., Giosan, L., Durcan, J., Duller, G.A.T., Macklin, M.G., & Fuller, D.Q., (2012). U-Pb zircon dating evidence for a Pleistocene Sarasvati River and capture of the Yamuna River. *Geology*. 40(3), 211–214. <https://doi.org/10.1130/G32840.1>
- Clift, P.D., Giosan, L., Henstock, T.J., Tabrez, A.R. (2014). Sediment storage and reworking on the shelf and in the Canyon of the Indus River-Fan System since the last glacial maximum. *Basin Research*. 26, 183-202. <http://doi.org/10.1111/bre.12041>
- Clift, P.D., Henstock, T.J. (2015). Kongsberg EM302 processed bathymetry data, Indus Canyon and shelf, Pelagia cruise PE300 (year 2008-2009, investigators Peter Clift and Tim Henstock). Interdisciplinary Earth Data Alliance (IEDA). <http://get.iedadata.org/doi/321848>
- Clift, P.D. (2017). Cenozoic sedimentary records of climate-tectonic coupling in the Western Himalaya. *Progress in Earth and Planetary Science*. 4(39), 1-22. <http://doi.org/10.1186/s40645-017-0151-8>
- Coleman, J.M., Huh, Q.K., Braud, D. Jr. (2008). Wetland loss in world deltas. *Journal of Coastal Research*. 24(1A), 1-14. <http://doi.org/10.2112/05-0607.1>
- Corney, R.K.T., Peakall, J., Parsons, D.R., Elliott, L., Amos, K.J., Best, J.L., Keevil, G.M., Ingham, D.B. (2006). The orientation of helical flow in curved channels. *Sedimentology*. 53, 249-257. <http://doi.org/10.1111/j.1365-3091.2006.00771.x>
- Covault, J.A. (2011). Submarine fans and canyon-channel systems: a review of processes, products, and models. *Nature Education Knowledge*, 3(10):4. Retrieved from <https://www.nature.com/scitable/knowledge/library/submarine-fans-and-canyon-channel-systems-a-24178428>
- Covault, J.A., Shelve, E., Traer, M., Hubbard, S.M., Romans, B.W., Fildani, A. (2012). Deepwater channel run-out length: insights from seafloor geomorphology. *Journal of Sedimentary Research*. 82(1), 25-40. <http://doi.org/10.2110/jsr.2012.2>
- Cross, N.E., Cunningham, A., Cook, R.J., Taha, A., Esmatie, E., Nasar, E.S. (2009). Three-dimensional seismic geomorphology of a deep-water slope-channel system: The Sequoia field, offshore west Nile Delta, Egypt. *American Association of Petroleum Geologists Bulletin*. 93, 1063-1086. <https://doi.org/10.1306/05040908101>
- Dailey, S.K., Clift, P.D., Kulhanek, D.K., Blusztajn, J., Routledge, C.M., Calvès, G., & Yu, Z. (2019). Large-scale mass wasting on the Miocene continental margin of western India. *Geological Society of America Bulletin*. <https://doi.org/10.1130/B35158.1>
- Damuth, J.E., Kumar, N. (1975). Amazon Cone: morphology, sediments, age, and growth pattern. *Geological Society of America Bulletin*. 86(6), 863-878. [https://doi.org/10.1130/0016-7606\(1975\)86<863:ACMSAA>2.0.CO;2](https://doi.org/10.1130/0016-7606(1975)86<863:ACMSAA>2.0.CO;2)

- Damuth, J.E., Flood, R.D. (1985). Amazon Fan, Atlantic Ocean. In: A.H., Bouma, W.R., Normark, N.E., Barnes (Eds.), *Submarine fans and related turbidite systems*. (1<sup>st</sup> ed.). Frontiers in Sedimentary Geology. New York, USA: Springer. [http://doi.org/10.1007/978-1-4612-5114-9\\_15](http://doi.org/10.1007/978-1-4612-5114-9_15)
- Darby, S.E., Peakall, J. (2012). Modelling the equilibrium bed topography of submarine meanders that exhibit reversed secondary flows. *Geomorphology*. 163-164, 99-109. <https://doi.org/10.1016/j.geomorph.2011.04.050>
- Deptuck, M.E., Steffens, G.S., Barton, M., Pirmez, C. (2003). Architecture and evolution of Upper Indus Fan channel-belts on the Niger Delta slope and in the Arabian Sea. *Marine and Petroleum Geology*. 20(6-8), 649-676. <http://doi.org/10.1016/j.marpetgeo.2003.01.004>
- Deptuck, M.E., Piper, D.J.W., Bruno, S., Gervais, A. (2008). Dimensions and architecture of late Pleistocene submarine lobes off the northern margin of East Corsica. *Sedimentology*. 55(4), 869-898. <http://doi.org/10.1111/j.1365-3091.2007.00926.x>
- Deptuck, M.E., Sylvester, Z. (2018). Submarine Fans and Their Channels, Levees, and Lobes. In: A., Micallef, S., Krastel, A., Savini. (Eds.), *Submarine Geomorphology*. Cham, Switzerland: Springer Geology. 273-299. [http://doi.org/10.1007/978-3-319-57852-1\\_15](http://doi.org/10.1007/978-3-319-57852-1_15)
- Dey, S. (Ed.). (2014). Fluvial processes: meandering and braiding. In: *Fluvial hydrodynamics, hydrodynamic and sediment transport phenomena*. GeoPlanet: Earth and Planetary Sciences. Heidelberg, Germany: Springer. 529-562. [https://doi.org/10.1007/978-3-642-19062-9\\_9](https://doi.org/10.1007/978-3-642-19062-9_9)
- Dipietro, J.A., Hussain, A., Ahmad, I., Khan, A.M. (2000). The main mantle thrust in Pakistan: its character and extent. In: M.A., Khan, P.J. Treloar, M.P., Searle, M.Q., Jan (Eds.), *Tectonics of the Nanga Parbat Syntaxis and the Western Himalaya*. Special Publications Vol 170. London, UK: The Geological Society. 375-393. <https://doi.org/10.1144/GSL.SP.2000.170.01.20>
- Emmel, F.J., Curray, J.R. (1985). Bengal Fan, Indian Ocean. In: A.H., Bouma, W.R., Normark, N.E., Barnes (Eds.), *Submarine fans and related turbidite systems*. (1st ed.). Frontiers in Sedimentary Geology. New York, USA: Springer. [http://doi.org/10.1007/978-1-4612-5114-9\\_16](http://doi.org/10.1007/978-1-4612-5114-9_16)
- Encyclopædia Britannica (2011) Potwar Plateau. Article in Encyclopaedia Britannica Online. <https://www.britannica.com/place/Potwar-Plateau>
- ESRI™, Environmental Systems Research Institute. Product: ArcMap® Tool Help. Retrieved from <https://desktop.arcgis.com/en/arcmap/>
- ESRI™ World Imagery (WGS84). Source: Esri, DigitalGlobe, GeoEye, Earthstar Geographics, CNES/Airbus DS, USDA, USGS, AEX, Getmapping, AeroGRID, IGN, IGP, swisstopo, and the GIS User Community. Retrieved from: <https://www.arcgis.com/home/item.html?id=52bdc7ab7fb044d98add148764eaa30a>
- FAO (2011) Indus River Basin. In: K., Frenken (Ed.), *Irrigation in Southern and Eastern Asia in figures*. AQUASTAT Survey – 2011, FAO Water Report 37, 129-142. Retrieved from <http://www.fao.org/3/i2809e/i2809e.pdf>
- Fairfield, J., Leymarie, P. (1991). Drainage networks from grid digital elevation models. *Water Resources Research*. 27(5), 709-717. <https://doi.org/10.1029/90WR02658>

- Flood, R.D., Damuth, J.E. (1987). Quantitative characteristics of sinuous distributary channels on the Amazon Deep-sea Fan. *Geological Society of America Bulletin*, 98(6), 728-738. [https://doi.org/10.1130/0016-7606\(1987\)98<728:QCOSDC>2.0.CO;2](https://doi.org/10.1130/0016-7606(1987)98<728:QCOSDC>2.0.CO;2)
- Florinsky, I.V. (2017). An illustrated introduction to general geomorphometry. *PPG: Earth and Environment*. 41(6), 723-752. <https://doi.org/10.1177/0309133317733667>
- Foreman, B.Z., Lai, S.Y.J., Komatsu, Y., Paola, C. (2015). Braiding of submarine channels controlled by aspect ratio similar to river. *Nature Geoscience*. 8, 700-703. <http://doi.org/10.1038/ngeo2505>
- Gaedicke, C., Schlüter, H.-U., Roeser, H.A., Prexl, A., Schreckenberger, B. Meyer, & Amjad, S. (2002). Origin of the northern Indus Fan and Murray Ridge, Northern Arabian Sea: interpretation from seismic and magnetic imaging. *Tectonophysics*. 355(1-4), 127-143. [https://doi.org/10.1016/S0040-1951\(02\)00137-3](https://doi.org/10.1016/S0040-1951(02)00137-3)
- Garbrecht, J., Martz, L.W. (1997). The Assignment of drainage direction over flat surfaces in raster digital elevation models. *Journal of Hydrology*. 193(1-4), 204-213. [https://doi.org/10.1016/S0022-1694\(96\)03138-1](https://doi.org/10.1016/S0022-1694(96)03138-1)
- Garzanti, E., Vezzoli, G., Ando, S., Paparella, P., Clift, P.D. (2005). Petrology of Indus River sands; a key to interpret erosion history of the western Himalayan syntaxis. *Earth and Planetary Science Letters*. 229(3-4), 287-302. <http://doi.org/10.1016/j.epsl.2004.11.008>
- Gaurav, K., Sinha, R., Panda, P.K. (2011). The Indus flood of 2010 in Pakistan: a perspective analysis using remote sensing data. *Natural Hazards*. 59:1815. <http://doi.org/10.1007/s11069-011-9869-6>
- Gee, E.R., Gee, D.G. (1989). Overview of the geology and structure of the salt range, with observations on related areas of northern Pakistan. *Special paper of the GSA*. 232, 95-112. <https://doi.org/10.1130/SPE232-p95>
- Ghahfarokhi, G.R.S., van Gelder, P.H.A.J.M., Vrijling, J.K. (2008). Evaluation of superelevation in open channel bends with probabilistic analysis methods. World Environmental and Water Resources Congress 2008 proceedings. [https://doi.org/10.1061/40976\(316\)244](https://doi.org/10.1061/40976(316)244)
- Giosan, L., Constantinescu, S., Clift, P.D., Tabrez, A.R., Danish, M., Inam, A. (2006). Recent morphodynamics of the Indus delta shore and shelf. *Continental Shelf Research*. 26(14), 1668-1684. <https://doi.org/10.1016/j.csr.2006.05.009>
- Google Earth™. Retrieved from [https://www.google.com/intl/en\\_in/earth/](https://www.google.com/intl/en_in/earth/)
- Govil, P., Naidu, P.D. (2008). Late Quaternary changes in depositional processes along the western margin of the Indus Fan. *Geo-Marine Letters*. 28(1), 1-6. <http://doi.org/10.1007/s00367-007-0083-1>
- Gupta, A. (Ed.). (2004). *Large rivers: geomorphology and management*. Chichester, UK: John Wiley & Sons. <https://doi.org/10.1002/9780470723722>
- Hansen, L., Callow, R., Kane, I., Gamberi, F., Rovere, M., Cronin, B., Kneller, B. (2015) Genesis and character of thin-bedded turbidities associated with submarine channels. *Marine and Petroleum Geology*. 67, 852-879. <https://doi.org/10.1016/j.marpetgeo.2015.06.007>
- Hansen, L., Janocko, M., Kane, I., Kneller, B. (2017). Submarine channel evolution, terrace development, and preservation of intra-channel thin-bedded turbidites: Mahin and Avon

- channels, offshore Nigeria. *Marine Geology*. 383(1), 146-167. <http://doi.org/10.1016/j.margeo.2016.11.011>
- Haq, B.U., Haq, S.M., Kullenberg, G., Stel, J.H. (Eds.). (1997). *Coastal zone management imperative for maritime developing nations*. Coastal Systems and Continental Margins (Vol 3). The Netherlands: Kluwer Academic Publishers. <http://doi.org/10.1007/978-94-017-1066-4>
- Harris, P.T. (2012). Seafloor Geomorphology—Coast, Shelf, and Abyss. In: P.T., Harris, E.K., Baker (Eds.), *Seafloor geomorphology as benthic habitat*. Elsevier. 109-115. <https://doi.org/10.1016/B978-0-12-385140-6.00006-2>
- Hawker, L., Bates, P., Neal, J., Rougier, J., (2018). Perspectives on Digital Elevation Model (DEM) Simulation for Flood Modeling in the Absence of a High-Accuracy Open Access Global DEM. *Frontiers in Earth Science*. 6, 233. <https://www.doi.org/10.3389/feart.2018.00233>
- Heiniö, P., Davies, R.J. (2007). Knickpoint migration in submarine channels in response to fold growth, western Niger Delta. *Marine and Petroleum Geology*. 24(6-9), 434-449. <http://doi.org/10.1016/j.marpetgeo.2006.09.002>
- Hsu, S.-K., Kuo, J., Lo, C.-L., Tsai, C.-H., Doo, W.-B., Ku, C.-Y., Sibuet, J.-C. (2008). Turbidity currents, submarine landslides and the 2006 Pingtung earthquake off SW Taiwan. *Terrestrial, Atmospheric and Oceanic Sciences Journal*.19(6), 767–772. [https://doi.org/10.3319/TAO.2008.19.6.767\(PT\)](https://doi.org/10.3319/TAO.2008.19.6.767(PT))
- Hull, E. (1912). Monograph on the sub-oceanic physiography of the North Atlantic Ocean. Cited in: Y., Qin (2017). Geological controls on the evolution of submarine channels in the Espírito Santo Basin, SE Brazil (Doctoral thesis). UK: Cardiff University. <https://orca.cf.ac.uk/104553/1/Thesis%20Yongpeng%20Qin.pdf>
- Hurtrez, J.E., Lucazean, F., Lave, J., Avouac, J.P. (1999). Investigation of the relationship between basin morphology, tectonic uplift and denudation from the study of an active fold belt in Siwalik Hills (Central Nepal). *Journal of Geophysical Research*, 104(B6), 12779-12796. <https://doi.org/10.1029/1998JB900098>
- Imran, J., Parker, G., Pirmez, C. (1999). A nonlinear model of flow in meandering submarine and subaerial channels. *Journal of Fluid Mechanics*. 400, 295-331. <http://doi.org/10.1017/S0022112099006515>
- Inam, A., Tahir, M. (2004). Channel-levee system - the major controlling mechanism for the sediment deposition on the Indus Fan. *Joint International Conference and First Annual Meeting of IGCP-475 DeltaMAP and APN project on the Mega-Deltas of Asia*.Icamg104/APN. Thailand, 15-20 January 2004. Retrieved from <http://citeseerx.ist.psu.edu/viewdoc/summary?doi=10.1.1.199.856>
- Inam, A., Clift, P.D., Giosan, L., Tabrez, A.R., Tahir, M., Rabbani, M.M., Danish, M. (2008). The geographic, geological and oceanographic setting of the Indus River. In: A., Gupta (Ed.), *Large rivers: geomorphology and management*. Chichester, UK: John Wiley & Sons. 333-346. <https://doi.org/10.1002/9780470723722.ch16>
- Jarvis, A., Reuter, H.I., Nelson, A., Guevara, E. (2008). Hole-filled SRTM for the globe Version 4. CGIAR-CSI SRTM 90 m Database. Retrieved from <http://srtm.csi.cgiar.org>

- Jégou, I., Savoye, B., Pirmez, C., Droz, L. (2008) Channel-mouth lobe complex of the recent Amazon Fan: The missing piece. *Marine Geology*. 252(1-2), 62-77. <https://doi.org/10.1016/j.margeo.2008.03.004>
- Jenson, S.K., Domingue, J.O. (1988). Extracting topographic structure from digital elevation data for geographic information system analysis. *Photogrammetric Engineering and Remote Sensing*. 54(11). 1593-1600. <http://pubs.er.usgs.gov/publication/70142175>
- Jervey, MT. (1988). Quantitative geological modeling of siliciclastic rock sequences and their seismic expression. In: C.K., Wilgus, B.S., Hastings, H., Posamentier, J.V., Wagoner, C.A., Ross, C., Kendall (Eds.), *Sea-level changes: an integrated approach*. Special Publication No. 42. SEPM Society for Sedimentary Geology. Tulsa, Oklahoma, USA: SEPM. <https://doi.org/10.2110/pec.88.01.0047>
- Jobe, Z.R., Howes, N.C., Auchter, N. (2016). Comparing submarine and fluvial channel kinematics: implications for stratigraphic architecture. *Geology*. 44(11), 931-934. <http://doi.org/10.1130/G38158.1>
- Johnson, M.R.W. (1994). Volume balance of erosional loss and sediment deposition related to Himalayan uplifts. *Journal of the Geological Society, London*. 151, 217-220. Retrieved from <http://citeseerx.ist.psu.edu/viewdoc/download?doi=10.1.1.850.6512&rep=rep1&type=pdf>
- Jones, L.S., Schumm, M. (1999). Causes of Avulsion: An Overview. In: N.D., Smith, J., Rogers (Eds.), *Fluvial Sedimentology VI*. Special Publication No. 28. The International Association of Sedimentologists. Oxford, London, UK: Blackwell Science Ltd. 169-178. <https://doi.org/10.1002/9781444304213.ch13>
- Juyal, N. (2014). Ladakh: the high altitude Indian cold desert. In: V.S., Kale (Ed.). *Landscapes and landforms of India*. Dordrecht, The Netherlands: Springer, 115-124. [http://doi.org/10.1007/978-94-017-8029-2\\_10](http://doi.org/10.1007/978-94-017-8029-2_10)
- Kane, I.A., Kneller, B.C., Dykstra, M., Kassem, A., McCaffrey, W.D. (2007). Anatomy of a submarine channel-levee: an example from Upper Cretaceous slope sediments, Rosario Formation, Baja California, Mexico. *Marine and Petroleum Geology*. 24(6-9), 540-563. <http://doi.org/10.1016/j.marpetgeo.2007.01.003>
- Kane I.A., McCaffrey, W.D., Peakall, J. (2008). Controls on sinuosity evolution within submarine channels. *Geology*. 36(4):287–290. <https://doi.org/10.1130/G24588A.1>
- Kazmi, A.H., Jan, M.Q. (1997). *Geology and Tectonics of Pakistan*. Karachi, Pakistan: Graphic Publishers. Retrieved from <https://lgc2016.files.wordpress.com/2016/03/geology-tectonics-of-pakistan-by-kazmi-qasimjan.pdf>
- Keevil, G.M., Peakall, J., Best, J.L., Amos, K.J. (2006). Flow structure in sinuous submarine channels: velocity and turbulence structure of an experimental submarine channel. *Marine Geology*. 229(3-4), 241-257. <http://doi.org/10.1016/j.margeo.2006.03.010>
- Keevil, G.M., Peakall, J., Best, J. (2007). The influence of scale, slope and channel geometry on the flow dynamics of submarine channels. *Marine and Petroleum Geology*. 24(6-9), 487-503. <http://doi.org/10.1016/j.marpetgeo.2007.01.009>
- Kenyon, N.H., Belderson, R.H., Stride, A.H. (1978). Channels, canyons and slump folds on the continental slope between South-West Ireland and Spain. *Oceanologica Acta*. 1(3), 369-380. <https://archimer.ifremer.fr/doc/00123/23393/21220.pdf>

- Kenyon, N.H., Amir, A., Bishop, D.G., Booth, D.G., Campbell, J.M., Danish, M., Davies, M.A., Hunter, P.M., Miles, P.R., Phipps, R.A., Robinson, A.D., Rothwell, R.G. (1987). GLORIA study of the Indus Fan, RRS Charles Darwin Cruise 20, 31 January-27 February 1987. *Institute of Oceanographic Sciences, Deacon Laboratory, Cruise Report, No. 198*. 1-17. <https://eprints.soton.ac.uk/14234/>
- Kenyon, N.H., Amir, A., Cramp, A. (1995). Geometry of the younger sediment bodies of the Indus Fan. In: K.T., Pickering, R.N., Hiscott, N.H., Kenyon, F.R., Lucchi, R.D.A., Smith (Eds.), *Atlas of deep-water environments: architectural style in turbidite systems*. London, UK: Chapman and Hall. 89-93. [https://doi.org/10.1007/978-94-011-1234-5\\_16](https://doi.org/10.1007/978-94-011-1234-5_16)
- Kenyon, N.H., Millington, J. (1995). Contrasting deep-sea depositional systems in the Bering Sea. In: K.T., Pickering, R.N., Hiscott, N.H., Kenyon, F.R., Lucchi, R.D.A., Smith (Eds.), *Atlas of deep-water environments: architectural style in turbidite systems*. London, UK: Chapman and Hall. 196-202. [https://doi.org/10.1007/978-94-011-1234-5\\_28](https://doi.org/10.1007/978-94-011-1234-5_28)
- Khan, M.A., Ahmed, R., Raza, H.A., Kemal, A. (1986). Geology of petroleum in Kohat-Potwar Depression, Pakistan. *American Association of Petroleum Geologists Bulletin*. 70(4), 393-414. <http://www.doi.org/10.1306/9488571E-1704-11D7-8645000102C1865D>
- Khan, M.Z., Akbar, G. (2012). In the Indus Delta it is no more the mighty Indus. In: P., Boon, B., Raven (Eds.), *River Conservation and Management*. Sussex, UK: John Wiley & Sons. 69-78. <http://www.doi.org/10.1002/9781119961819>
- Khan, I.H., Clyde, W.C. (2013). Lower Paleogene tectonostratigraphy of Balochistan: evidence for time-transgressive Late Paleocene-Early Eocene uplift. *Geosciences*, 3(3), 466-501. <https://doi.org/10.3390/geosciences3030466>
- Khan, A.D., Ghoraba, S., Arnold, J.F., Luzio, M.D. (2014). Hydrological Modeling of Upper Indus Basin and assessment of deltaic ecology. *International Journal of Modern Engineering Research*. 4(1), 73-85. Retrieved from <http://agris.fao.org/agris-search/search.do?recordID=US201500107627>
- Khan, G., Chen, X., Bao, A., Wang, Y., Meng, F. (2017). Hydrological modeling of the Upper Indus Basin: a case study from a high-altitude glacierized catchment Hunza. *Water*. 9(17), 1-20. <https://doi.org/10.3390/w9010017>
- Khim, B.-K., Horikawa, K., Asahara, Y., Kim, J.-E., Ikehara, M. (2018). Detrital Sr-Nd isotopes, sediment provenances and depositional processes in the Laxmi Basin of the Arabian Sea during the last 800 ka. *Geological Magazine*. 1-13. <https://doi.org/10.1017/S0016756818000596>
- Khonde, N.S., Singh, S.K., Maurya, D.M., Rai, V.K., Chamyal, L.S., Giosan, L. (2017). Tracing the Vedic Saraswati River in the Great Rann of Kachchh. *Scientific Reports*. 7, 5476 (2017). <https://doi.org/10.1038/s41598-017-05745-8>
- Kodagali, V.N., Jauhari, P. (1999). The meandering Indus channels: study in a small area by the multibeam swath bathymetry system-Hydrosweep. *Current Science*. 76(2), 240-243. <http://drs.nio.org/drs/handle/2264/1777>
- Kolla, V., Henderson, L., Biscaye, P.E. (1976) Clay mineralogy and sedimentation in the western Indian Ocean. *Deep-Sea Research and Oceanographic Abstracts*. 23(10),949-961. [https://doi.org/10.1016/0011-7471\(76\)90825-1](https://doi.org/10.1016/0011-7471(76)90825-1)

- Kolla, V., Buffler, R.T. (1985). Magdalena Fan, Caribbean. In: A.H., Bouma, W.R., Normark, N.E., Barnes (Eds.), *Submarine fans and related turbidite systems*. (1<sup>st</sup> ed.). Frontiers in Sedimentary Geology. New York, USA: Springer. 71-78. [http://doi.org/10.1007/978-1-4612-5114-9\\_12](http://doi.org/10.1007/978-1-4612-5114-9_12)
- Kolla, V., Coumes, F. (1987). Morphology, internal structure, seismic stratigraphy, and sedimentation of Indus Fan. *American Association of Petroleum Geologists Bulletin*. 71(6), 650-677. Retrieved from <https://pubs.geoscienceworld.org/aapgbull/article-abstract/71/6/650/38261/morphology-internal-structure-seismic-stratigraphy?redirectedFrom=fulltext>
- Kolla, V., Bourges, P., Urruty, J.-M., Safa, P. (2001). Evolution of deep-water sinuous channels offshore Angola (West Africa) and implications for reservoir architecture. *American Association of Petroleum Geologists Bulletin*. 85, 1373–1405. <https://doi.org/10.1306/8626CAC3-173B-11D7-8645000102C1865D>
- Kolla, V. (2007). A review of sinuous channel avulsion patterns in some major deep-sea fans and factors controlling them. *Marine and Petroleum Geology*. 24(6-9), 450-469. <http://doi.org/10.1016/j.marpetgeo.2007.01.004>
- Kolla, V., Posamentier, H.W., Wood, L.J. (2007). Deep-water and fluvial sinuous channels—characteristics, similarities and dissimilarities, and modes of formation. *Marine and Petroleum Geology*. 24(6-9), 388-405. <http://doi.org/10.1016/j.marpetgeo.2007.01.007>
- Kolla, V., Bandyopadhyay, A., Gupta, P., Mukherjee, B., Ramana, D.V. (2012). Morphology and internal structure of a Recent Upper Bengal Fan-valley complex. In: B.E., Prather, M.E., Deptuck, D., Mohrig, B.V., Hoorn, R.B., Wynn (Eds.), *Application of the principles of seismic geomorphology to continental slope and base-of-slope systems: case studies from seafloor and near-seafloor analogues*. Special Publication No. 99. SEPM (Society for Sedimentary Geology). Oklahoma, USA: SEPM. 347-369. <https://doi.org/10.2110/pec.12.99.0347>
- Konsoer, K., Zinger, J., Parker, G. (2013). Bankfull hydraulic geometry of submarine channels created by turbidity currents: relations between bankfull channel characteristics and formative flow discharge. *Journal of Geophysical Research Earth Surface*. 118(1), 216-228. <http://doi.org/10.1029/2012JF002422>
- Kumar, A., Srivastava, P. (2018). Landscape of the Indus River. In: D., Singh (Ed.), *The Indian Rivers*. Springer Hydrogeology Series. Singapore: Springer Nature. 47-59. [http://doi.org/10.1007/978-981-10-2984-4\\_4](http://doi.org/10.1007/978-981-10-2984-4_4)
- Kumar, A., Dutt, S., Saraswat, R., Gupta, A.K., Clift, P.D., Pandey, D.K., & Kulhanek, D. (2019) A late Pleistocene sedimentation in the Indus Fan, Arabian Sea, IODP Site U1457. *Geological Magazine*, 1-9. <https://doi.org/10.1017/S0016756819000396>
- Lai, S.Y.J., Samuel, S.C.H., Foreman, B.Z., Limaye, A.B., Grimaud, J-L., Paola, C. (2017). Stream power controls the braiding intensity of submarine channels similarly to rivers. *Geophysical Research Letters*. 44, 5062-5070. <https://doi.org/10.1002/2017GL072964>
- Lajeunesse, E., Malverti, L., Lancien, P., Armstrong, L., Métivier, F., Coleman, & Parker, G. (2010). Fluvial and submarine morphodynamics of laminar and near-laminar flows: a synthesis. *Sedimentology*. 57, 1-26. <http://doi.org/10.1111/j.1365-3091.2009.01109.x>

- Lazarus, E.D., Constantine, J.A. (2013). Generic theory for channel sinuosity. *Proceedings of the National Academy of Sciences*. 110(21), 8447-8452. <https://doi.org/10.1073/pnas.1214074110>
- Leopold, L.B. Wolman, M.G. (1960). River Meanders. *Geological Society of America Bulletin*. 71(6), 769-793. [https://doi.org/10.1130/0016-7606\(1960\)71\[769:RM\]2.0.CO;2](https://doi.org/10.1130/0016-7606(1960)71[769:RM]2.0.CO;2)
- Lin, W.T., Choub, W.C., Lin C.Y., Huang, P.H. and Tsai, J.S. (2008). Win Basin: using improved algorithms and the GIS technique for automated watershed modelling analysis from digital elevation models. *International Journal of Geographical Information Science*. 22(1), 47-69. <https://doi.org/10.1080/13658810701300121>
- Lomas, S.A., Joseph, P. (Eds.). (2004). *Confined Turbidite Systems*. Special Publications No. 222. London, UK: The Geological Society. <https://doi.org/10.1144/GSL.SP.2004.222>
- Lu, H., Liu, R., Cheng, L., Feng, H., Zhang, H., Wang, Y., & Clift, P.D. (2020) Phased evolution and variation of the South Asian monsoon, and resulting weathering and surface erosion in the Himalaya–Karakoram Mountains, since late Pliocene time using data from Arabian Sea core. *Geological Magazine*. 1-15. <https://doi.org/10.1017/S0016756820000291>
- Mackin, J.H. (1948). Concept of a graded river. *Geological Society of America Bulletin*. 59(5): 463-512. <https://pdfs.semanticscholar.org/53fb/2f5368f0c08d496243df458106439fb6996e.pdf>
- Makaske, B. (2001). Anastomosing rivers: a review of their classification, origin and sedimentary products. *Earth Science Reviews*. 53(3-4), 149-196. [https://doi.org/10.1016/S0012-8252\(00\)00038-6](https://doi.org/10.1016/S0012-8252(00)00038-6)
- Mayall, M., Jones, E., Casey, M. (2006). Turbidite channel reservoirs—key elements in facies prediction and effective development. *Marine and Petroleum Geology*. 23(8), 821-841. <https://doi.org/10.1016/j.marpetgeo.2006.08.001>
- McDougall, J.W., Khan, S.H. (1990). Strike-slip faulting in a foreland foldthrust belt: The Kalabagh fault and western salt range, Pakistan. *Tectonics*, 9(5), 1061-1075. <https://doi.org/10.1029/TC009i005p01061>
- McGregor, B., Stubblefield, W.L., Ryan, W.B.F., Twichell, D.C. (1982). Wilmington Submarine Canyon: A marine fluvial-like system. *Geology*. 10(1), 27-30. [https://doi.org/10.1130/0091-7613\(1982\)10<27:WSCAMF>2.0.CO;2](https://doi.org/10.1130/0091-7613(1982)10<27:WSCAMF>2.0.CO;2)
- McHargue, T.R., Webb, J.E. (1986). Internal geometry, seismic facies, and petroleum potential of canyons and inner fan channels of the Indus submarine fan. *American Association of Petroleum Geologists Bulletin*. 70(2), 161-180. Retrieved from <https://www.osti.gov/biblio/6968606>
- McHargue, T.R. (1991). Seismic facies, processes, and evolution of Miocene Inner Fan Channels, Indus Submarine Fan. In: P., Weimer, M.H., Link (Eds.), *Seismic facies and sedimentary processes of submarine fans and turbidite systems*. Frontiers in Sedimentary Geology. New York, USA: Springer. [https://doi.org/10.1007/978-1-4684-8276-8\\_22](https://doi.org/10.1007/978-1-4684-8276-8_22)
- Menard, H.W. (1955). Deep-sea channels, topography, and sedimentation. *American Association of Petroleum Geologists Bulletin*. 39, 236-255. Cited in: J.A., Covault (2011). Submarine fans and canyon-channel systems: a review of processes, products, and models. *Nature Education Knowledge*, 3(10), 4. Retrieved from

- <https://www.nature.com/scitable/knowledge/library/submarine-fans-and-canyon-channel-systems-a-24178428>
- Metz, J.M., Grotzinger, J.P., Mohrig, D., Milliken, R., Prather, B., Pirmez, & A.S., Weitz, C.M. (2009). Sublacustrine depositional fans in southwest Melas Chasma. *Journal of Geophysical Research*. 114, E10002. <https://doi.org/10.1029/2009JE003365>
- Miall, A.D. (2002). Architecture and sequence stratigraphy of pleistocene fluvial systems in the Malay Basin, based on seismic time-slice analysis. *American Association of Petroleum Geologists Bulletin*. 86(7), 1201-1216. <https://doi.org/10.1306/61EEDC56-173E-11D7-8645000102C1865D>
- Middleton, G.V. (1993). Sediment deposition from turbidity currents. *Annual Review of Earth and Planetary Sciences*. 21, 89-114. <https://doi.org/10.1146/annurev.ea.21.050193.000513>
- Miller, T.K. (1988). An analysis of the relation between stream channel sinuosity and stream channel gradient. *Computers, Environment and Urban Systems*. 12(3), 197-207. [https://doi.org/10.1016/0198-9715\(88\)90022-1](https://doi.org/10.1016/0198-9715(88)90022-1)
- Miller, J.R., Miller, S.M.O.(Eds.). (2007). *Contaminated rivers: a geomorphological-geochemical approach to site assessment and remediation*. Dordrecht, The Netherlands: Springer. 235-270. <https://doi.org/10.1007/1-4020-5602-8>
- Milliman, J.D., Meade, R.H. (1983). World-wide delivery of river sediment to the oceans. *The Journal of Geology*. 91(1), 1-21. <https://doi.org/10.1086/628741>
- Mishra, R., Pandey, D.K., Ramesh, P. (2015). Active channel systems in the middle Indus Fan: results from high-resolution bathymetry surveys. *Current Science*. 108(3), 409-412. Retrieved from <https://www.currentscience.ac.in/Volumes/108/03/0409.pdf>
- Mishra. R., Pandey, D.K., Ramesh, P., Clift, P.D. (2016). Identification of new deep sea sinuous channels in the eastern Arabian Sea. *Springer Plus*. 5:844, <http://doi.org/10.1186/s40064-016-2497-6>
- Molnar, P., Tapponnier, P. (1975). Cenozoic tectonics of Asia: effects of a continental collision. *Science*. 189(4201), 419-426. <https://doi.org/10.1126/science.189.4201.419>
- Molnar, P., Tapponnier, P. (1977). The Collision between India and Eurasia. *Scientific American*. 236, 30-41. <https://www.jstor.org/stable/24953979>
- Mountjoy J., Micallef A. (2018). Submarine Landslides. In: A., Micallef, S., Krastel, A., Savini. (Eds.), *Submarine geomorphology*. Cham, Switzerland: *Springer Geology*. 235-250. [http://doi.org/10.1007/978-3-319-57852-1\\_13](http://doi.org/10.1007/978-3-319-57852-1_13)
- Mukherjee, S. (2015). A review on out-of-sequence deformation in the Himalayas. In: S., Mukherjee, R., Carosi, P., van der Beek, B.K., Mukherjee, D.M. Robinson (Eds.), *Tectonics of the Himalaya*. Geological Society, London, Special Publications (Vol 412). London, UK: The Geological Society. 67-109. <https://doi.org/10.1144/SP412.13>
- Mulder, T. (2011). Gravity processes and deposits on continental slope, rise and abyssal plains. In: H., Heiko, T., Mulder (Eds.), *Deep-sea sediments*. Developments in Sedimentology. Elsevier. 63, 25-148. <https://doi.org/10.1016/B978-0-444-53000-4.00002-0>
- Murphy, M.A., Yin, A., Kapp, P., Harrison, T.M., Lin, D., Guo, J. (2000). Southward propagation of the Karakoram fault system, southwest Tibet: timing and magnitude of slip. *Geology*, 28(5), 451-454. [https://doi.org/10.1130/0091-7613\(2000\)28<451:SPOTKF>2.0.CO;2](https://doi.org/10.1130/0091-7613(2000)28<451:SPOTKF>2.0.CO;2)

- Mutti, E., Ricci Lucchi, F. (1978). Turbidites of the northern Apennines: introduction to facies analysis. *International Geology Review*, 20(2), 125-166. Translation of: Mutti, E., Ricci Lucchi, F. (1972). Le toribiditi dell'Appennino settentrionale: introduzione all'analisi di facies by Nilson, T.H., USGS. <https://doi.org/10.1080/00206817809471524>
- Naini, B.R., Kolla, V. (1982). Acoustic character and thickness of sediments of the Indus Fan and the continental margin of western India. *Marine Geology*. 47(3-4), 181-195. [http://doi.org/10.1016/0025-3227\(82\)90068-8](http://doi.org/10.1016/0025-3227(82)90068-8)
- Najman, Y., Garzanti, E., Pringle, M., Bickle, M., Stix, J., Khan, I. (2003). Early-Middle Miocene paleodrainage and tectonics in the Pakistan Himalaya. *Geological Society of America Bulletin*. 115(10), 1265–1277. <https://doi.org/10.1130/B25165.1>
- NCPOR, n.d. Processed bathymetric data. Survey of the EEZ.
- Nomark, W.R. (1970). Growth patterns of deep sea fans. Cited in: H., Heiko, T., Mulder (Eds.), *Deep-sea sediments*. Developments in Sedimentology. 63, 25-148. <https://doi.org/10.1016/B978-0-444-53000-4.00002-0>
- NRSC. (2011). Evaluation of Indian National DEM from Cartosat-1 Data. Indian Space Research Organisation, National Remote Sensing Center. Retrieved from: [https://bhuvan-app3.nrsc.gov.in/data/download/tools/document/CartoDEMReadme\\_v1\\_u1\\_23082011.pdf](https://bhuvan-app3.nrsc.gov.in/data/download/tools/document/CartoDEMReadme_v1_u1_23082011.pdf)
- Nyberg, B, Helland-Hansen, W., Gawthorpe, R.L., Sandbakken, P., Eide, C.H., Sømme, T., & Leiknes, S. (2018). Revisiting morphological relationships of modern source-to-sink segments as a first-order approach to scale ancient sedimentary systems. *Sedimentary Geology*. 373. 111-133. <https://doi.org/10.1016/j.sedgeo.2018.06.007>
- O'Callaghan, J.F., Mark, D.M. (1984). The extraction of drainage networks from digital elevation data. *Computer Vision, Graphics and Image Processing*. 28(3), 323-344. [https://doi.org/10.1016/S0734-189X\(84\)80011-0](https://doi.org/10.1016/S0734-189X(84)80011-0)
- Owen, L.A. (1988). Terraces, uplift and climate, Karakoram Mountains, Northern Pakistan (Doctoral Thesis).UK: University of Leicester. <http://hdl.handle.net/2381/35081>
- Pandey, D.K., Clift, P.D., Kulhanek, D.K., Andò, S., Bendle, J.A.P., Bratenkov, S., & Yu, Z. (2016). Expedition 355 summary. In: D.K., Pandey, P.D., Clift, D.K., Kulhanek (Eds.), *Arabian Sea monsoon: proceedings of the International Ocean Discovery Program*. Volume 355. Texas, USA: International Ocean Discovery Program. <https://doi.org/10.14379/iodp.proc.355.101.2016>
- Peakall, J., McCaffrey, B., Kneller, B. (2000). A process model for the evolution, morphology, and architecture of sinuous submarine channels. *Journal of Sedimentary Research*. 70(3), 434-448. <https://doi.org/10.1306/2DC4091C-0E47-11D7-8643000102C1865D>
- Peakall, J., Sumner, E.J. (2015). Submarine channel flow processes and deposits: A process-product perspective. *Geomorphology*. 244, 95-120. <http://doi.org/10.1016/j.geomorph.2015.03.005>
- Pettingill, H.S., Weimer, P. (2002). Worldwide deep water exploration and production: past, present, and future. *The Leading Edge*. 21(4), 371-376. <http://dx.doi.org/10.1190/1.1471600>
- Pickering, K.T., Coleman, J., Cremer, M., Droz, L., Kohl, B., Normark, W., O'Connell, S., Stow, D., Meyer-Wright, A. (1986). A high sinuosity, laterally migrating submarine fan channel-levee-overbank: results from DSDP Leg 96 on the Mississippi Fan, Gulf of

- Mexico. *Marine and Petroleum Geology*. 3(1), 3-18. [https://doi.org/10.1016/0264-8172\(86\)90052-8](https://doi.org/10.1016/0264-8172(86)90052-8)
- Picot, M., Droz, L., Marsset, T., Bernard, D., Bez, M. (2016). Controls on turbidite sedimentation: Insights from a quantitative approach of submarine channel and lobe architecture (Late Quaternary Congo Fan). *Marine and Petroleum Geology*. 72, 423-446. <http://doi.org/10.1016/j.marpetgeo.2016.02.004>
- Pike, R.J. (1963) Landform regions of southern New England—a quantitative delimitation. Cited in: R.J., Pike, S.E. Wilson (1971). Elevation relief ratio, hypsometric integral, and geomorphic area-altitude analysis. *Geological Society of America Bulletin*. 82, 1079-1084. [https://doi.org/10.1130/0016-7606\(1971\)82\[1079:ERHIAG\]2.0.CO;2](https://doi.org/10.1130/0016-7606(1971)82[1079:ERHIAG]2.0.CO;2)
- Pike, R.J., Wilson, S.E. (1971). Elevation-relief ratio, hypsometric integral, and geomorphic area-altitude analysis. *Geological Society of America Bulletin*. 82, 1079-1084. [https://doi.org/10.1130/0016-7606\(1971\)82\[1079:ERHIAG\]2.0.CO;2](https://doi.org/10.1130/0016-7606(1971)82[1079:ERHIAG]2.0.CO;2)
- Pike, R.J. (1995). Geomorphometry-diversity in quantitative surface analysis. *PPG: Earth and Environment*. 24(1), 1-20. <https://doi.org/10.1177/030913330002400101>
- Piper, D.J.W., Shor, A.N., Clarke, J.E.H. (1988). The 1929 “Grand Banks” earthquake, slump, and turbidity current". In: H.E. Clifton (Ed.), *Sedimentologic consequences of convulsive geologic events*. Volume 229. Colorado, USA: Geological Society of America. <https://doi.org/10.1130/SPE229-p77>
- Pirmez, C., Flood, R.D. (1995). Morphology and structure of Amazon channel. In: R.D., Flood, D.J.W., Piper, A., Klaus (Eds.), *Proceedings of the Ocean Drilling Program*. Initial report (Vol 155).23-45. Texas A&M University, USA: Ocean Drilling Program. <http://doi.org/10.2973/odp.proc.ir.155.103.1995>
- Posamentier, H.W. (2003). Depositional elements associated with a basin floor channel-levee system: case study from the Gulf of Mexico. *Marine and Petroleum Geology*. 20(6-8), 677-690. <http://doi.org/10.1016/j.marpetgeo.2003.01.002>
- Prell, W.L., Niitsuma, N., Emeis, K.-E., Anderson, D., Barnes, R., Bilak, R.A., & Weedon, G.P. (1989). *Proceedings of the Ocean Drilling Program*. Initial report (Vol 117). 157-195. Texas A&M University, USA: Ocean Drilling Program. <http://doi.org/10.2973/odp.proc.ir.117.104.1989>
- Perna, R., Pandey, D.K. Mishra, R. (2015). Approximation of flow patterns for submarine channel systems in the Arabian Sea using a GIS approach. *International Journal of Advanced Remote Sensing and GIS*. 4(1), 1142-1160. <http://technical.cloud-journals.com/index.php/IJARSG/article/view/Tech-429>
- Perna, R., Pandey, D.K., Mahender, K. (2018). Longitudinal profiling and elevation-relief analysis of the Indus. *Arabian Journal of Geosciences*.11:343. <https://doi.org/10.1007/s12517-018-3657-5>
- Perna, R., Kotha, M. (2020) Geomorphometric comparison of submarine channel-levee complexes with fluvial river systems: observations from the Indus. *Geo-Marine Letters*, Springer. <https://www.doi.org/10.1007/s00367-020-00654-8>
- Prins, M.A., Postma, G., Cleveringa, J., Cramp, A., Kenyon, N.H. (2000). Controls on terrigenous sediment supply to the Arabian Sea during the late Quaternary: The Indus Fan. *Marine Geology*. 169(3-4), 327-349. [http://doi.org/10.1016/S0025-3227\(00\)00086-4](http://doi.org/10.1016/S0025-3227(00)00086-4)

- Qayyum, M., Niem, A.R., Lawrence, R.D. (1996). Newly discovered Paleogene deltaic sequence in Katawaz Basin, Pakistan, and its tectonic implications. *Geology*. 24(9), 835-838. [https://doi.org/10.1130/0091-7613\(1996\)024<0835:NDPDSI>2.3.CO;2](https://doi.org/10.1130/0091-7613(1996)024<0835:NDPDSI>2.3.CO;2)
- Qin, Y., Alves, T.M., Constantine, J., Gamboa, D. (2016). Quantitative seismic geomorphology of a submarine channel system in SE Brazil (Espírito Santo Basin): scale comparison with other submarine channel systems. *Marine and Petroleum Geology*. 78, 455-473. <http://doi.org/10.1016/j.marpetgeo.2016.09.024>
- Quadri, V., Shuaib, S.M. (1986). Hydrocarbon prospects of Southern Indus Basin, Pakistan. *American Association of Petroleum Geologists Bulletin*. 70, 430-747. <https://doi.org/10.1306/94886344-1704-11D7-8645000102C1865D>
- Ramaswamy, V., Nair, R.R., Manganini, S., Haake, B., Ittekkot, V. (1991). Lithogenic fluxes to the deep Arabian Sea measured by sediment traps. *Deep-Sea Research Part A. Oceanographic Research Papers*. 38(2), 169-184. [https://doi.org/10.1016/0198-0149\(91\)90078-T](https://doi.org/10.1016/0198-0149(91)90078-T)
- Ritter, D.F., Kochel, R.C., Miller, J.R. (2002). Process geomorphology. Cited in: O., Singh, A., Sarangi (2008). Hypsometric analysis of the lesser Himalayan watersheds using geographical information system. *Indian Journal of Soil Conservation*. 36(3), 148-154. <http://krishikosh.egranth.ac.in/bitstream/1/37880/1/S-Hypsometric%20analysis.pdf>
- Rosgen, D.L. (1994). A classification of natural rivers. *Catena*. 22, 169-199. [https://doi.org/10.1016/0341-8162\(94\)90001-9](https://doi.org/10.1016/0341-8162(94)90001-9)
- Rust, B.R. (1978). A classification of alluvial channel systems. In: A.D., Miall (Ed.), *Fluvial sedimentology*. Canadian Society of Petroleum Geologists Memoir (Vol 116, 5). Calgary, Canada: Geological Magazine, Cambridge University Press. 187-198. <https://doi.org/10.1017/S0016756800044101>
- Schumm, S.A. (1969). River metamorphosis. *Journal of the Hydraulics Division*. 95(1), 255-274. Retrieved from <https://cedb.asce.org/CEDBsearch/record.jsp?dockey=0015935>
- Schumm, S.A., Khan, H.R. (1972). Experimental study of channel patterns. *Geological Society of America Bulletin*. 83(6), 1755-1770. [https://doi.org/10.1130/0016-7606\(1972\)83\[1755:ESOCP\]2.0.CO;2](https://doi.org/10.1130/0016-7606(1972)83[1755:ESOCP]2.0.CO;2)
- Schumm, S.A. (1985). Patterns of alluvial rivers. *Annual Review of Earth and Planetary Sciences*. 13, 5-27. <https://doi.org/10.1146/annurev.earth.13.050185.000253>
- Schumm, S.A., Dumont, J.F., Holbrook, J.M. (Eds.). (2000). *Active tectonics and alluvial rivers*. Cambridge, UK: University Press. Retrieved from [https://books.google.co.in/books/about/Active\\_Tectonics\\_and\\_Alluvial\\_Rivers.html?id=yTc3jmYKS6EC&redir\\_esc=y](https://books.google.co.in/books/about/Active_Tectonics_and_Alluvial_Rivers.html?id=yTc3jmYKS6EC&redir_esc=y)
- Searle, M.P. (1996). Geological evidence against large-scale pre-Holocene offsets along the Karakoram fault: implications for the limited extrusion of the Tibetan plateau. *Tectonics* 15(1), 171-186. <https://doi.org/10.1029/95TC01693>
- Shah, Z.U.H. (1997) Deep crustal studies of Indus offshore Basin (Pakistan) using seismic and gravity data. *Geological Bulletin*. 30, 13-40. Retrieved from: <http://nceg.uop.edu.pk/GeologicalBulletin/Vol-30-1997/Vol-30-1997-Paper2.pdf>
- Shanmugam, G., Moiola, R.J. (1988). Submarine fans: characteristics, models, classification, and reservoir potential. *Earth-Science Reviews*. 24(6), 383-428. [http://doi.org/10.1016/0012-8252\(88\)90064-5](http://doi.org/10.1016/0012-8252(88)90064-5)

- Shanmugam, G. (2016). Submarine fans: a critical retrospective. *Journal of Palaeogeography*. 5(2), 110-184. <http://dx.doi.org/10.1016/j.jop.2015.08.011>
- Shareef, N.M., Dinesh, A.C., Venkateswara, R., Jayaprakash, C., Rajarama, K.N., Varghese, S., Girishbai, D. (2018). Evidences of shallow marine sediments as channel fill in the Lower Indus Fan. *Indian Journal of Geo-Marine Sciences*. 47, 67-72. Retrieved from <http://nopr.niscair.res.in/handle/123456789/43453>
- Shepard, F.P. (1934). Detailed surveys of submarine canyons. *Science*. 80(2079), 410-411. <https://doi.org/10.1126/science.80.2079.410>
- Shepard, F.P., Drill, R.F., von Rad, U. (1969). Physiography and sedimentary processes of La Jolla submarine fan and fan valley. *Bulletin of the American Association of Petroleum Geologists*. 53, 390-420. <http://archives.datapages.com/data/bulletns/1968-70/data/pg/0053/0002/0350/0390.htm>
- Shreve, R.L. (1966). Statistical law of stream numbers. *The Journal of Geology*. 74(1). 17-37. <https://doi.org/10.1086/627137>
- Shuaib, S.M. (1982). Geology and hydrocarbon potential of offshore Indus Basin, Pakistan. *American Association of Petroleum Geologists Bulletin*. 66(7), 940-946. <https://doi.org/10.1306/03B5A363-16D1-11D7-8645000102C1865D>
- Sinclair, H., Mudd, S.M., Dingle, E., Hobley, D.E.J., Robinson, R., Walcott, R. (2017). Squeezing river catchments through tectonics: shortening and erosion across the Indus Valley, NW Himalaya. *Geological Society of America Bulletin*. 129(1-2), 203-217. <http://doi.org/10.1130/B31435.1>
- Singh, O., Sarangi, A. (2008). Hypsometric analysis of the lesser Himalayan watersheds using geographical information system. *Indian Journal of Soil Conservation*. 36(3), 148-154. <http://krishikosh.egranth.ac.in/bitstream/1/37880/1/S-Hypsometric%20analysis.pdf>
- Singh, O. (2009). Hypsometry and erosion proneness: a case study in the lesser Himalayan Watersheds. *Journal of Soil and Water Conservation*. 8(2), 53-59. <http://www.environmentportal.in/files/Hypsometry.pdf>
- Singh, A., Thomsen, K.J., Sinha, R., Buylaert, J.-P., Carter, A., Mark, D.F., & Gupta, S. (2017). Counter-intuitive influence of Himalayan river morphodynamics on Indus civilisation urban settlements. *Nature Communications*. 8. Article number: 1617. <http://doi.org/10.1038/s41467-017-01643-9>
- Smith, W.H.F., Sandwell, D.T. (1997). Global seafloor topography from satellite altimetry and ship depth soundings. *Science*. 277(5334), 1957-1962. <https://doi.org/10.1126/science.277.5334.1956>
- Sømme, T.O., Helland-Hansen, W., Martinsen, O.J., Thurmond, J.B. (2009). Relationships between morphological and sedimentological parameters in source-to-sink systems: a basis for predicting semi-qualitative characteristics in subsurface systems. *Basin Research*. 21. 361-387. <https://doi.org/10.1111/j.1365-2117.2009.00397.x>
- Sonam, S., Jain, V. (2018). Geomorphic effectiveness of a long profile shape and the role of inherent geological controls in the Himalayan hinterland area of the Ganga River basin, India. *Geomorphology*. 304, 15-29. <https://doi.org/10.1016/j.geomorph.2017.12.022>
- Spencer, J.W. (1903). Submarine valleys off the American coast and in the North Atlantic. *Geological Society of America Bulletin*. 14(1), 207-226. <https://doi.org/10.1130/GSAB-14-207>

- Strahler, A.N. (1952). Hypsometric (area-altitude) analysis of erosional topology. *Geological Society of America Bulletin*. 63(11), 1117-1142. [https://doi.org/10.1130/0016-7606\(1952\)63\[1117:HAAOET\]2.0.CO;2](https://doi.org/10.1130/0016-7606(1952)63[1117:HAAOET]2.0.CO;2)
- Strahler, A., Strahler, A.N. (Eds.). (1996). Fluvial processes and landforms. In: *Physical geography: science and systems of the human environment*. (2<sup>nd</sup> ed.). New Delhi, India: John Wiley & Sons. <https://trove.nla.gov.au/work/8254783>
- Stelting, C.E., DSDP Leg 96 Shipboard Scientists. (1985). Migratory characteristics of a mid-fan meander belt, Mississippi Fan. In: A.H., Bouma, W.R., Normark, N.E., Barnes (Eds.), *Submarine fans and related turbidite systems*. (1<sup>st</sup> ed.). Frontiers in Sedimentary Geology. New York, USA: Springer. 283-290. [https://doi.org/10.1007/978-1-4612-5114-9\\_41](https://doi.org/10.1007/978-1-4612-5114-9_41)
- Stow, D.A.V., Howell, D.G., Nelson, C.H. (1985). Sedimentary, tectonic, and sea-level controls. In: A.H., Bouma, W.R., Normark, N.E., Barnes (Eds.), *Submarine fans and related turbidite systems*. (1st ed.). Frontiers in Sedimentary Geology. New York, USA: Springer. [http://doi.org/10.1007/978-1-4612-5114-9\\_4](http://doi.org/10.1007/978-1-4612-5114-9_4)
- Subrahmanyam, V., Krishna, K.S., Ramana, M.V., Murthy, K.S.R. (2008). Marine geophysical investigations across the submarine canyon (Swatch-of-No-Ground), northern Bay of Bengal. *Current Science*. 94(4), 507-513. <http://drs.nio.org/drs/handle/2264/962>
- Syvitski, J.P.M., Brakenridge, G.R. (2013). Causation and avoidance of catastrophic flooding along the Indus River, Pakistan. *Geological Society of America Today*. 23(1), 4-10. <http://doi.org/10.1130/GSATG165A.1>
- Tada, R., Zheng, H., Clift, P.D. (2016). Evolution and variability of the Asian monsoon and its potential linkage with uplift of the Himalaya and Tibetan Plateau. *Progresses in Earth and Planetary Science*. 3:4. <https://doi.org/10.1186/s40645-016-0080-y>
- Tappin, D.R., Grilli, S.T., Harris, J.C., Geller, R.J., Masterlark, T., Kirby, J.T., & Mai, M. (2014) Did a submarine landslide contribute to 2011 Tohoku tsunami? *Marine Geology*. 357, 344-361. <https://doi.org/10.1016/j.margeo.2014.09.043>
- Taylor, B., Smoot, N.C. (1984). Morphology of Bonin fore-arc submarine canyons. *Geology*. 12(12), 724-727. [https://doi.org/10.1130/0091-7613\(1984\)12<724:MOBFSC>2.0.CO;2](https://doi.org/10.1130/0091-7613(1984)12<724:MOBFSC>2.0.CO;2)
- Timár, G. (2003). Controls on channel sinuosity changes: a case study of the Tisza River, the Great Hungarian Plain. *Quaternary Science Reviews*. 22(20), 2199-2207. [http://doi.org/10.1016/S0277-3791\(03\)00145-8](http://doi.org/10.1016/S0277-3791(03)00145-8)
- Veatch, A.C., Smith, P.A. (1939). Atlantic submarine valleys of the United States and the Congo submarine valley. *Geological Society of America*. Special Papers, No. 7. <https://searchworks.stanford.edu/view/80600>
- Vittori, J., Morash, A., Savoye, B., Marsset, T., Lopez, M., Droz, L., Cremer, M. (2000). The Quaternary Congo deep-sea fan: preliminary results on reservoir complexity in turbiditic systems using 2D high-resolution seismic and multibeam data. In: P., Weimer, R.M., Slatt, J., Coleman, N.C., Rosen, H., Nelson, A.H., Bouma, M.J., Styzen, D.T., Lawrence (Eds.), *Deep-water reservoirs of the world*. Texas, USA: SEPM Society for Sedimentary Geology. <https://doi.org/10.5724/gcs.00.20>
- von Rad, U., Tahir, Md. (1997). Late Quaternary sedimentation on the outer Indus shelf and slope (Pakistan): evidence from high-resolution seismic data and coring. *Marine Geology*. 138(3-4), 193-236. [http://doi.org/10.1016/S0025-3227\(96\)00090-4](http://doi.org/10.1016/S0025-3227(96)00090-4)

- Ward, B. (2007). Anammox and denitrification in the ODZ of the Arabian Sea. Cruise: KNOX09RR, Kongsberg EM120 multibeam sonar data. Princeton University. R/v Roger Revelle, Scripps Institution of Oceanography. *Marine Geophysical Data System*. <https://doi.org/10.7284/903735>
- Warwick, P.D. (2007). Overview of the geography, geology, and structure of the Potwar regional framework assessment project study area, northern Pakistan. In: P.D., Warwick, B.R., Wardlaw (Eds.), *Regional studies of the Potwar plateau area, Northern Pakistan*. US Geological Survey Bulletin. 2078, A1-A9. Retrieved from <https://pubs.usgs.gov/bul/2078/>
- White, R. (Ed.). (2001). Evacuation of sediments from reservoirs. In: *Numerical model case study*. London, UK: Thomas Telford Publishing. 163-169. <https://doi.org/10.1680/eosfr.29538.bm04>
- Whitmarsh, R. B., Weser, O. E., Ali, S., Boudreaux, J. E., Fleisher, R. L., Jipa, D., & Hamilton, N. (1974a). *Deep Sea Drilling Project*. Initial report (Vol 23). Site 220. 117-166. Texas A&M University, USA: Ocean Drilling Program. <http://doi.org/10.2973/dsdp.proc.23.104.1974>
- Whitmarsh, R. B., Weser, O. E., Ali, S., Boudreaux, J. E., Fleisher, R. L., Jipa, D., & Hamilton, N. (1974b). *Deep Sea Drilling Project*. Initial report (Vol 23). Site 221. 167-210. Texas A&M University, USA: Ocean Drilling Program. <http://doi.org/10.2973/dsdp.proc.23.105.1974>
- Willgoose, G., Hancock, G. (1998). Revisiting the hypsometric curve as an indicator of form and process in transport-limited catchment. *Earth Surface Processes and Landforms*. 23(7), 611–623. [https://doi.org/10.1002/\(SICI\)1096-9837\(199807\)23:7<611::AID-ESP872>3.0.CO;2-Y](https://doi.org/10.1002/(SICI)1096-9837(199807)23:7<611::AID-ESP872>3.0.CO;2-Y)
- Williams, S.C.P. (2016) Skimming the surface of underwater landslides. *PNAS* February 16, 2016. 113(7), 1675-1678. <https://doi.org/10.1073/pnas.1524012113>
- Winston, Y., Yang, Y-C., Savitsky, A., Alford, D., Brown, C., Wescoat., J., Debowicz, D., Robinson, S., (Eds.) (2013). Hydrology and glaciers in the Upper Indus Basin. In: *The Indus Basin of Pakistan: the impacts of climate risks on water and agriculture*. Washington D.C.: The World Bank, 57-75. <https://doi.org/10.1596/978-0-8213-9874-6>
- Wood, W. F., Snell, J. B., U.S. Army Natick Laboratories. (1960). A quantitative system for classifying landforms. Cited in: R.J., Pike, S.E. Wilson (1971). Elevation-relief ratio, hypsometric integral, and geomorphic area-altitude analysis. *Geological Society of America Bulletin*. 82, 1079-1084. [https://doi.org/10.1130/0016-7606\(1971\)82\[1079:ERHIAG\]2.0.CO;2](https://doi.org/10.1130/0016-7606(1971)82[1079:ERHIAG]2.0.CO;2)
- Wohl, E.E. (2008). Hydrology and discharge. In: A., Gupta (Ed.), *Large rivers: geomorphology and management*. Chichester, UK: John Wiley & Sons.29-44. <https://doi.org/10.1002/9780470723722.ch3>
- Wynn, R.B., Cronin, B.T., Peakall, J. (2007). Sinuous deep-water channels: genesis, geometry and architecture. *Marine and Petroleum Geology*. 24(6-9), 341-387. <https://doi.org/10.1016/j.marpetgeo.2007.06.001>
- Yin, A.N. (2006). Cenozoic tectonic evolution of the Himalayan orogen as constrained by along-strike variation of structural geometry, exhumation history, and foreland

- sedimentation. *Earth-Science Reviews*. 76, 1-131.  
<https://doi.org/10.1016/j.earscirev.2005.05.004>
- Zámolyi, A., Székely, B., Draganits, E., Timára, G. (2010). Neotectonic control on river sinuosity at the western margin of the Little Hungarian Plain. *Geomorphology*. 122(3-4), 231-243. <http://doi.org/10.1016/j.geomorph.2009.06.028>
- Zeitler, P.K., Koons, P.O., Bishop, M.P., Chamberlain, C.P., Craw, D., Edwards, M.A., & Shroder, J.F. (2001). Crustal reworking at Nanga Parbat, Pakistan: metamorphic consequences of thermal mechanical coupling facilitated by erosion. *Tectonics*. 20(5), 712-728. <https://doi.org/10.1029/2000TC001243>
- Ziring, L., Burki, S.J. (2019). Pakistan. Article in Encyclopædia Britannica Online. <https://www.britannica.com/place/Pakistan>

**PUBLICATIONS**  
**AND**  
**PARTICIPATIONS**

## **Publications**

1. Prerna R., Pandey D.K., and Mahender, K. (2018) Longitudinal Profiling and Elevation-Relief Analysis of the Indus. Arabian Journal of Geosciences, Springer. Vol 11:343. <http://www.doi.org/10.1007/s12517-018-3657-5>
2. Prerna R., and Mahender, K. (2020). Geomorphometric comparison of submarine channel-levee complexes with fluvial river systems: observations from the Indus. Geo-Marine Letters, Springer. <https://www.doi.org/10.1007/s00367-020-00654-8>

## **Conference participations**

1. Presented paper titled ‘Longitudinal Profiling and Elevation-Relief Ratio of the Indus’ at the 17<sup>th</sup> ESRI India User Conference, held at New Delhi, 13-14 December, 2017 (Annexure I).
2. Presented paper titled ‘Fluvial rivers and submarine channels: their inherent differences’ at the NRSC-ISRO User Interaction Meet, held at Hyderabad, 22-23 January, 2019 (Annexure II).

\*\*\*



**UC**  
**Esri India**  
User Conference  
13-14 December 2017 | Delhi

Certificate of Award

This certificate is presented to R Sneha  
for presenting a paper on National Centre for Antarctic +  
Ocean Research (NCAOR)  
during Esri India User Conference 2017.

*Agendra Kumar*

**Agendra Kumar**  
President, Esri India

14/12/2017  
Date



# User Interaction Meet - 2019

22<sup>nd</sup> & 23<sup>rd</sup>, January 2019

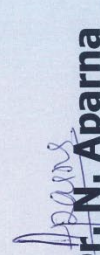
NRSC, Balanagar, Hyderabad

**nrsc**

## **PARTICIPATION CERTIFICATE**

*This is to certify that R.Premna, Project Scientist -B, NCPOR, Goa has participated and presented a paper in "User Interaction Meet - 2019" held at NRSC, Balanagar, Hyderabad during 22<sup>nd</sup> & 23<sup>rd</sup>, January 2019.*

**23<sup>rd</sup> JAN 2019**

  
**Dr. N. Aparna**  
**Group Head**  
ग्रुप हेड/Group Head  
అధ్యక్షురాలు/Chief Scientist  
NRSC U... Centre